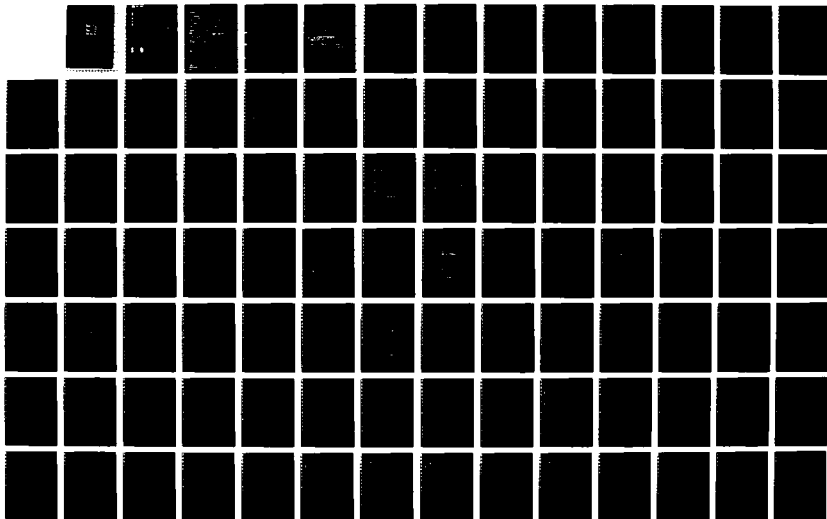AD-A181 504    BORON ASSISTED HYDROCARBON COMBUSTION MODEL AND          1/2
               SENSITIVITY ANALYSIS(U) AERODYNE RESEARCH INC BILLERICA
               MA   R C BROWN ET AL. MAR 87 ARI-RR-580 AFOSR-TR-87-0627
UNCLASSIFIED   F49620-86-C-0087                          F/G 21/2      NL

②

ARI-RR-580

AD-A181 834

AFOSR-TR- 87 - 0 6 27

BORON ASSISTED HYDROCARBON COMBUSTION MODEL
AND SENSITIVITY ANALYSIS

APR 13 1987

Prepared by:

R.C. Brown and C.E. Kolb
Aerodyne Research, Inc.
45 Manning Road
Billerica, MA  01821

and

R.A. Yetter and F.L. Dryer
Department of Mechanical and Aerospace Engineering
Princeton University

and

H.R. Rabitz
Department of Chemistry
Princeton University

DTIC
ELECTE
JUN 1 2 1987
C4D

Prepared for:

Major L. Davis
Chemical and Atmospheric Sciences Division
Air Force Office of Scientific Research
Bolling Air Force Base, Washington, DC  20331

March 1987

87   5  20  073

AD-A181504

# REPORT DOCUMENTATION PAGE

| REPORT SECURITY CLASSIFICATION<br>Unclassified | 1b. RESTRICTIVE MARKINGS |
|---|---|
| SECURITY CLASSIFICATION AUTHORITY | 3. DISTRIBUTION/AVAILABILITY OF REPORT<br>Distribution unlimited; approved for<br>public release |
| DECLASSIFICATION/DOWNGRADING SCHEDULE | |
| PERFORMING ORGANIZATION REPORT NUMBER(S)<br>ARI-RR-580 | 5. MONITORING ORGANIZATION REPORT NUMBER(S)<br>AFOSR-TR- 87-0627 |

| NAME OF PERFORMING ORGANIZATION<br>Aerodyne Research, Inc. | 6b. OFFICE SYMBOL<br>(If applicable) | 7a. NAME OF MONITORING ORGANIZATION<br>Air Force Office of Scientific Research/NC |
|---|---|---|
| ADDRESS (City, State, and ZIP Code)<br>45 Manning Road<br>Billerica, MA. 01821 | | 7b. ADDRESS (City, State, and ZIP Code)<br>Directorate of Chemical & Atmospheric Sciences<br>Building 410<br>Bolling AFB, D.C. 20332-6448 |
| NAME OF FUNDING/SPONSORING<br>ORGANIZATION<br>AFOSR | 8b. OFFICE SYMBOL<br>(If applicable)<br>NC | 9. PROCUREMENT INSTRUMENT IDENTIFICATION NUMBER<br>F49620-86-C-0087 |

| ADDRESS (City, State, and ZIP Code)<br>Directorate of Chemical & Atmospheric Sciences<br>Building 410<br>Bolling AFB, D.C. 20332-6448 | 10. SOURCE OF FUNDING NUMBERS | | | |
|---|---|---|---|---|
| | PROGRAM<br>ELEMENT NO.<br>61102F | PROJECT<br>NO.<br>3005 | TASK<br>NO.<br>A1 | WORK UNIT<br>ACCESSION NO. |

TITLE (Include Security Classification)
Boron Assisted Hydrocarbon Combustion Model and Sensitivity Analysis

PERSONAL AUTHOR(S)
R.C. Brown, C.E. Kolb, R. A. Yetter, F.L. Dryer, and H.R. Rabitz

| 13a. TYPE OF REPORT<br>Final Report | 13b. TIME COVERED<br>FROM | 14. DATE OF REPORT (Year, Month, Day) | 15. PAGE COUNT<br>122 |
|---|---|---|---|

SUPPLEMENTARY NOTATION

| COSATI CODES | | | 18. SUBJECT TERMS (Continue on reverse if necessary and identify by block number) |
|---|---|---|---|
| FIELD | GROUP | SUB-GROUP | Boron Combustion; Sensitivity Analysis; Propulsion |
| | | | |

ABSTRACT (Continue on reverse if necessary and identify by block number)

Solid boron has long been recognized as a potential high volumetric density propellant for volume limited air breathing propulsion systems. However, achieving this potential has proved difficult due to low combustion and heat release efficiencies encountered when solid boron slurries are added to conventionally designed combustors. The combustion of solid boron particles with an oxygen based oxidizer has long been known to be a complex process involving both heterogeneous (gas/solid) and homogeneous (gas/gas) chemical kinetics. The difficulties in achieving the anticipated potential of boron assisted propellants in practical applications has created a need for improved understanding of the basic chemical and physical processes in these systems.

This report presents the results of an AFOSR sponsored project to model the homogeneous gas phase oxidation kinetics for boron assisted hydrocarbon combustion and use kinetic sensitivity analysis to determine critical reaction pathways and assess uncertainties in the currently available thermochemical and kinetic data.

| 20. DISTRIBUTION/AVAILABILITY OF ABSTRACT<br>☐ UNCLASSIFIED/UNLIMITED  ☒ SAME AS RPT.  ☐ DTIC USERS | 21. ABSTRACT SECURITY CLASSIFICATION<br>Unclassified |
|---|---|
| 22a. NAME OF RESPONSIBLE INDIVIDUAL<br>Major Larry Davis | 22b. TELEPHONE (Include Area Code)<br>(202) 767-4960 | 22c. OFFICE SYMBOL<br>NC |

DD FORM 1473, 84 MAR          83 APR edition may be used until exhausted.          SECURITY CLASSIFICATION OF THIS PAGE

## 19. Abstract (Contd.)

In addition, a preliminary evaluation of the modifications and/or extensions to sensitivity analysis techniques for future applications to the heterogeneous phases of boron combustion was performed.

The basic foundation has been developed for initiating experimental and/or theoretical studies to further refine the kinetic and thermochemical parameters identified to be of critical importance to gas phase oxidation and to help validate the present gas phase combustion model. At the same time, a fairly comprehensive gas phase combustion model now exists for studying a number of boron based combustion systems.

CERTIFICATION OF TECHNICAL DATA CONFORMITY (OCT 1985) (DoD FAR SUP 52.227-7036)

The Contractor, _Aerodyne Research Inc._ , hereby certifies that, to the best of its knowledge and belief, the technical data delivered herewith under Contract No. _F19620-86-C-0087_ is complete, accurate, and complies with all requirements of the contract.

_April 6 1986_
Date

_Robert C. Brown , Senior Research Scientist._
Name and Title of Certifying Official

Aerodyne Research, Inc.
F49620-86-C-0087

| Accesion For | |
|---|---|
| NTIS CRA&I | ☑ |
| DTIC TAB | ☐ |
| Unannounced | ☐ |
| Justification | |
| By | |
| Dist ibution / | |
| Availability Codes | |
| Dist | Avail and/or Special |
| A-1 | |

# SUMMARY

Solid boron has long been recognized as a potential high volumetric density propellant for volume limited air breathing propulsion systems. However, achieving this potential has proved difficult due to low combustion and heat release efficiencies encountered when solid boron slurries are added to conventionally design combustors. The difficulties in achieving the anticipated potential of boron-assisted propellants in practical applications has created a need for improved understanding of the basic chemical and physical processes in these systems.

The combustion of solid boron particles with an oxygen based oxidizer has long been known to be a complex process involving both heterogeneous (gas/solid) and homogeneous (gas/gas) chemical kinetics. The combustion process begins with an initial heterogeneous phase of particle oxidation, ignition and volatilization of partially oxidized boron species. The volatilized boron species undergo further homogeneous gas-phase oxidation to form a mixture of gaseous boron oxide and boron oxyhydride species. Finally, as these combustion gases cool, the complex B-O-H mixture must condense to liquid or solid $B_2O_3$ in a third (heterogeneous) combustion phase in order to complete the heat release necessary for an efficient boron assisted propellant.

This study presents the results of an AFOSR sponsored project to model the homogeneous gas phase combustion sub-process and use kinetic sensitivity analysis to determine critical reaction pathways and uncertainties in the currently available thermochemical and kinetic data. An additional objective was to evaluate the extensions of sensitivity analysis that would permit its future application to heterogeneous boron combustion. Eventually, the models for each of the three sub-processes would be coupled to develop a complete model for the full combustion process.

From the modeling work and sensitivity analysis summarized in this report, several important results have been obtained. These include the following:

1) Thermodynamically, the dominant equilibrium boron species in the boundary layer surrounding a hot boron particle in hydrocarbon combustion gases consists of $HBO$ and $B_2O_2$ for fuel rich systems and $HBO_2$ and $B_2O_3$ for oxygen rich systems.

2) The initial identity of boron sub-oxides and oxyhydride species evolved from the particulate boron influences the gas phase oxidation kinetics only during the first few micro seconds. The species and temperature profiles, as well as sensitivity gradients are only weakly dependent on the identity of initially vaporized species during the subsequent oxidation chemistry.

3) The presence of hydrogen containing species has a significant impact on the homogeneous combustion. In general hydrogen tends to have a favorable effect because it aids vaporization of $B(s)$ and promotes reactions of $BO$ and $BO_2$ to form $HBO_2$ and $B_2O_3$. On the other hand, larger quantities of hydrogen promote the formation of $HBO_2$, and the product condensation stage becomes more complicated.

4) The gas phase oxidation kinetics is dominated by a relatively small set of kinetic and equilibrium processes. These have been identified for further experimental and/or theoretical study.

5) $HBO_2$ and $B_2O_2$ are the two principal gas phase combustion products with $B_2O_3(g)$ favored at higher combustion temperatures. For most systems modeled, $HBO_2$ is favored. Consequently, the product condensation stage of boron combustion is probably more typically a complex heterogeneous process. However, the ability to shift the product distribution to $B_2O_3$ via special additives would allow condensation to proceed as a simple nucleation which could significantly increase combustion efficiency.

6)  A preliminary analysis has identified key issues and viable
    approaches for extending the current model and sensitivity analysis
    to the heterogeneous burn phase of boron combustion.

The basic foundation has now been developed for initiating experimental
and/or theoretical studies to further refine the kinetic and thermochemical
parameters identified to be of critical importance to gas phase oxidation and
to help validate the present gas phase combustion model.  At the same time, a
fairly comprehensive gas phase combustion model now exists for studying a
number of boron based combustion systems of important to the Department of
Defense community.

## TABLE OF CONTENTS

Table of Contents (Continued)

# LIST OF ILLUSTRATIONS

List of Illustrations (Continued)

List of Illustrations (Continued)

# LIST OF TABLES

# 1. INTRODUCTION

For several decades boron has been proposed as an advanced fuel for use in combustion and propulsion systems because of its high energy density. Considering heats of combustion, the gravimetric heating value of boron is approximately 35% greater than JP4, a widely used conventional liquid hydrocarbon fuel, and approximately 80% greater than metallic aluminum, another advanced fuel candidate currently used in solid fueled rockets. On a volumetric basis, boron is even more appealing with a heating value approximately 30% greater than JP4 and 60% greater than aluminum. These potential advantages have sparked a great deal of interest in the enhancement of conventional liquid hydrocarbon combustion via the addition of particular boron in the form of slurry suspensions. To date however, these potential gains have not been fully realized in either research or practical combustors.

Two major unresolved combustion problems are the poor combustion efficiency and the inadequate ignition characteristics of boron particles. The heat of combustion advantage of boron assisted hydrocarbon fuels noted above is based on the assumption of complete combustion (i.e., final products of gaseous $H_2O$, gaseous $CO_2$, and liquid boria, $B_2O_3$); the poor combustion efficiency results from slow kinetically controlled condensation processes to form the liquid phase metal oxide which do not reach the desired equilibria during the short residence times available in most combustion devices. The ignition problem is a result of the overall inhibiting process of oxide scale formation on unburned boron fuel particles and its subsequent inhibition of boron particle surface vaporization during the initial heat-up phase of the particle.

The current understanding of boron combustion consists of, at best, an overall description of the most probable physical and chemical processes; i.e., knowledge of the detailed elementary processes is significantly lacking. It is apparent from previous research in this field, that if

solutions to the current problems preventing practical application of boron are to be found, additional research efforts will be required, particularly at the elementary level.

This report presents the results of an initial AFOSR sponsored program to construct a detailed model for describing the homogeneous boron combustion phase of an overall hydrocarbon assisted boron combustion model. This homogeneous combustion phase model is the first part of an overall program designed to obtain a better fundamental under-standing of the elementary processes of boron combustion and the role these processes play during the entire hydrocarbon assisted boron combustion process.

The modeling program included in this report relies on gradient sensitivity analysis to aid the development and validation of the model and to efficiently interface modeling and experimental programs. Furthermore, the necessary extension of sensitivity analysis techniques to surface chemistry problems will be a significant component of future work. The extension of gradient sensitivity analysis techniques to heterogeneous kinetic processes such as particle ignition and product condensation is not only necessary to successfully treat boron combustion, but will be a major contribution to models of other inherently heterogeneous chemical systems including solid rocket propellant and pulverized coal combustion, upper atmospheric and near space degradation of space vehicle materials, combustion and atmospheric pollutant driven surface corrosion, and chemical deposition and plasma etching processes for advanced electronic and electro-optical materials.

The ultimate goal of any boron combustion model development program is to provide combustion engineers with a predictive tool which will allow the design of advanced combustors capable of efficiently burning liquid hydrocarbon fuels loaded with particulate boron. However, as mentioned above, a very important initial goal is to analyze model results with the help of kinetic sensitivity analysis techniques in order to identify the most important physical processes and chemical reactions which control effective boron combustion. This will allow subsequent experimental and theoretical

studies to focus effort on quantifying only those model parameters, including reaction rate constants and thermochemical parameters, which control effective boron combustion. This process is, of course, an iterative procedure with model predictions and sensitivity analyses becoming more accurate as input data for important physical and chemical parameters are improved.

A crucial set of model parameters for hydrocarbon assisted boron combustion is the gas phase reaction rate constants governing the oxidation of suboxide and suboxyhydride species volatilized during the combustion of solid particulate boron. Chemical equilibrium calculations predict that solid boron burning in the presence of hydrocarbon fuels will evolve substantially to gaseous boron oxyhydride compounds such as HOBO. Since the chemical environment in the boundary layer around each boron particle will almost certainly be oxidizer poor, it is likely that a B/O ratio of less than two will prevail in the vaporized species. Depending on the currently uncertain details of gas/surface thermochemistry and kinetics, it is expected that the volatilization of species such as $BO$, $HBO$, $BOH$, $B_2O$, and $B_2O_2$ as the boron/boron oxide surface layer of the particle is heated by radiative and convective heat transfer and reacts with hydrocarbon combustion intermediates and products including $H$, $OH$, $H_2O$, $CO$, and $CO_2$.

The initial modeling effort, presented in this report, concentrates on the homogeneous gas phase portion of boron combustion for several related reasons. First, an extensive gas phase reaction rate set for boron assisted combustion was developed by Kolb and co-workers under DARPA and AFOSR funding in the late 1970's,[1-2,1-3,1-4] and this reaction set with its estimated rate constant parameters can serve as the basis for initial model development. Second, while a few key reactions in the gas phase boron oxidation scheme have been measured over the past several years, (generally confirming the rate estimates of Kolb and co-workers)[1-1] and several experimental groups have the capability to measure more, it is clear that a kinetic sensitivity analysis study of the system will help specify which of the many unmeasured rate constants should be the focus of dedicated experimental or theoretical efforts. Finally, kinetic sensitivity studies of

1-3

combustion systems have so far been limited to homogeneous, gas phase systems; thus, the gas phase portion of the boron combustion process is most amenable to immediate kinetic sensitivity analysis.

An important secondary task of our initial effort is to map out the theoretical extensions necessary to extend the gradient kinetic sensitivity analysis technique to the heterogeneous problems of boron particle ignition and burnout and boron oxyhydride/boron oxide condensation kinetics necessary for a complete boron combustion model.

Section 2 of this report will present elements of the overall model for boron assisted combustion of hydrocarbon fuels. Section 3 presents the homogenous combustion model developed to date and the results of initial model runs and sensitivity analysis. Section 4 summarizes conclusions and presents recommendations for further work.

## 1.1 References for Section 1

1-1 Faeth, G.M., "Status of Boron Combustion Research," Report of the Boron Combustion Specialists Workshop, Air Force Office of Scientific Research, (October 1984), also partially published under the same title in the Proceedings of the 21st JANNAF Combustion Meeting, Laurel, MD (October 1984).

1-2 Wolfhard, H.G., Draper, J.S., Rieger, T.J., and Kolb, C.E., "Determination of the Infrared Emissions of Rocket Plumes and Their Emitting Species," IDA Paper P-1117, Institute for Defense Analysis (June 1975).

1-3 Gersh, M.E. and Kolb, C.E., "Exhaust Plume Infrared Signatures of Advanced Liquid Propellant Rockets," Minutes of the 10th JANNAF Plume Technology Meeting, Report No. NWC TD6011, Naval Weapons Center, China Lake, CA (March 1978).

1-4 Bernstein, L.S., Gersh, M.E., and Kolb, C.E., "Analysis of CALSPAN High Energy Propellant Data and Full Scale Signature Predictions," Minutes of the 11th JANNAF Plume Technology Meeting, Army Missile Command, Hunstville, AL (May 1979).

1-5 Rabitz, H., "Sensitivity Analysis of Combustion Systems," in The Mathematics of Combustion, J. Buckmaster, Ed., SIAM, Philadelphia (1985).

## 2. COMBUSTION MODEL DEVELOPMENT AND SENSITIVITY ANALYSIS

### 2.1 Model Overview

Particulate boron combustion in conjunction with hydrocarbon combustion is a complex, multiphase process.[2-1] Initial analysis indicates that the process can be viewed as involving at least three stages. These are: 1) boron particle surface oxidation, ignition and volatilization of suboxides and suboxyhydrides; 2) a largely homogeneous, gas phase oxidation of the volatile suboxides and suboxyhydride which pass through the oxidizer poor boundary layers of the particle; and 3) condensation of the gaseous high temperature boron oxyhydride products to liquid boria ($B_2O_3$) as the combustion exhaust temperature and pressure approach ambient values.

A schematic of these combustion stages is shown in Figure 2.1. Each of these is discussed in more detail in subsequent subsections.

| COMBUSTION PHASE | DESCRIPTION | TYPICAL SPECIES | |
|---|---|---|---|
| I | BORON PARTICLE OXIDATION, IGNITION AND VOLATILIZATION | $B(s)$ $B_2O_3(s,l)$ | $O_2(g)$ $CO_2(g)$ $H_2O(g)$ |
| II | HOMOGENEOUS REACTIONS OF BORON SUBOXIDES AND OXYHYDRIDES | $HOBO(g)$ $HBO(g)$ $B_2O_3(g)$ $B_2O_2(g)$ $BO_2(g)$ $BO(g)$ | $H_2O(g)$ $OH(g)$ $O_2(g)$ $O(g)$ $CO_2(g)$ |
| III | CONDENSATION OF BORON OXYHYDRIDES TO $B_2O_3(l)$ | $HOBO$ $(HOBO)_3$ $B_2O_3(g)$ $H_xO_yB_z(l)$ $B_2O_3(l)$ | |

Figure 2.1. Schematic of Boron Particle Combustion Processes

2-1

## 2.2 Particle Ignition and Volatilization

The ignition process involves the heating of an initially cold boron particle covered with an oxide layer. As the particle temperature rises (due initially to the hot external environment from the surrounding hydrocarbon combustion, but eventually to some self-heating), two competing processes occur involving the removal of and the formation of the oxide layer. The oxide layer is removed at the surface through vaporization. At high temperatures, this process can involve chemical transformations, and therefore, the composition of the surrounding gases can significantly alter the rates of oxidelayer removal.[2-2] For example, water vapor has been observed to promote ignition.

Some controversy has recently arisen regarding the mechanism for oxide formation. Early works[2-3] postulated that oxygen dissolves in the oxide layer and diffuses to the boron – boron oxide surface where it reacts to form boron oxide. More recently,[2-4] it has been argued that a more likely mechanism would involved the diffusion of boron to the boron oxide – gas surface where subsequent heterogeneous reaction with oxygen to form the oxide would occur.

Most of the past work on boron particle ignition has involved studies of boron in oxygen or air. However, as noted above, water vapor can have a significant promotional effect on boron ignition kinetics.[2-2] In a boron assisted hydrocarbon combustion process, not only water vapor but a number of other hydrocarbon combustion intermediates and products including $H_2$, CO, OH, H, $CO_2$, and possibly partially oxidized hydrocarbons such as aldehydes will all interact with the surface of the boron particles.

It is probable that it is the chemical reaction of these species, not O and $O_2$ which control particle ignition and vaporization in mixed hydrocarbon/boron combustion systems. Since both thermochemical models,[2-5-2-6] and flame sampling studies[2-7] indicate that boron oxyhydride species such as HOBO are the dominant high temperature boron containing combustion products, it seems possible that a third process dominates boron particle ignition and volatilization kinetics in hydrocarbon combustion

systems. This process would involve the removal of the boron oxide layer itself through surface reaction with hydrogen containing species such as H, OH, $H_2$, and $H_2O$ to form volatile boron oxyhydride species such as HBO, BOH, and HOBO. As the depth of the boron oxide layer is reduced, new surface will be available to reform boron oxides, through interaction with $CO_2$, OH, $H_2O$, and whatever O and $O_2$ penetrate the oxygen poor region around the particle.

Indeed the reactive chemistry of atomic boron as well as electronically analogous atomic aluminum provides a strong hint that oxyhydride species form efficiently and preferentially. These electron deficient atoms each combine with water in bimolecular reactions in both the gas phase[2-8-2-12] and in cold argon matrices[2-13] to form an excited H-M-OH species which efficiently sheds its excess energy through radiative decay.

$$B, Al + H_2O \rightarrow H\text{-}B\text{-}OH^* \text{ or } H\text{-}Al\text{-}OH^* \rightarrow H\text{-}B\text{-}OH \text{ or } H\text{-}Al\text{-}OH + h\nu \quad (2.3.1)$$

Theoretical studies confirm that these remarkable reactions occur with surprisingly small activation energies.[2-14-2-15] It is not difficult to imagine that the high combustion temperatures coupled with the presence of surface to stabilize reactions may well promote very efficient oxyhydride formation.

As surface reactions and heat transfer raise the particle temperature, boron suboxide species such as BO, $B_2O$, and $B_2O_2$ may vaporize along with the boron oxyhydride species.

Thus, it is quite possible that under hydrocarbon combustion conditions the boron oxide layer which strongly inhibits particle ignition and vaporization under clean boron/oxygen system conditions becomes a reactive layer promoting particle vaporization when the particle boundary layer is oxidizer poor.

A better understanding of the thermochemical, solubility, transport, and reaction properties of the layer is required to resolve the actual ignition and vaporization mechanism. Thermodynamically, the oxide formation process is exothermic whereas the removal process for oxides is endothermic. Thus, the criteria for ignition in the "clean" boron/oxygen system is that the oxide vaporization rate exceeds its production rate so that the layer itself is removed. The degree to which hydrocarbon combustion products and intermediates change this picture is an important question.

## 2.3 Combustion Kinetics

Once the oxide layer is removed, the particle burns rapidly with a surrounding flame sheet which is detached from but near the surface. Since the volatility of boron is low, boron burns much like a carbon particle vs. a hydrocarbon liquid droplet.[2-4] Here, gasification of the boron occurs by chemical transformation into more volatile components. Thus, heterogeneous and homogeneous chemistry play a more dominant role in the gasification of boron than for liquid hydrocarbons. For example, liquid hydrocarbon droplets gasify primarily by a simple vaporization process which proceeds in the presence or absence of oxidant. The volatile component formed during boron gasification is believed to be BO, but as noted above there may be significant levels of $HOBO$, $HBO$, $BOH$, $B_2O$, or $B_2O_2$. $CO_2$ is the major product of carbon combustion which diffuses back to the carbon particle surface to react heterogeneously to form more CO. Boron oxides and oxyhydrides may play similar roles in boron combustion. Indeed, there may be a strong similarity between boron and carbon combustion; even the homogeneous gas phase kinetics may have similarities. For example, CO oxidation is controlled by the presence of the hydrogen containing OH radical and boron sub-oxide oxidation will be clearly affected by oxyhydride formation.

Evolution of gas-phase boron compounds in the boundary layer around the burning particle is most likely under kinetic control and must be modeled as a homogeneous kinetic process. This requires estimated or measured rate constants for a large number of individual reactions. Fortunately, previous

DOD interest in boron assisted liquid rocket propellants and their exhaust plumes resulted in considerable activity in this area.[2-16] Section 3 presents an updated and extensive version of this reaction rate constant set, including, of course, the results of available experimental data obtained since 1979.

## 2.4 Product Condensation

Estimates for the high volumetric energy density potential of boron-based fuels are based on heats of combustion for complete oxidation with condensed boron oxide, e.g., $B_2O_3$ (l), as the principal product. Thus, realizing the full theoretical potential depends, in part, on achieving complete energy conversion as combustion product vapors cool during the expansion process. This has been difficult to achieve, however, because chemical recombination reaction rates are typically slow relative to the short residence-times for expansions in typical combustion devices. This significantly reduces combustion efficiency as energy is effectively trapped in the vapor phase. It is currently estimated that as much as 20 - 30 percent of the estimated available energy may be lost by this mechanism. The problem is particularly acute for high altitude operation where reaction rates are even slower due to the reduced pressure in the nozzle exhaust flow.

Equilibrium calculations for boron oxidation in wet flames indicate large concentrations of HOBO in the product vapors. Studies of the boron-oxide surface layers properties also suggest the heterogeneous formation of HOBO during combustion in the presence of $H_2O$. Taking HOBO(g) as the principal vapor phase product, boron oxidation at temperatures near the onset of nucleation (T ~2000 K) may be represented as

$$2B + O_2 + H_2 \rightarrow 2HOBO \text{ (g)} \qquad \Delta H = 1151 \text{ KJ/mol} \qquad (2.4.1)$$

In contrast, complete combustion to condensed boron oxide,

$$2B + 2O_2 + 2 + H_2 \rightarrow B_2O_3(1) + H_2O \qquad \Delta H = 1468 \text{ KJ/mol} \qquad (2.4.2)$$
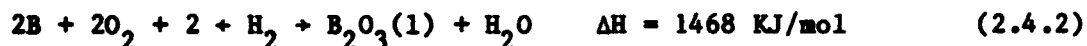
is approximately 20 percent more exothermic. Since, at T = 2000 K, the
constant pressure equilibrium constants for reactions 2.4.1 and 2.4.2 are to a
first approximation equal, failure of HOBO(g) to convert to $B_2O_2$ and
subsequently condense significantly reduces combustion efficiency. Equations
(2.4.1) and (2.4.2) do not represent the reaction mechanisms for boron
oxidation, but only serve to indicate the increased energy available upon
condensation. Obtaining this extra energy, however, is dependent upon
condensation.

The mechanism for formation of $B_2O_3(1)$ remains one of the most poorly
understood components of boron combustion. Edelmann et. al. characterized
it as a nucleation process and developed a model for the finite-rate kinetics
and condensation during nozzle expansions which agreed reasonably well with
experiment.[2-17] In contrast, Miller has argued that the mechanism is more
complex than just a simple nucleation process and actually involves many
intermediates and reactions not considered in Edelmann's model.[2-7] Miller's
arguments are based on studies of the boron combustion products at low
pressures, ca. 0.1 atm, in which mass spectrometry was used to determine the
species present in an oxygen-rich flame under conditions appropriate for
nucleation. These results indicated the presence of a variety of complex
boron oxyhydroxide species in addition to simple monomers, dimers and trimers
of HOBO.[2-7] Since polymerization reactions are typically fast (k ~$10^{-10}$ cm$^3$
molecule sec for dimer and trimer formation), Miller concluded that
elimination of $H_2O$ from the polymer chain was the more likely kinetic
bottleneck to condensation. Moreover, it appeared that $H_2O$ elimination
occurred gradually during nucleation rather than in a single discrete step.

From this data, Miller formulated a hypothetical polymerization mechanism. However, the experimental studies were unable to probe specific reaction pathways, and many reasonable pathways were left out of the model, so that no quantitative predictions that could be compared with experiment were made. It has been suggested that some of the discrepancy between Edelman et. al. and Miller may be attributed to the fact that they had examined the combustion products in very different pressure ranges. However, since neither study provided definite measurements to test reaction mechanisms, both models are subject to a great deal of uncertainty. Since the formation of condensed boron oxide is so important to combustion efficiency, it is imperative to gain a more reliable grasp of the key reactions and parameters which control this process.

## 2.5 References for Section 2

2-1 Faeth, G.M., "Status of Boron Combustion Research," Report of the Boron Combustion Specialists Workshop, Air Force Office of Scientific Research, (October 1984), also partially published under the same title in the Proceedings of the 21st JANNAF Combustion Meeting, Laurel, MD (October 1984).

2-2 Turns, S.R., Holl, J.T., Solomon, A.S.P., and Faeth, G.M., Combust. Sci. and Tech. 43, 287 (1985).

2-3 King, M.K., "Single Particle Boron Ignition Modeling," proceedings of the 19th JANNAF Combustion Meeting, CPIA, Pub. 366, Vol. 11, p. 27 (1982).

2-4 Glassman, I., Williams, F., and Antaki, P., Twentieth Symposium (International) on Combustion, the Combustion Institute, Pittsburgh, PA (1984).

2-5 Wolfhard, H.G., Draper, J.S., Riger, T.J., and Kolb, C.E., "Determination of the Infrared Emissions of Rocket Plumes and Their Emitting Species," IDA Paper P-1117, Institute for Defense Analysis (June 1975).

2-6 Gersh, M.E. and Kolb, C.E., "Exhaust Plume Infrared Signatures of Advanced Liquid Propellant Rockets," Minutes of the 10th JANNAF Plume Technology Meeting, Report No. NWC TD6011, Naval Weapons Center, China Lake, CA (March 1978).

2-7    Miller, W.J., "Boron Combustion Product Chemistry," Report No. TP-349, AeroChem Research Laboratories, Inc., (October 1976).

2-8    Gole, J.L. and Kolb, C.E., "On the Upper Atmospheric Chemiluminescent Emission Observed Upon Release of Aluminum Vapor and Its Compounds," J. Geophys. Res. 86, 9125 (1981).

2-9    Oblath, S.B. and Gole, J.L., "Aluminum Hydration in the Vapor Phase," J. Chem. Phys. 20, 581 (1979).

2-10   Oblath, S.B. and Gold, J.L., "On the Continuum Emissions Observed Upon Oxidation of Aluminum and its Compounds," Combust. Flame 37, 293 (1980).

2-11   DiGiuseppe, T.G., Estes, R., and Davidovits, P., "Boron Atom Reactions and Rate Constants with $H_2O$, $H_2O_2$, Alcohols and Ethers," J. Phys. Chem. 86, 260 (1982).

2-12   Gole, J.L. and Pace, S.A., "Chemiluminescence From the Interaction of Boron Atoms and Water Vapor," J. Phys. Chem. 85, 2651 (1981).

2-13   Hauge, R.H., Kaufman, J.W., Billups, W.E., and Margrave, J.L., "Infrared Matrix-Isolated Studies of the Interactions and Reactions of Group III A Metal Atoms With Water," J. Amer. Chem. Soc. 102, 6005 (1980).

2-14   Kurtz, H.A. and Jordan, K.D., "Comment On the Electronic Structure of HAlOH and $H_2AlO$," J. Amer. Chem. Soc. 102, 1177 (1980).

2-15   Sokal, S. and Jordan, K.D., "Comment On the $B(^2P) + H_2O \rightarrow BO(X\ ^2\Sigma, A\ ^2\pi) + H_2(X\ ^1\Sigma_g)$ Reaction," J. Phys. Chem. 87, 2243 (1983).

2-16   Bernstein, L.S., Gersh, M.E., and Kolb, C.E., "Analysis of CALSPAN High Energy Propellant Data and Full Scale Signature Predictions," Minutes of the 11th JANNAF Plume Technology Meeting, Army Missile Command, Hunstville, AL (May 1979).

2-17   Edelmann, R.B., et al., "Gas Generator Fueled Scramjet Program, Part II: Theoretical and Experimental Investigation of Metal Particle Combustion In a Supersonic Gas Stream," AFAPF-TR-70-84, Part III (1974).

## 3. HOMOGENEOUS BORON COMBUSTION: MODEL DEVELOPMENT AND KINETIC SENSITIVITY ANALYSIS

### 3.1 Overview of Model Development

The model development and concomitant sensitivity analysis program described in the report consisted of the following tasks:

1) The collection and evaluation of currently available thermochemical and kinetic data for chemical species and elementary reactions that may be important to boron combustion (Subsection 3.2).

2) A series of thermodynamic calculations for air oxidation of a mixture of solid boron and a typical hydrocarbon fuel (JP4) to determine equilibrium boron speciation (Subsection 3.3).

3) The development of a homogeneous combustion model consisting of a detailed list of plausible elementary reactions and estimated (or measured values when available) rate constants followed by kinetic calculations to determine species concentrations and temperature profiles under various initial conditions. (Subsection 3.4).

4) The application of kinetic sensitivity analysis to determine the response of system observables to changes in the input parameters, e.g., initial species concentrating, rate parameters, etc.

5) An in depth analysis of the gradient sensitivity data to identify the critical reaction pathways and key uncertainties in currently available thermochemical and kinetic parameters (Subsection 3.6).

6) and lastly, a brief analysis of the research strategies needed to extend the applicability of sensitivity analysis to heterogeneous process.

Each phase of this work is briefly described in the following subsections.

## 3.2 Collection and Evaluation of Relevant Thermochemical and Kinetic Data

During the initial stage of this program, a comprehensive literature search was performed to develop a data base containing the most up-to-date values for the thermochemical and kinetics parameters that would be needed in developing a model for gas phase boron oxidation kinetics. The data base was periodically re-evaluated and updated as new or more reliable results become available. In this section, we summarize the more important results from this survey.

### 3.2.1 Thermochemical Data

Table 3-1 contains the standard enthalpies of formation $\Delta H_{f,298}$ and entropies $S_{298}$ for the atomic and molecular species that are important to boron assisted hydrocarbon combustion systems. (This list intentionally concentrates on species containing boron since the corresponding carbon-containing species are well-known and well-documented.) With one notable exception (BOH), this data has been collected from the most recent publication of the JANAF thermochemical tables.[3-1] The heavier boron oxyhydrides (e.g. $H_3BO_3$, $H_4B_2O_4$, etc.) are probably not critical to a description of the high temperature gas phase boron combustion chemistry. They will be important, however, to future modeling of the condensation phase (Subsection 2.3) and are included in Table 3-1 for completeness.

The HBO species has long been thought to be an important intermediate in boron combustion systems containing hydrogen. It is pertinent, therefore, to consider the possible role of the BOH isomer. At present there is no experimental data available for this species. Ab initio calculations, however, have been performed to characterize the potential energy and minimum energy path for the intramolecular rearrangement BOH $\rightarrow$ HBO.[3-2] These results indicate that the ground configuration for BOH is approximately 40 kcal above the ground configuration for HBO. The potential barrier for rearrangement is approximately 50 kcal. The optimum geometric parameters for the BOH species

**Table 3-1 - $\Delta H_{f,298}$ and $S_{298}$ for Atomic and Molecular Species of Importance to Boron Assisted Hydrocarbon Combustion**

| | $\Delta H_{f,298}$ (kcal/mole) | $S_{298}$ (cal/mole-deg) |
|---|---|---|
| B(s) | 0 | 1.41 ± 0.02 |
| B(l) | [11.841] | [6.432] |
| B | 133.8 ± 3.0 | 36.646 ± 0.00 |
| BO | 0 ± 2.0 | 48.6 ± 0.1 |
| $BO_2$ | -68 ± 2.0 | 54.90 ± 0.05 |
| $B_2$ | 198.3 ± 8.0 | 48.27 ± 0.04 |
| $B_2O$ | 23 ± 25 | [54.67] |
| $B_2O_2$ | -109. ± 2.0 | 57.958 |
| $B_2O_3$(s) | -304.0 ± 0.5 | 12.90 ± 0.1 |
| $B_2O_3$ (l) | -299.56 ± 0.6 | 18.75 ± 0.01 |
| $B_2O_3$ | -199.8 ± 1.0 | 67.8 ± 1 |
| HBO | -47.2 ± 3.0 | 48.4 ± 0.5 |
| BOH | | |
| $HBO_2$(s) | -191.87 ± 0.20 | [11.7 ± 1.0] |
| $HBO_2$ | -134.0 ± 1.0 | [57.273] |
| $H_2BO_2$ | [-114 ± 15] | [58.116] |
| $H_3BO_3$ | -237.16 ± 0.6 | [70.5387] |
| $H_4B_2O_4$ | -307. ± 5.0 | [83.37] |
| $H_3B_3O_3$ | -291. ± 10.0 | [69.7] |
| $H_3B_3O_4$ | -543 ± 3 | [83.041] |

Table 3-1 - $\Delta H_{f,298}$ and $S_{298}$ for Atomic and Molecular Species of Importance to Boron Assisted Hydrocarbon Combustion (Continued)

| | $\Delta H_{f,298}$ (kcal/mole) | $S_{298}$ (cal/mole-deg) |
|---|---|---|
| CO | -26.42 ± 0.04 | 47.21 ± 0.01 |
| CO$_2$ | -94.054 ± 0.011 | 51.07 ± 0.03 |
| H$_2$O(l) | -68.315 ± 0.01 | 16.718 ± 0.019 |
| H$_2$O | -57.795 ± 0.01 | 45.106 ± 0.01 |
| O$_2$ | 0 | 49.005 ± 0.008 |
| H$_2$ | 0 | 31.207 ± 0.008 |
| O | 39.554 ± 0.024 | 38.468 ± 0.005 |
| H | 52.103 ± 0.001 | 27.392 ± 0.004 |
| OH | 9.318 ± 0.29 | 43.890 ± 0.01 |

(in atomic units) are $R_{B-O} = 2.46$, $R_{O-H} = 1.79$ and the BOH angle is 125°. From this data $\Delta H_{f,293}$ and $S_{298}$ for BOH have been estimated to be Kcal/mole and cal/mole deg respectively.

From Table 3-1, it is immediately apparent that the uncertainties in the thermodynamic parameters for the B/O/H combustion system are several orders of magnitude larger than for the same parameters associated with molecular species important to conventional hydrocarbon combustion. For example, the uncertainties in the standard enthalpies and entropies for CO and $CO_2$ range from one to two orders of magnitude smaller than the corresponding uncertainties their isoelectronic boron analogs HBO and $HBO_2$.

The heats of formation in Table 3-1 have been used to establish bond energies for several relevant B-H, B-O, and B-B bonds. These are summarized in Table 3-2.

Table 3-2 - Bond Energies for Boron Assisted Hydrocarbon Combustion

| Bond | $D_o$ (kcal/mole) | $D_o$ (eV) |
|------|-------------------|------------|
| B - O | 192.8 ± 3.5 | 8.37 |
| HOB - O | 145.8 ± 2.0 | 6.33 |
| H - OBO | 117.0 ± 3.0 | 5.08 |
| OBOB - O | 149.8 ± 27.0 | 6.50 |
| OBO - BO | 131.0 ± 5.0 | 5.68 |
| OB - O | 127.0 ± 4.5 | 5.51 |
| H - BO | 98.7 ± 5.5 | 4.28 |
| OBB - O | 191.0 ± 27.0 | 8.29 |
| OB - BO | 109.0 ± 6.0 | 4.73 |
| H - H | 103 ± 0.5 | 4.47 |
| O - O | 118 ± 0.1 | 5.12 |
| O - H | 101 ± 0.3 | 4.38 |
| HO - H | 118 ± 0.1 | 5.12 |
| C - O | 256 ± 0.04 | 11.11 |
| OC - O | 127.6 ± 0.06 | 5.54 |

### 3.2.2 Experimental Kinetic Data

Reliable data for kinetic parameters associated with the B/O/H combustion
system is even more lacking than for the thermodynamic parameters. One
important exception is the recent work by Baughcum and Oldenborg[3-3] at Los
Alamos National Laboratory on the reactions of B and BO with molecular
oxygen.

$$B + O_2 \rightarrow BO + O \qquad k_f = 1.19 \ (\pm 0.004) \times 10^{-10} \ e^{-(158 \pm 13)/T} \ cm^3/sec$$

$$BO + O_2 \rightarrow BO_2 + O \qquad k_f = 1.7 \ (\pm 0.4) \times 10^{-11} (T/1000) \ 2.23 \pm 0.5$$
$$e^{-(716 \pm 288)/T} \ cm^3/sec$$
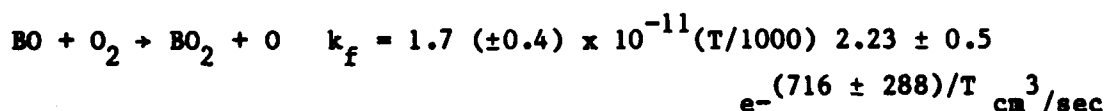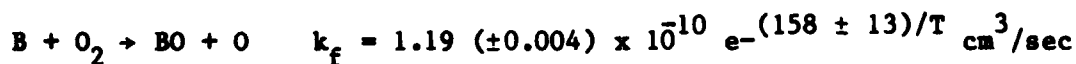
This work extends the earlier room temperature work on $B + O_2$ by DiGiusspe and
Davidovits[3-4] and $BO + O_2$ by Llewellyn, Fontijn and Clyne.[3-5] We have also
drawn on the experimental work of DiGiusseppe et. al.,[3-4 - 3-6] for the
reaction of B with $CO_2$ and B with $H_2O$.

### 3.3 Combustion Thermochemistry

Equilibrium calculations were performed to establish initial estimates of
the boron speciation in the boundary layer surrounding each boron particle.
The results of these calculations were used to extend the list of relevant
reaction (Subsection 3.4.1) and as guides in choosing initial species
concentrations for the subsequent kinetic calculations (Subsection 3.4.3).

The equilibrium calculations were performed using the PACKAGE code
(Plasma Analysis, Chemical Kinetics, and Generator Efficiency) developed at
ARI to predict multiphase combustion product parameters including mixture
composition and thermodynamic properties. Originally based on the NASA CED
code, the present PACKAGE program has been extended to include a multiple
ideal solution model, a phase rule check when condensed phases are present,
and improved methods for dealing with numerical difficulties.

The equilibrium calculations were performed for oxidation of a JP4/solid boron mixture (fuel) in air (oxidizer). Initial concentrations of the fuel reactants (moles of fuel reactant/total moles of fuel) and of the components of the oxidizing medium (moles of oxidizer species/total moles of oxidizer) are given in Table 3-3 and were the same for each calculation. The actual reactant concentrations in the fuel-oxidizer mixture were varied by adjusting the fuel/oxidizer (F/O) equivalence ratio. Calculations were performed for F/O equivalence ratios ranging from 0.3 (oxidizer rich) to 4.5 (fuel rich). However, since the chemical environment in the boundary layer is almost certainly fuel rich, the calculations for F/O > 2.0 are probably more representative of the boron species concentrations near a boron particle.

Table 3-3 - Initial Fuel and Oxidizer Species Concentrations for Equilibrium Calculations

|  | Species | Mole Fraction |
|---|---|---|
| Fuel: | JP4 | 0.1 |
|  | B(s) | 0.9 |
|  |  |  |
| Oxidizer: | $N_2$ | 0.78 |
|  | $O_2$ | 0.21 |
|  | Ar | 0.0095 |
|  | $CO_2$ | 0.0005 |

Figures 3.1a and 3.1b show constant pressure equilibrium species concentrations as a function of temperature for F/O equivalence ratios of 0.3 and 4.5, respectively. The pressure was 1.0 atm and the temperature was varied from 1400 K to 2400 K. Similar results for pressures of 3.0 atm and 6.0 atm did not indicate any substantial change in the thermodynamically predicted boron speciation.
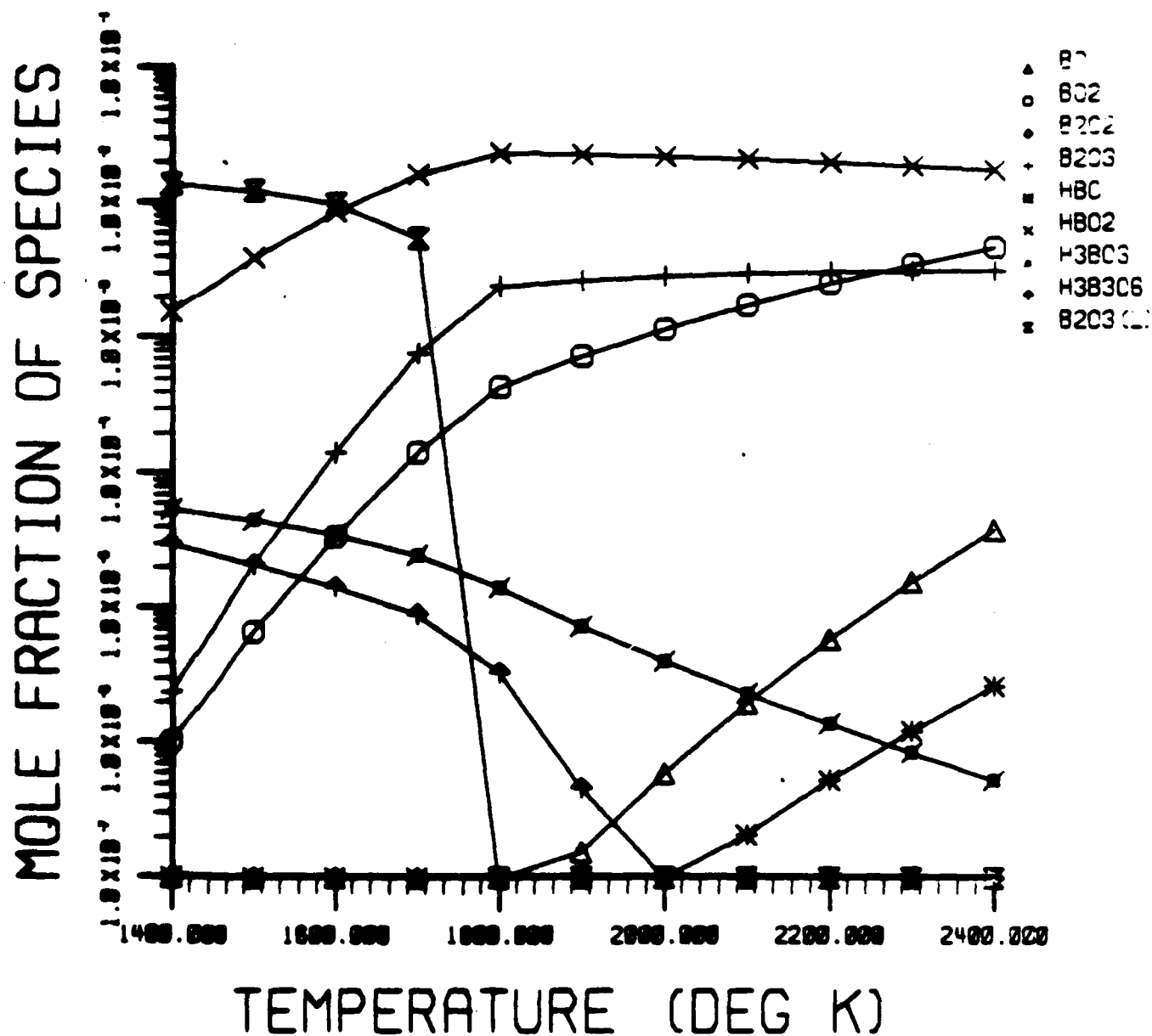
Figure 3.1a. Equilibrium Concentration Versus Temperature for Boron
Speciation in the Boundary Layer of a Hot Boron Particle
in Hydrocarbon Combustion Gases. (P = 1.0 atm; F/O
Equivalence Ratio = 0.3)
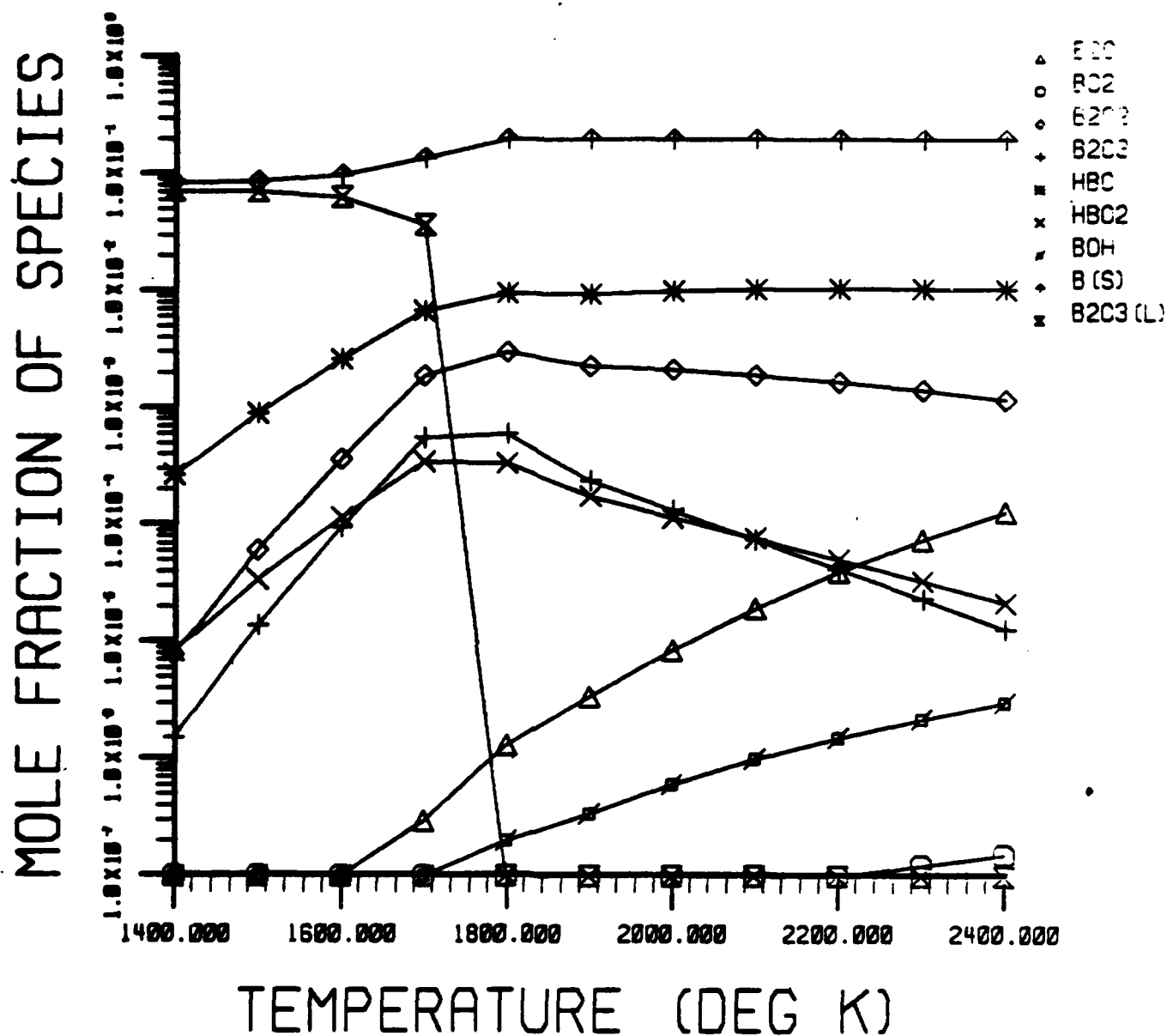
**Figure 3.1b. Equilibrium Concentration Versus Temperature for Boron Speciation in the Boundary Layer of a Hot Boron Particle in Hydrocarbon Combustion Gases. (P = 1.0 atm; F/O Equivalence Ratio = 4.5 atm)**

For F/O = 0.3, Figure 3.1a, the system is oxidizer rich and the initial solid boron phase, excluding the liquid boria component [$B_2O_3(l)$] below 1800 K, is completely oxidized to gas phase oxides and oxyhydrides. The dominant gas phase species are HOBO, $B_2O_3$, and $BO_2$ for T > 1600 K. The concentrations for the heavier oxyhydrides $H_3BO_3$ and $H_3B_3O_6$, although comparable to the concentrations of $B_2O_3$ and $BO_2$ for T < 1600 K, are more than 3 orders of magnitude smaller then the concentration of HOBO for T = 1800 K. Thus, although these species will be important in modeling the condensation stage of boron combustion, they are not going to be important to the gas phase kinetics considered in this report. Beginning at about 2200 K, entropy terms begin to become important and there is a gradual increase in the concentrations of smaller species, BO and HBO, with increasing temperature. However, they remain minor species over the temperature range considered with concentrations at least 3 orders of magnitude smaller then the the dominant species HOBO.

The equilibrium boron species distribution changes markedly with as the F/O equivalence ratio increases. Figure 3.1b shows the species concentrations for an equivalence ratio of 4.5. These results are typical for fuel rich systems (F/O > 2.0). In this case, a solid boron phase persists throughout the temperature range considered. In contrast to oxidizer rich systems, the primary equilibrium gas phase species for fuel rich systems are HBO and $B_2O_2$. Gaseous $B_2O_3$ and HOBO are comparatively minor species with concentrations approximately 2 orders of magnitude smaller.

Table 3-4 summarizes the dominant equilibrium boron speciation in the boundary layer surrounding a hot boron particle. These results show an interesting correlation with conventional hydrocarbon combustion. Specifically, the dominant combustion products for boron combustion, $HBO_2$ (oxidizer rich) and HBO (fuel rich), are isoelectronic with the primary hydrocarbon oxidation products $CO_2$ (complete combustion) and CO (incomplete combustion), respectively. Similarly, the secondary equilibrium constituents show expected trends in the B/O mole ratio as the F/O equivalence ratio

Table 3-4 - Dominant Equilibrium Gas Phase Boron Speciation at T=1800 K

| F/O Equivalence Ratio: | 0.3 | | 4.5 | |
|---|---|---|---|---|
| | Species | Mole Fraction | Species | Mole Fraction |
| | HOBO | $10^{-2}$ | HBO | $10^{-2}$ |
| | $B_2O_3$ | $10^{-3}$ | $B_2O_2$ | $10^{-3}$ |
| | $BO_2$ | $10^{-4}$ | $B_2O_3$ | $10^{-4}$ |
| | | | HOBO | $10^{-4}$ |

increases. Thus, for oxidizer rich systems, the $B_2O_3$ species has a B/O mole
ratio of 2/3, whereas for fuel rich systems, the second major constituent $B_2O_2$
has a B/O mole ratio of 1.

## 3.4  Homogeneous Combustion Kinetics

### 3.4.1  Elementary Reactions and Rate Parameters

There is currently not enough known about the initial ignition and
volatilization phase of boron assisted combustion to accurately characterize
the boron species distributions dominating the homogeneous kinetics. Kinetic
and transport effects may significantly alter the predicted species
concentrations based on an assumption of local equilibrium. The equilibrium
results do serve as guides, however, which help identify the species and
elementary reactions which should be included in a homogeneous boron
combustion model. Thus, from the list of boron species in Table 3-1, the
small subset given in Table 3-5 has been selected for initial study. The
principal species not included are the heavier boron oxyhydrides ($H_xBO_y$
with x,y > 2) which appear to only be important for temperatures below 1600 K
and those species ($B_2O$ and BOH) which because of their large positive
enthalpies of formation tend to be important only in extremely high
temperature regimes, i.e. T > 2400 K.

Table 3-5 - Boron Species List for Homogeneous Combustion Models

| | | |
|---|---|---|
| B | $B_2O_3$ | |
| BO | HBO | |
| $BO_2$ | HOBO | |
| $B_2O_2$ | | |

Based on the thermodynamically predicted boron speciation in the boundary layer a list of elementary reactions for boron assisted hydrocarbon combustion was developed. This reaction list, which is summarized in Table 3-6, includes most of the thermodynamically allowed reactions between boron containing species and hydrocarbon intermediates. Reactions which were spin forbidden, sterically improbable, or not thought to be fundamental were not included in Table 3-6.

Developing an accurate model for the homogeneous boron oxidation kinetics requires a knowledge of the rate parameters for a large number of elementary reactions. Unfortunately, with but a few important exceptions, detailed experimental and/or theoretical studies are notably lacking for the reactions listed in Table 3.4. This has forced this initial modeling effort to rely on estimated rate constants.

Rate constants for the bimolecular rate constants were estimated using transition state theory (TST) and/or by scaling the rate constants for similar reactions. Both approaches are subject to large uncertainties. For TST, general questions concerning the validity of a statistical theory are relatively minor for the present application; rather, the primary source of uncertainty stems from not knowing the relevant transition state configurations and activation energies. Rate constants based on scaling the rate parameters for similar reactions do not necessarily fare much better since the specific scaling relationship used may also require either structural and dynamical information which is unknown, or be forced to rely on unsupported assumptions. Because of these inherent uncertainties, the principal aim has been to establish rate constants which are at least physically reasonable and, to a certain extent, collectively self-consistent.

For the sets of reactions

$$A + HBO \rightarrow AH + BO \qquad A=(H, O, and OH) \qquad (3.1)$$

and

$$A + HBO \rightarrow H + ABO \qquad A = (O, OH, and BO) \qquad (3.2)$$
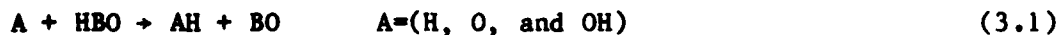
## Table 3-6 - Reactions and Rate Constants for Boron Assisted Hydrocarbon Combustion

| Reaction | $\Delta H^{\circ}$(eV) | $k_f$(cm$^3$/sec or cm$^6$/sec) |
|---|---|---|
| B + O$_2$→BO + O | -3.16 | $1.19(\pm0.004)\times10^{-10}\, e^{-(158\pm13)/T}$ |
| BO + O$_2$→BO$_2$ + O | -0.34 | $1.7(\pm0.4)\times10^{-11}(T/1000)^{2.23\pm0.5}\, e^{-(716\pm288)/T}$ |
| BO$_2$ + H$_2$→HBO$_2$ + H | -0.60 | $3\times10^{-12}\, e^{-1500/T}$ |
| B + OH→BO + H | -3.90 | $1\times10^{-10}$ |
| BO + OH→BO$_2$ + H | -1.08 | $4\times10^{-12}$ |
| BO$_2$ + OH→HBO$_2$ + O | -0.69 | $3\times10^{-12}\, e^{-500/T}$ |
| BO$_2$ + BO$_2$→B$_2$O$_3$ + O | -0.18 | $1\times10^{-13}\, e^{-5000/T}$ |
| B + H$_2$O→HBO + H | -2.29 | $4\times10^{-10}\, e^{-1350/T}$ |
| BO + H$_2$O→HBO$_2$ + H | -1.0 | $1\times10^{-13}\, e^{-5000/T}$ |
| HBO$_2$ + OH→BO$_2$ + H$_2$O | -0.05 | $2\times10^{-12}\, e^{-1000/T}$ |
| B$_2$O$_3$ + H$_2$O→2HBO$_2$ | -0.42 | $1\times10^{-15}\, e^{-6000/T}$ |
| B + BO$_2$→2BO | -2.28 | $6\times10^{-11}$ |

Table 3-6 -- Reactions and Rate Constants for Boron Assisted Hydrocarbon Combustion - Continued

| Reaction | $\Delta H^o$(eV) | $k_f$(cm$^3$/sec or cm$^6$/sec) |
|---|---|---|
| $B + CO_2 \rightarrow BO + CO$ | -2.82 | $7.0\ (\pm\ 2.8) \times 10^{-14} e^{1000/T}$ |
| $BO + O + M \rightarrow BO_2 + M$ | -5.46 | $3 \times 10^{-33} e^{+1000/T}$ |
| $BO_2 + H + M \rightarrow HBO_2 + M$ | -5.07 | $5 \times 10^{-33} e^{+1000/T}$ |
| $BO + OH + M \rightarrow HBO_2 + M$ | -6.16 | $1 \times 10^{-33} e^{+1000/T}$ |
| $BO + BO_2 + M \rightarrow B_2O_3 + M$ | -5.64 | $2 \times 10^{-34} e^{+1000/T}$ |
| $BO_2 + CO \rightarrow CO_2 + BO$ | 0.0 | $5 \times 10^{-11} e^{-1000/T}$ |
| $BO + H + M \rightarrow HBO + M$ | -4.28 | $3 \times 10^{-33} e^{+1000/T}$ |
| $HBO + H \rightarrow BO + H_2$ | -0.20 | $2 \times 10^{-11}$ |
| $HBO + O \rightarrow BO + OH$ | -0.01 | $8 \times 10^{-11}$ |
| $HBO + O \rightarrow BO_2 + H$ | -1.23 | $8 \times 10^{-12}$ |
| $HBO + OH \rightarrow BO + H_2O$ | -0.84 | $8 \times 10^{-11}$ |
| $HBO + OH \rightarrow HOBO + H$ | -1.94 | $8 \times 10^{-12}$ |

Table 3-6 - Reactions and Rate Constants for Boron Assisted Hydrocarbon Combustion - Continued

| Reaction | $\Delta H^o$(eV) | $k_f$(cm$^3$/sec or cm$^6$/sec) |
|---|---|---|
| $HBO + OH \rightarrow BO_2 + H_2$ | -1.31 | $10^{-20}e^{-35200/T}$ |
| $HBO + O_2 \rightarrow BO_2 + OH$ | -0.49 | $10^{-20}e^{-35200/T}$ |
| $HBO + O + M \rightarrow HOBO + M$ | -6.43 | $10^{-27}xT^{-0.5}e^{-25200/T}$ |
| $HBO + BO \rightarrow B_2O_2 + H$ | -10.3 | $1 \times 10^{-12}$ |
| $2BO + M \rightarrow B_2O_2 + M$ | -4.73 | $1 \times 10^{-34}e^{+1000/T}$ |
| $B_2O_2 + O \rightarrow BO + BO_2$ | -0.78 | $6 \times 10^{-11}$ |
| $B_2O_2 + O_2 \rightarrow 2BO_2$ | -1.17 | $1 \times 10^{-15}e^{-40300/T}$ |
| $B_2O_2 + OH \rightarrow BO + HOBO$ | -1.49 | $6 \times 10^{-11}$ |
| $B_2O_2 + OH \rightarrow BO_2 + HBO$ | -0.68 | $1 \times 10^{-15}e^{-35200/T}$ |

the rate constants were first estimated using TST by assuming a linear transition state. The rate constants for the reactions (3.2) were subsequently decreased by about an order of magnitude to offset the effect of assuming a linear complex. Rate constants for reactions (3.1) were also calculated by scaling the corresponding reactions for the isoelectronic HCN using the ratio of classical partition functions for the reactants. These values were typically larger than the rate constants calculated using TST. Since TST tends to yield rate constants which are slower than experimentally observed, the TST rate constants for both sets of reactions were increased slightly to give the final values in Table 3.4.

Rate constants for the reactions

$$B_2O_2 + O \rightarrow BO + BO_2$$

and

$$B_2O_2 + OH \rightarrow BO + HOBO$$
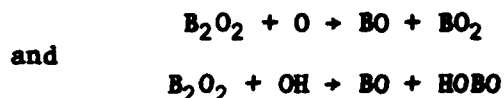
were more difficult to estimate because of they involve 5 and 6 atom transition states. Initial estimates were obtained by simply doubling the rate constants for the corresponding HBO reactions (3.2) due to the symmetry of the $B_2O_2$ species giving $k_f = 1.6 \times 10^{-11}$. This value was then scaled by the reactant partition function ratio for the HBO and $B_2O_2$ reaction giving the value in Table 3-4, $k_f = 6 \times 10^{-11}$. The reactions

$$HBO + OH \rightarrow BO_2 + H_2 \quad k_f = 10^{-20} x e^{-35200/T}$$

$$HBO + O_2 \rightarrow BO_2 + OH \quad k_f = 10^{-20} x e^{-35200/T}$$

$$B_2O_2 + OH \rightarrow BO_2 + HBO \quad k_f = 10^{-15} x e^{-35200/T}$$

$$B_2O_2 + O_2 \rightarrow BO_2 + BO_2 \quad k_f = 10^{-15} x e^{-35200/T}$$
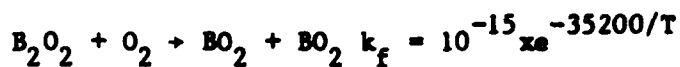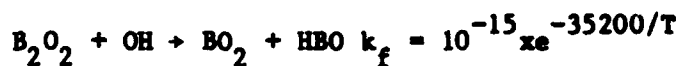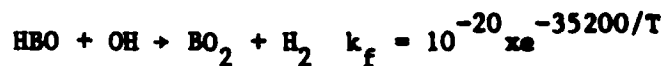
probably involve 4-center reaction complexes and, consequently, were estimated to proceed very slowly.

## 3.4.2  System Equations

Two types of systems have been investigated; an adiabatic, constant pressure system and an isothermal constant volume system. The adiabatic constant pressure system is described by the set of equations,

$$\frac{dY_i}{dt} = \frac{\dot{\omega}_i W_i}{\rho} \quad (i = 1, \ldots, N) \tag{3.4.1}$$

$$\frac{dT}{dt} = - \frac{1}{\rho \bar{C}_p} \sum_{i=1}^{N} h_i \dot{\omega}_i W_i \tag{3.4.2}$$

where $Y_i$ is the mass fraction of the i-th chemical species, $T$ is the temperature, $\rho$ is the mixture mass density, $\bar{C}_p$ is the mass weighted mean specific heat at constant pressure, $h_i$ is the specific enthalpy of the i-th chemical species, $\dot{\omega}_i$ is the molar production rate of the i-th chemical species, $W_i$ is the molecular weight of the i-th chemical species, and $t$ is time. The mass density is defined via the perfect gas law

$$\rho = \frac{P \bar{W}}{R^0 T} \tag{3.4.3}$$

where $P$ is the system pressure, $R^0$ is the universal gas constant and $\bar{W}$ is the mixture molecular weight, i.e.,

$$\bar{W} = \frac{1}{\sum_{i=1}^{N} \frac{Y_i}{W_i}} \tag{3.4.4}$$

the molar net rate of production of species i is given by,

$$\dot{\omega}_i = \sum_{k=1}^{N} (v''_{i,k} - v'_{i,k}) \dot{\omega}'_k \quad (i=1, \ldots, N) \tag{3.4.5}$$

these

$$\omega_k^{'} = k_{f,k} \prod_{i=1}^{N} C_i^{v_{i,k}^{'}} - k_{b,k} \prod_{i=1}^{N} C_i^{v_{i,k}^{''}} \quad (k=1, \ldots M) \qquad (3.4.6)$$

where $k_{f,k}$ and $k_{b,k}$ are the specific reaction rate constants for the forward and backward reactions, respectively and where $v_{i,k}^{'}$ and $v_{i,k}^{''}$ are the stoichiometric coefficients for species i appearing as reactant and as product, respectively, in the arbitrary chemical reaction

$$\sum_{i=1}^{N} v_{i,k}^{'} M_i \rightarrow \sum_{i=1}^{N} v_{i,k}^{''} M_i \quad (k=1, \ldots, M) \qquad (3.4.7)$$

with $M_i$ denoting the chemical symbol for species i.

The mass weighted mean specific heat at constant pressure is

$$\bar{C}_p = \sum_{i=1}^{N} C_{p_i} Y_i \qquad (3.4.8)$$

The mass weighted specific heats at constant pressure and the mass weighted enthalpies for each species are given by,

$$C_{p_i} = \frac{C_{p_i}}{W_i} \qquad (3.4.9)$$

and

$$h_i = \frac{H_i^o}{W_i} . \qquad (3.4.10)$$

The reference state specific heats at constant pressure, enthalpies, and entropies for each species are obtained from the NASA polynominal fits to the JANAF data.

$$C^o_{P_i} = a_{1i} + a_{2i}T + a_{3i}T^2 + a_{4i}T^3 + a_{5i}T^4 \qquad (3.4.11)$$

$$\frac{H_i^o}{R^oT} = a_{1i} + \frac{a_{2i}}{2}T + \frac{a_{3i}}{3}T^2 + \frac{a_{4i}}{4}T^3 + \frac{a_{5i}}{5}T^4 + \frac{a_{6i}}{T} \qquad (3.4.12)$$

and

$$\frac{S_i^o}{R^o} = a_{1i}\ln(T) + a_{2i}T + \frac{a_{3i}}{2}T^2 + \frac{a_{4i}}{3}T^3 + \frac{a_{5i}}{4}T^4 + a_{7i} \qquad (3.4.13)$$

The elementary reaction rate constant is expressed in modified Arrhenius form,

$$k_{f,k} = P_k A_k T^{n_k} \exp(-E_{a,k}/R^oT) \qquad (3.4.14)$$

where $A_k$ is the pre-exponential factor, $n_k$ the temperature exponent, and $E_{a,k}$ the activation energy. $P_k$ is the constant parameter perturbed in the sensitivity analysis, $P_i$ for each reaction equals unity. The backward rate constant is obtained from the forward reaction rate constant and the reaction equilibrium constant using the relation

$$k_{b,k} = \frac{k_{f,k}}{K_k} , \qquad (3.4.15)$$

The equilibrium constants for the reactions are obtained from

$$K_{c,k} = K_{p,k} \left(\frac{1}{R^0 T}\right)^{\sum_{i=1}^{N}(v''_{i,k} - v'_{i,k})} \qquad (3.4.16)$$

where $K_{p,k}$ is determined from

$$K_{p,k} = \exp\left(\frac{\Delta S_k^0}{R^0} - \frac{\Delta H_k^0}{RT}\right) \qquad (3.4.17)$$

where

$$\frac{\Delta S_k^0}{R^0} = \sum_{i=1}^{N}(v''_{i,k} - v'_{i,k})\frac{S_i^0}{R^0} \qquad (3.4.18)$$

and

$$\frac{\Delta H_k^0}{R^0 T} = \sum_{i=1}^{N}(v''_{i,k} - v'_{i,k})\frac{H_i^0}{R^0 T} \qquad (3.4.19)$$

All termolecular reactions are assumed to be in their low pressure limiting regimes. The third body $M_k$ for each reaction is defined as the sum of the product of all species concentrations times the corresponding chaperon efficiency

$$M_k = \sum_{i=1}^{N} e_{k,i} c_i \qquad (3.4.20)$$

where $e_{k,i}$ is the chaperon efficiency for the i-th species and the k-th reaction and $c_i$ is the concentration of the i-th chemical species.

The governing equations for the isothermal, constant volume system are

$$\frac{dc_i}{dt} = \dot{\omega}_i W_i \quad (i=1,\ldots\ldots,N) \; . \tag{3.4.21}$$

The species concentrations are related to the species mass fractions and mole fractions through the following equations

$$c_i = \frac{P Y_i}{R^0 T \left( \sum\limits_{i=1}^{N} \frac{Y_i}{W_i} \right)} = \frac{P \bar{W} Y_i}{R^0 T} = \rho Y_i \tag{3.4.22}$$

$$X_i = \frac{Y_i}{W_i \left( \sum\limits_{i=1}^{N} \frac{Y_i}{W_i} \right)} \tag{3.4.23}$$

The system equations are solved using LSODE and several modified subroutines from CHEMKIN.

### 3.4.3 <u>Response of Species Concentration and Temperature Profile to System Parameters</u>

General characteristic behavior of high temperature B-C-H-O chemistry was investigated by examining the response of the species concentrations and temperature profiles to various different initial conditions. The initial conditions studied covered a wide range of temperature, pressure, and initial species concentrations. These conditions were chosen to be representative of some of the gas phase environments surrounding metallic boron particle combustion. Several of these systems are illustrated below. The initial conditions for each system are tabulated in Table 3-7.

In the first example (Run 1), the initial conditions were derived from equilibrium calculations for a fuel rich mixture of JP4 and B(s) in air at a a pressure of 1 atm and an equivalence ratio of 4.5. Results from these

Table 3-7 - Initial Conditions for Kinetic Calculations

| RUN | 1 | 2 | 3 | 4 | 5 | 6 | 7 | 8 |
|---|---|---|---|---|---|---|---|---|
| T(k) | 1800 | 1800 | 1800 | 1800 | 1800 | 1800 | 1800 | 1800 |
| P(atm) | 1 | 1 | 1 | 1 | 1 | 1 | 1 | 1 |
| H | 1.04(-4) | 1.31(-4) | 0 | 0 | 0 | 0 | 0 | 0 |
| O | 0 | 0 | 0 | 0 | 0 | 0 | 0 | 0 |
| OH | 0 | 0 | 0 | 0 | 0 | 0 | 0 | 0 |
| $H_2$ | 2.00(-1) | 2.52(-1) | 0.04 | 0.04 | 0 | 0.09 | 0.09 | 0 |
| $O_2$ | 4.35(-2) | 0 | 0.17 | 0.17 | 0.17 | 0.17 | 0.17 | 0.17 |
| $H_2O$ | 1.04(-5) | 1.31(-5) | 0 | 0 | 0.04 | 0 | 0 | 0.09 |
| $HO_2$ | 0 | 0 | 0 | 0 | 0 | 0 | 0 | 0 |
| $H_2O_2$ | 0 | 0 | 0 | 0 | 0 | 0 | 0 | 0 |
| CO | 1.80(-1) | 2.27(-1) | 0.04 | 0.04 | 0 | 0.04 | 0.04 | 0 |
| $CO_2$ | 0 | 0 | 0 | 0 | 0.04 | 0 | 0 | 0.04 |
| HCO | 0 | 0 | 0 | 0 | 0 | 0 | 0 | 0 |
| B | 0 | 0 | 0 | 0 | 0 | 0 | 0 | 0 |
| BO | 0 | 0 | 0 | 0 | 0 | 0.05 | 0.05 | 0.05 |
| $BO_2$ | 0 | 0 | 0 | 0 | 0 | 0 | 0 | 0 |
| $B_2O_2$ | 2.80(-3) | 3.53(-3) | 0 | 0 | 0 | 0 | 0 | 0 |
| $B_2O_3$ | 5.00(-4) | 6.31(-4) | 0 | 0 | 0 | 0 | 0 | 0 |
| HBO | 9.00(-3) | 1.14(-2) | 0.05 | 0.05 | 0.05 | 0 | 0 | 0 |
| $HBO_2$ | 3.00(-4) | 3.78(-4) | 0 | 0 | 0 | 0 | 0 | 0 |
| $N_2$ | 5.14(-1) | 5.05(-1) | 0.70 | 0.70 | 0.70 | 0.65 | 0.65 | 0.65 |
| ADIABATIC | Y | Y | Y | ___ | Y | Y | ___ | Y |
| ISOTHERMAL | ___ | ___ | ___ | Y | ___ | ___ | Y | ___ |

constant pressure, constant temperature calculations over a temperature range of 1400 - 2400 K are shown in Figure 3.1b. The initial conditions for the kinetic calculations were taken at a temperature of 1800 K. Here, all species with mole fractions greater than $1 \times 10^{-5}$ were considered as initial reactants. The solid boron was replaced by an equivalent amount of air (where air is assumed as 21% $O_2$ and 79% $N_2$). The results of species mole fractions and temperature versus time for an adiabatic, constant pressure system are shown in Figure 3.2. Part (a) of the figure presents the boron containing compounds; part (b) presents the species of the $CO/H_2/O_2$ system; and part (c) presents the temperature.
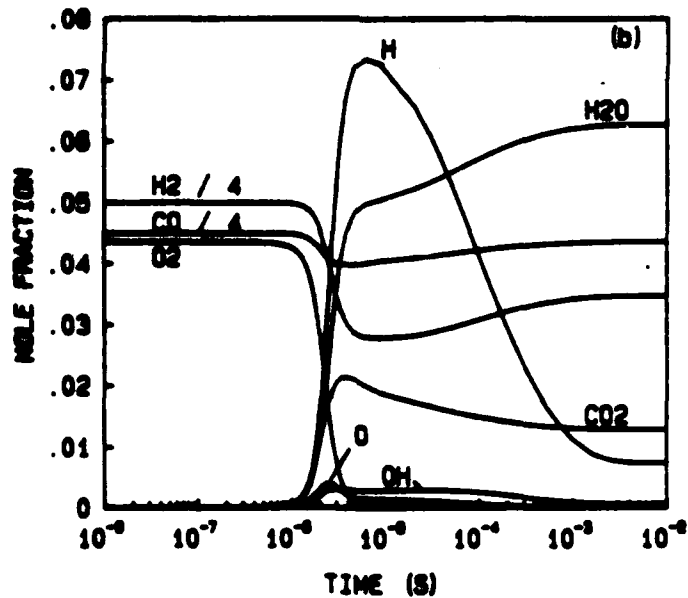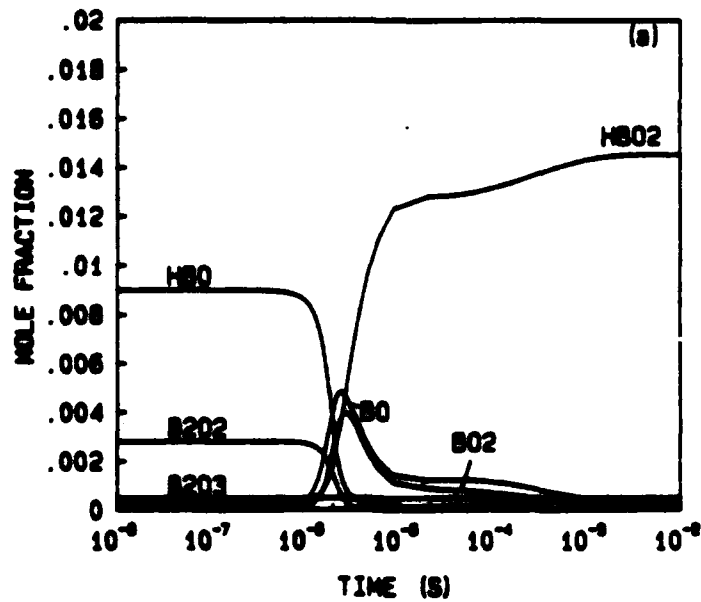
Figure 3.2. Species and Temperature Profiles for an Adiabatic, Constant Pressure, Oxygen Rich System. Initial Reactants Derived From Fuel Rich (F/O = 4.5) Equilibrium Gas Phase Boron Species.
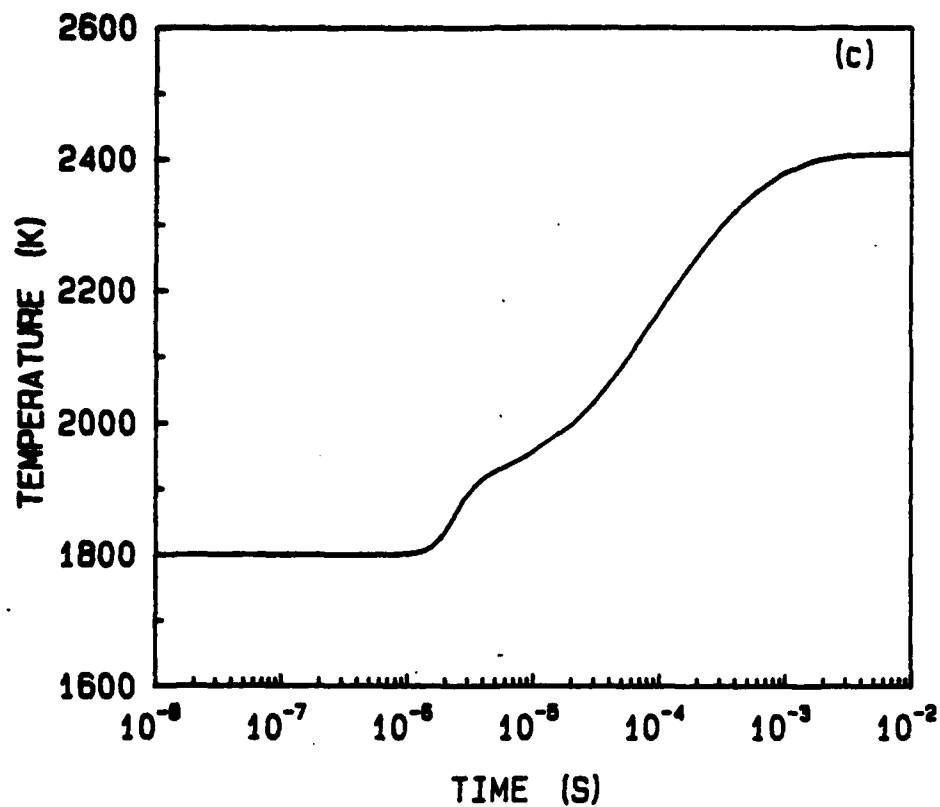
Figure 3.2. (Continued) Species and Temperature Profiles for an Adiabatic, Constant Pressure, Oxygen Rich System. Initial Reactants Derived From Fuel Rich (F/O = 4.5) Equilibrium Gas Phase Boron Species.

Run 2, Figure 3.3, is the same as run 1 except that the metallic boron removed from the system in run 1 was not replaced with any species, and the existing equilibrium mole fractions were normalized to equal 1.0, neglecting solid B.

Runs 3 through 5, Figures 3.4 through 3.6, make a set for comparison. Run 3 is for an initial mixture consisting of HBO, $H_2$, CO, $O_2$ and $N_2$ as reactants. This case represents an extreme assuming all the initial boron (e.g., coming from the solid boron surface) is in the form of HBO. Run 4 is the same as run 3 except the reaction is isothermal, constant pressure. Run 5 is the same as run 3 except the initial $H_2$ is replaced by $H_2O$ and the initial CO is replaced by $CO_2$.

Run 6-8, Figures 3.7 through 3.9, again make a set. Run 6 is for an initial mixture consisting of BO, $H_2$, CO, $O_2$ and $N_2$. This case represents another extreme assuming all the initial boron is in the form of BO. In comparison to run 3, the amount of BO is equal to the amount of HBO. The H originally in HBO (in run 3) is put into $H_2$ in run 6. Run 7 is the same as run 6 except the reaction is isothermal, constant pressure. Run 8 is the same as run 6 except the $H_2$ is replaced by $H_2O$ and CO by $CO_2$.

Run 9, Figure 3.10, shows the results from a constant volume, isothermal system. Relative to run 3, the initial $O_2$ concentration was reduced and the initial temperature was increased. In Figure 3.11, the profiles of boron containing species for 4 related cases are presented. In part (a) of the figure, the initial CO mole fraction was converted to $H_2$ (i.e., the system is carbon free); in part (b), the initial $H_2$ mole fraction was converted to CO; in part (c), the initial $O_2$ mole fraction was reduced from 0.07 to 0.005, by volume; and in part (d), the initial $H_2$ and CO mole fraction were converted to $N_2$.

As a final set of examples (Runs 11 and 12), the series of runs 9 and 10 were repeated, but with the initial HBO replaced by BO + 1/2 $H_2$. The results from this series of runs are reported in Figures 3.12 and 3.13.
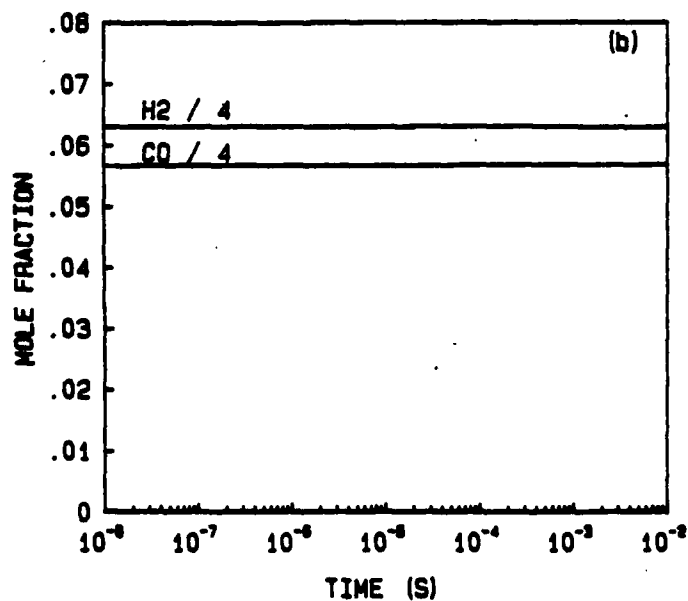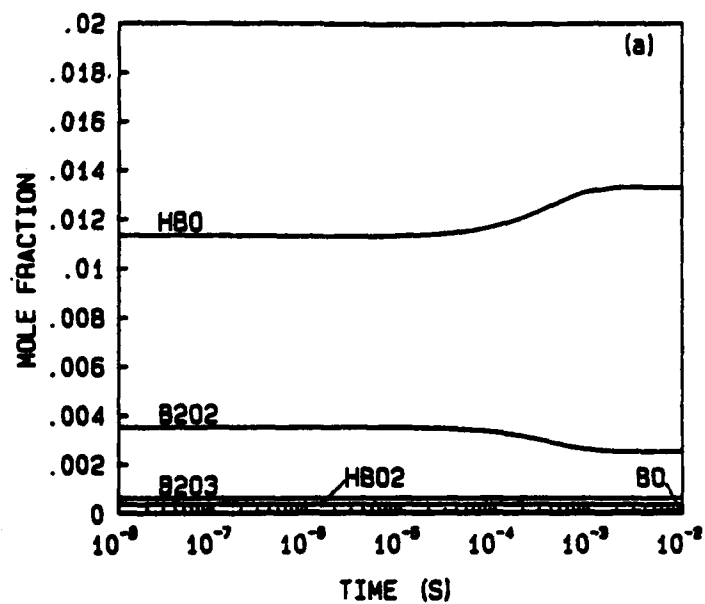
**Figure 3.3.** Species and Temperature Profiles for an Adiabatic, Constant Pressure, Oxygen Poor System. Initial Reactants Derived From Fuel Rich (F/O = 4.5) Equilibrium Gas Phase Boron Species.
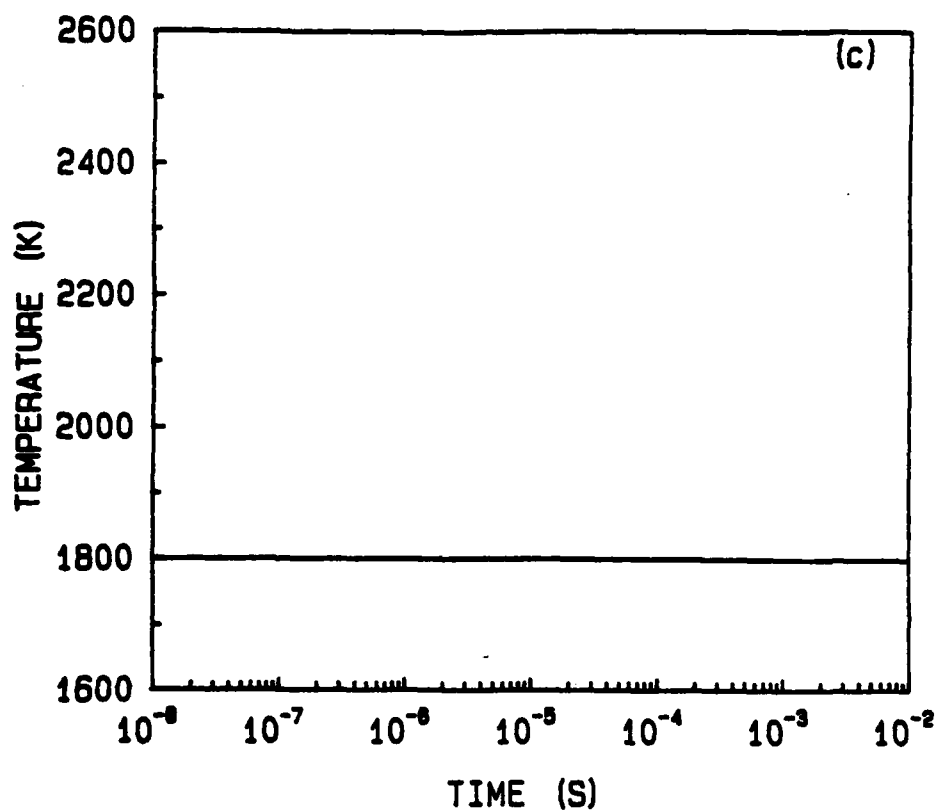
Figure 3.3. (Continued) Species and Temperature Profiles for an Adiabatic,
Constant Pressure, Oxygen Poor System. Initial Reactants
Derived From Fuel Rich (F/O = 4.5) Equilibrium Gas Phase
Boron Species.
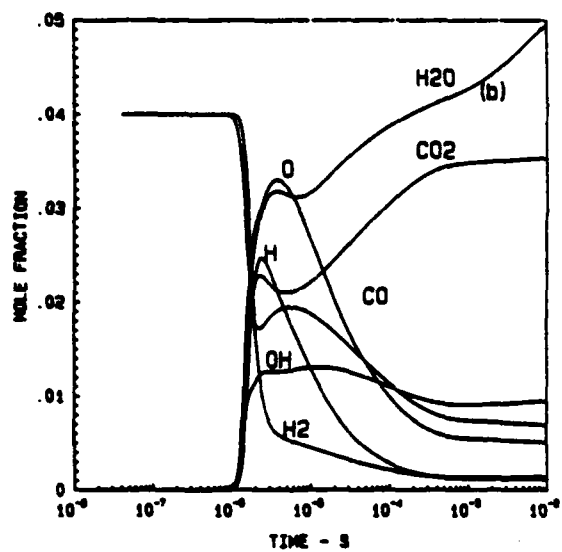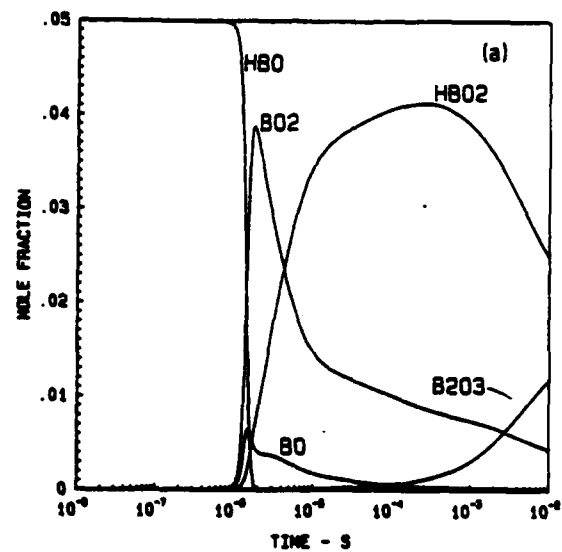
Figure 3.4.  Species and Temperature Profiles for an Adiabatic, Constant Pressure Mixture of HBO, $H_2$, CO, $O_2$ and $N_2$

3-28
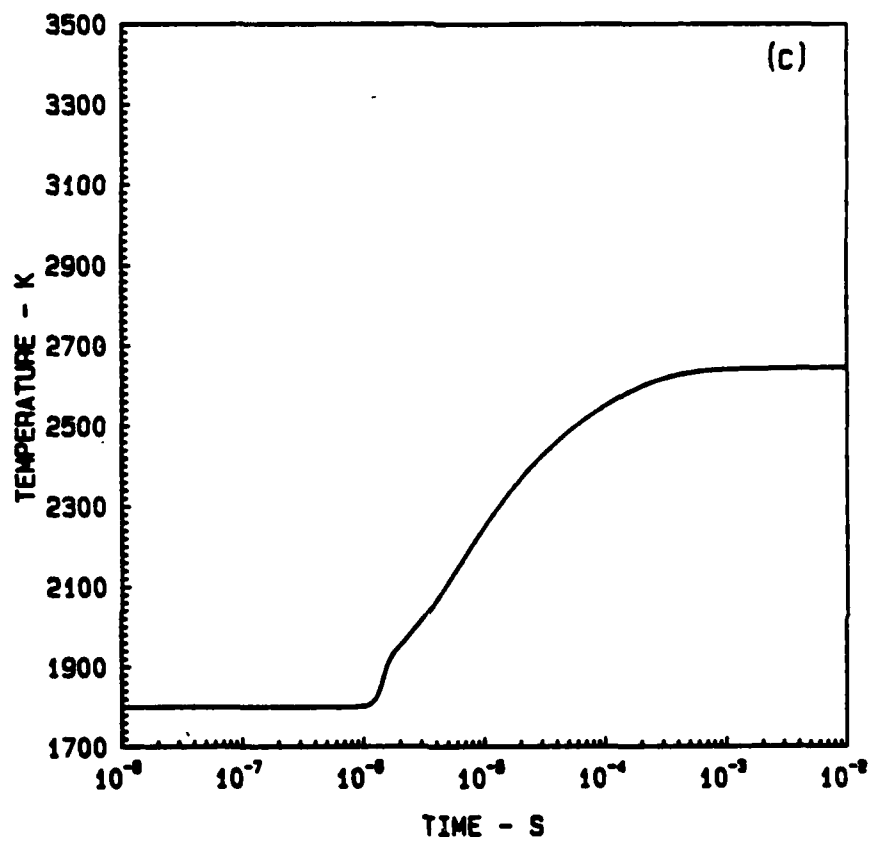
Figure 3.4. (Continued) Species and Temperature Profiles for an Adiabatic, Constant Pressure Mixture of HBO, $H_2$, CO, $O_2$ and $N_2$
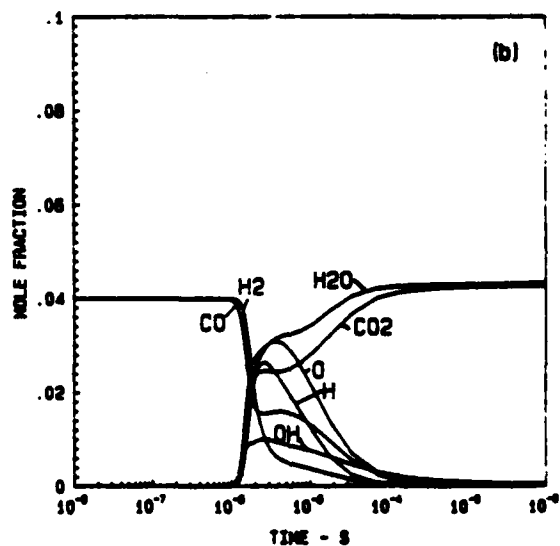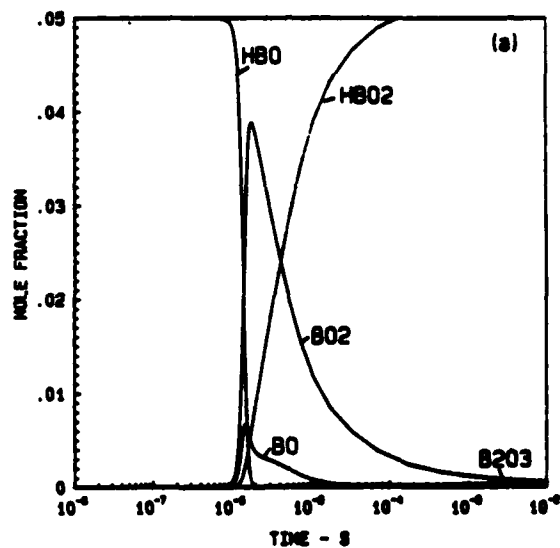
Figure 3.5. Species and Temperature Profiles for an Isothermal, Constant Pressure Mixture of HBO, $H_2$, CO, $O_2$ and $N_2$
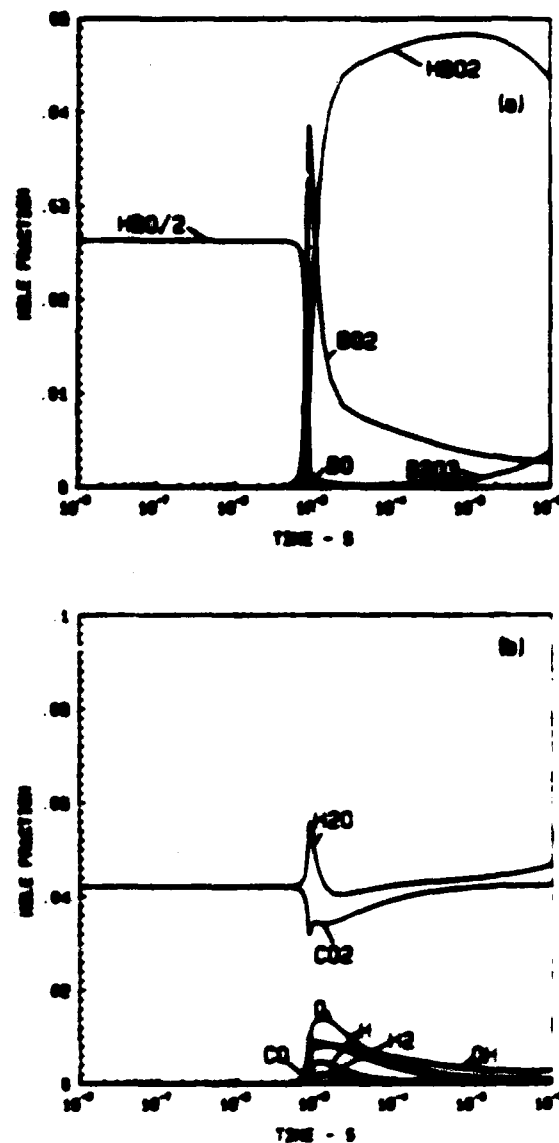
Figure 3.6. Species and Temperature Profiles for an Adiabatic, Constant Pressure Mixture of HBO, $H_2O$, $CO_2$, $O_2$ and $N_2$
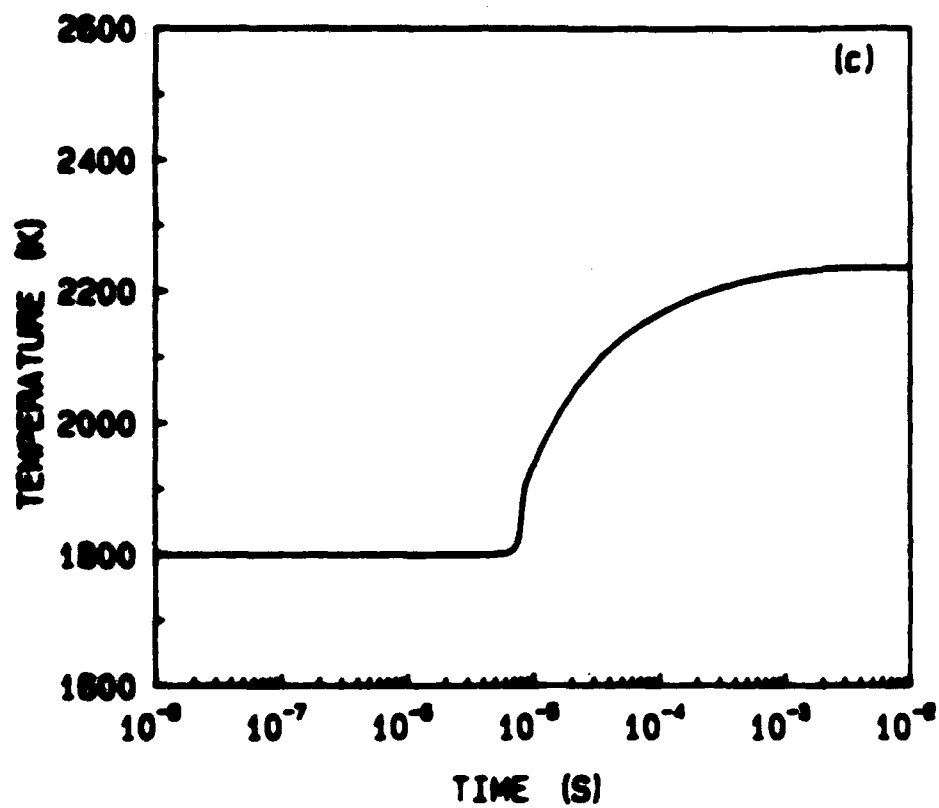
Figure 3.6. (Continued) Species and Temperature Profiles for an Adiabatic, Constant Pressure Mixture of $HBO$, $H_2O$, $CO_2$, $O_2$ and $H_2$
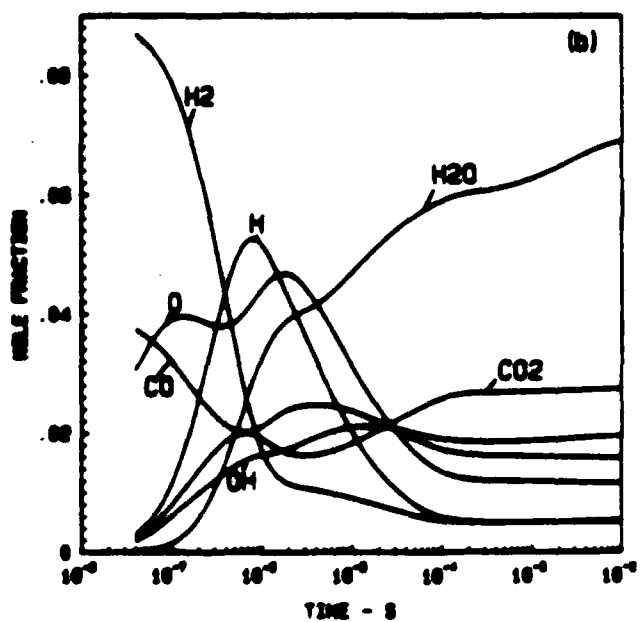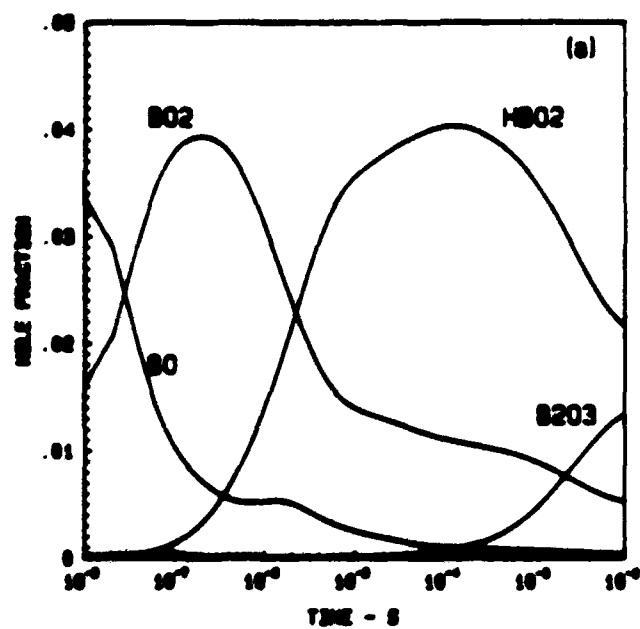
Figure 3.7. Species and Temperature Profiles for an Adiabatic, Constant Pressure Mixture of BO, $H_2$, CO, $O_2$ and $N_2$
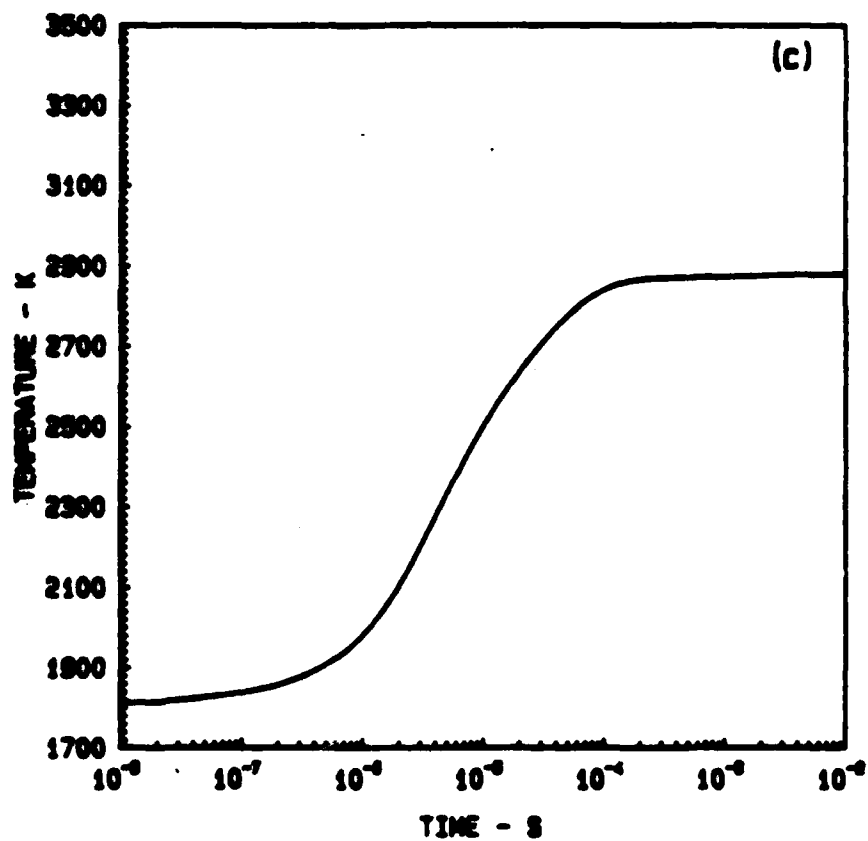
Figure 3.7. (Continued) Species and Temperature Profiles for an Adiabatic, Constant Pressure Mixture of BO, $H_2$, CO, $O_2$ and $N_2$
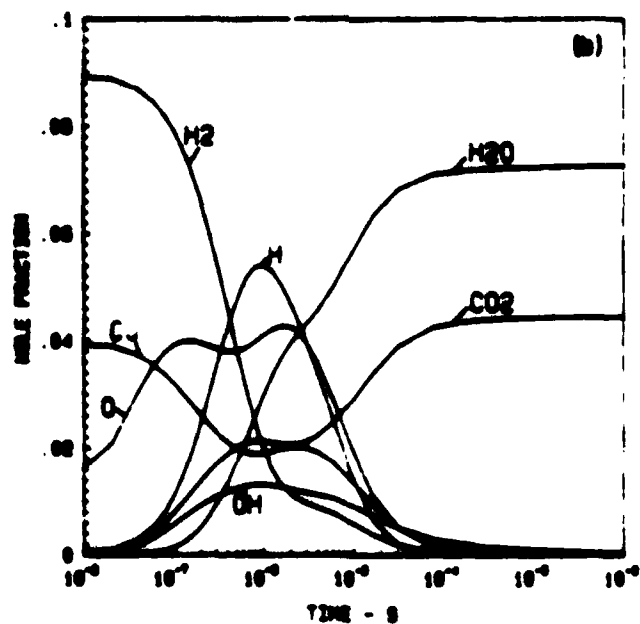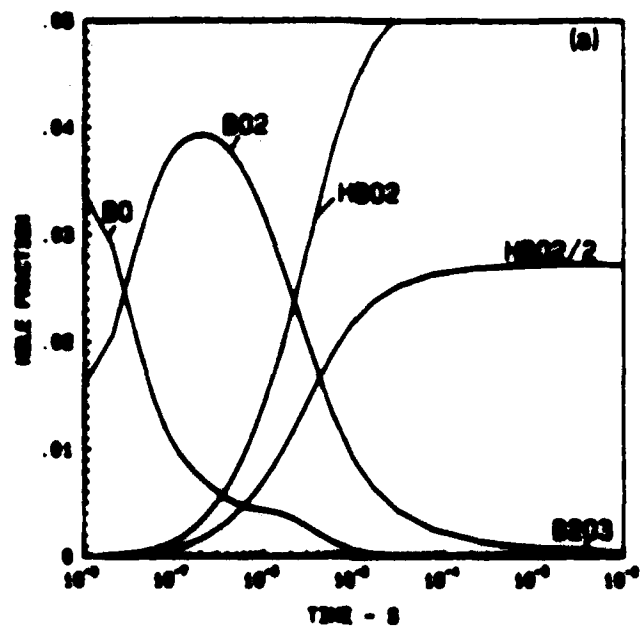
Figure 3.8. Species and Temperature Profiles for an Isothermal, Constant Pressure Mixture of $BO$, $H_2$, $CO$, $O_2$ and $N_2$
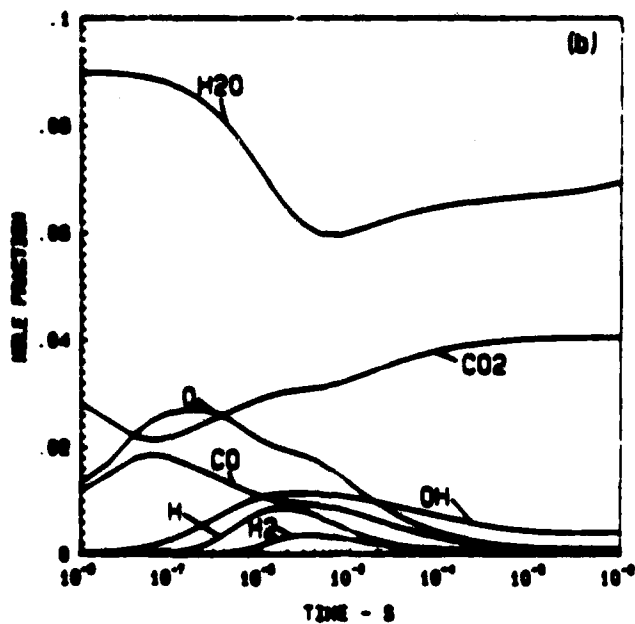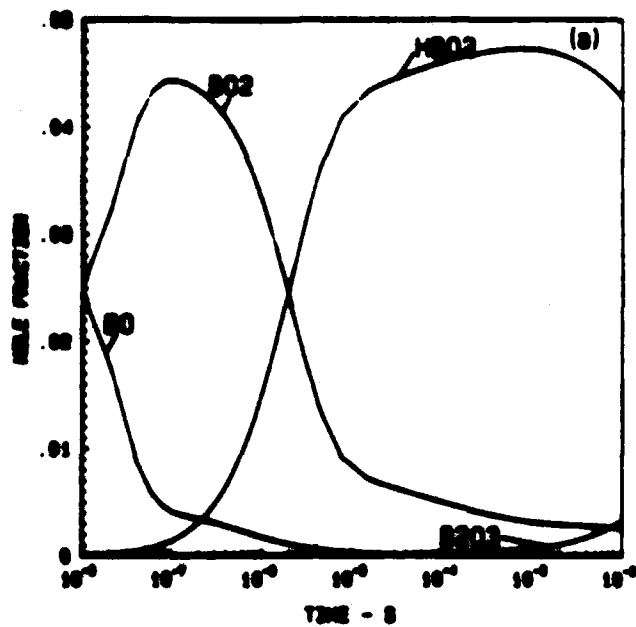
Figure 3.9. Species and Temperature Profiles for an Adiabatic, Constant
Pressure Mixture of $NO$, $H_2O$, $CO_2$, $O_2$ and $N_2$

Figure 3.9. (Continued) Species and Temperature Profiles for an Adiabatic,
Constant Pressure Mixture of BO, $H_2O$, $CO_2$, $O_2$ and $N_2$
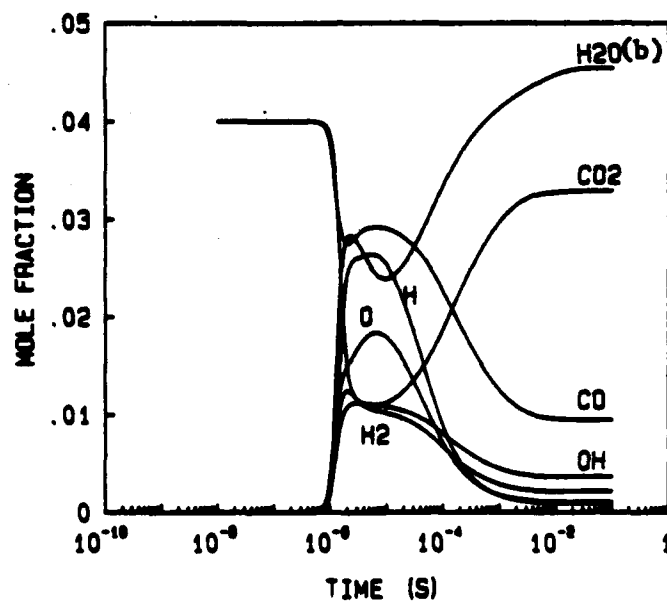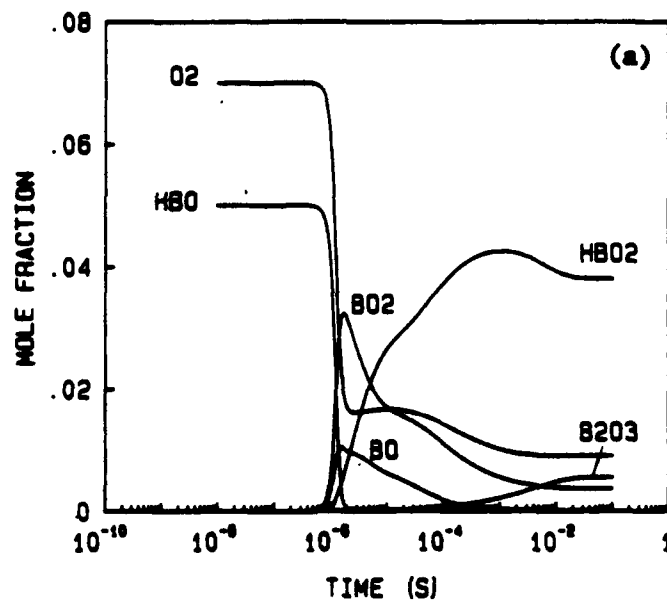
Figure 3.10. Species and Temperature Profiles for an Isothermal, Constant Volume Mixture of HBO, $H_2$, $CO_2$, $O_2$ and $N_2$
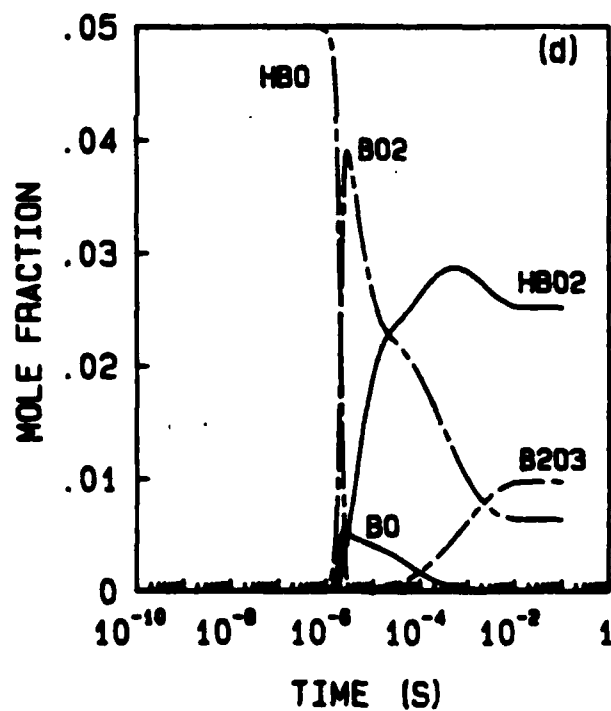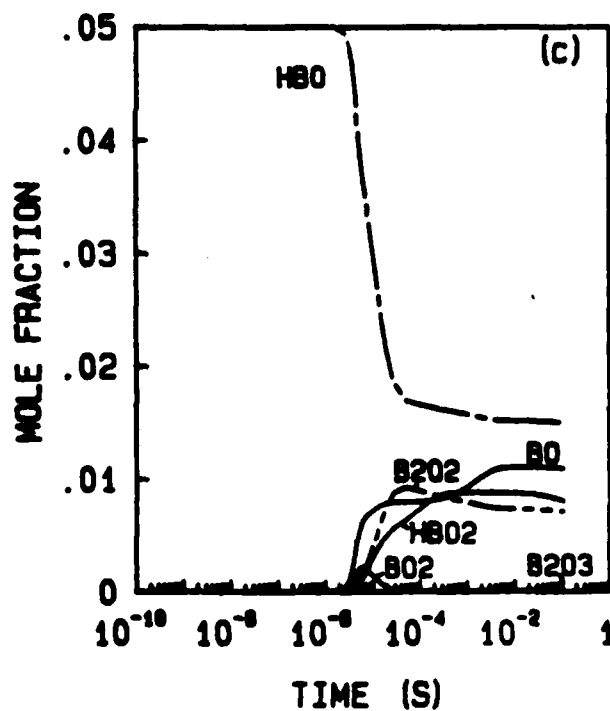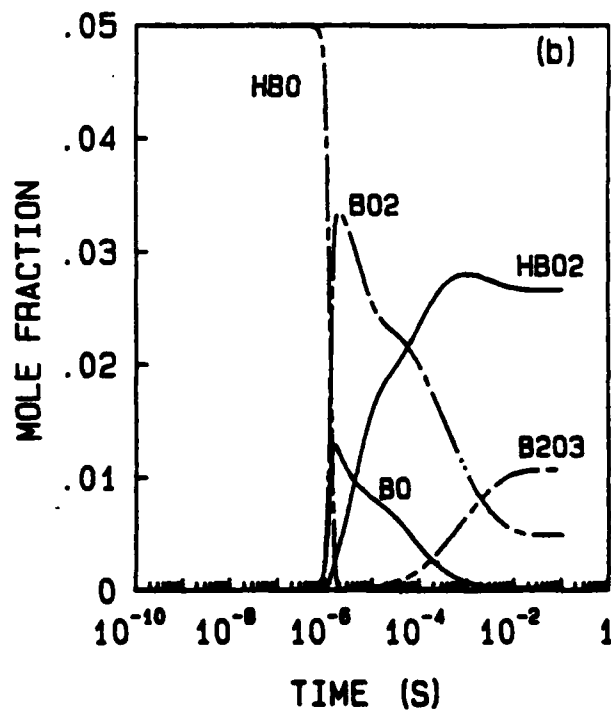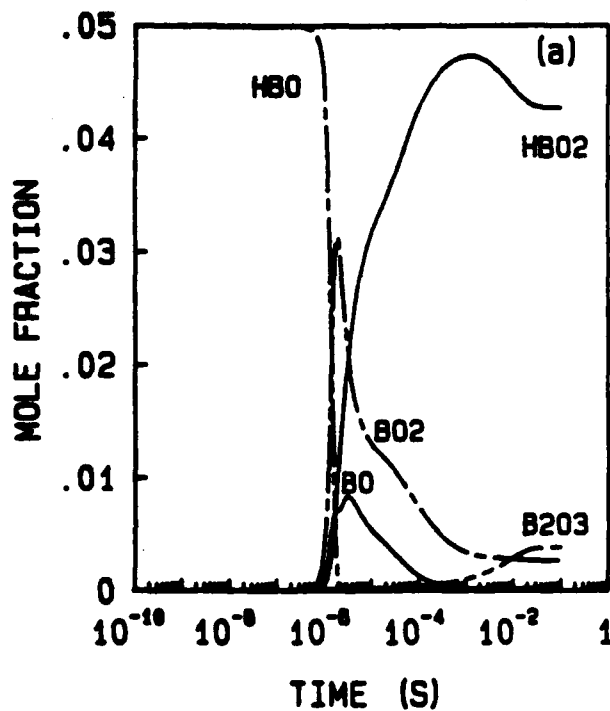
Figure 3.11.  Boron Speciation Profiles for Four Related HBO, $H_2$, CO, $O_2$ and $N_2$ Mixtures:  (a) system is carbon-free; (b) system is free of $H_2$; (c) system is oxygen deficient; and (d) system is free of $H_2$ and carbon.
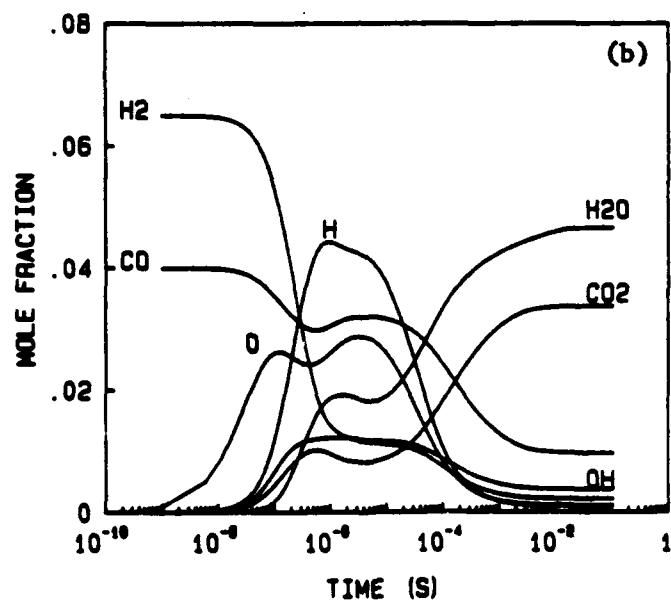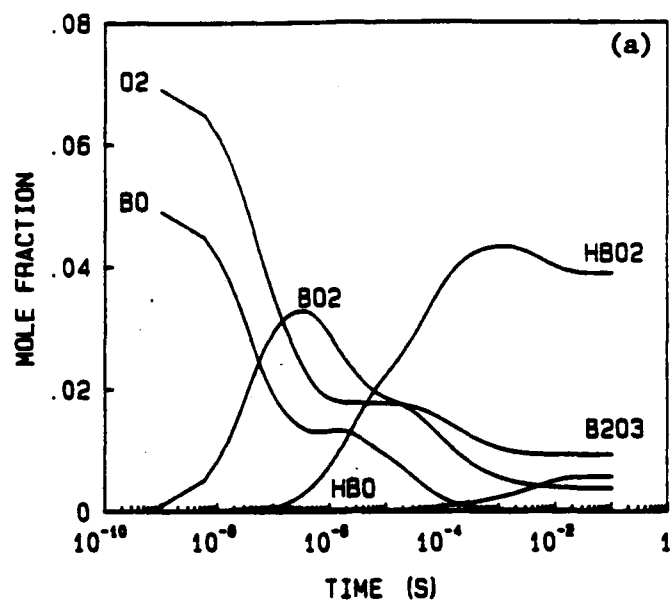
**Figure 3.12.** Species and Temperature Profiles for an Isothermal Constant Volume Mixture of BO, $H_2$, $CO_2$, $O_2$ and $N_2$
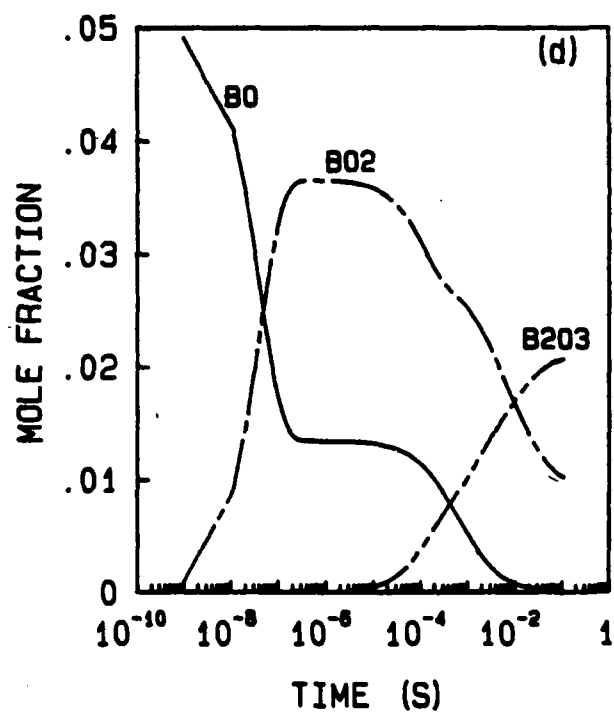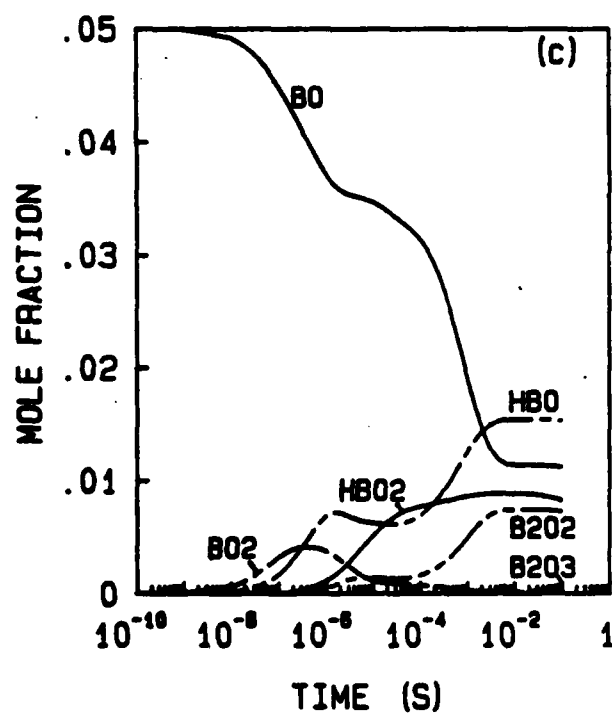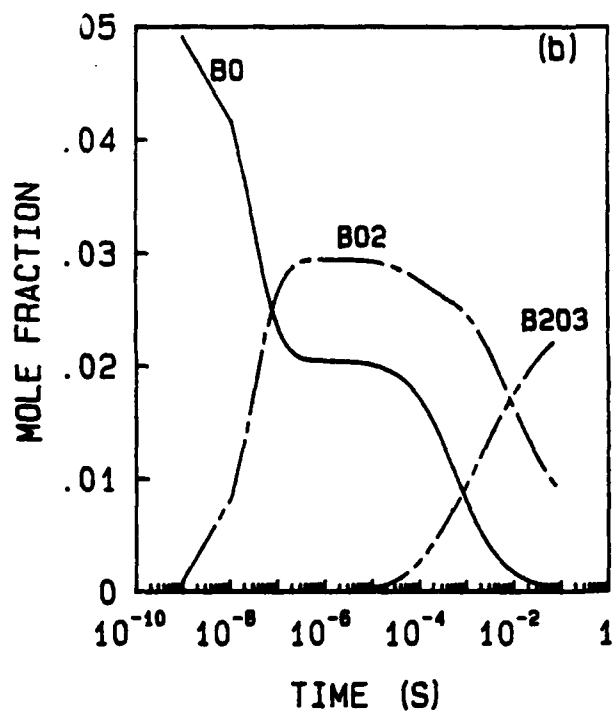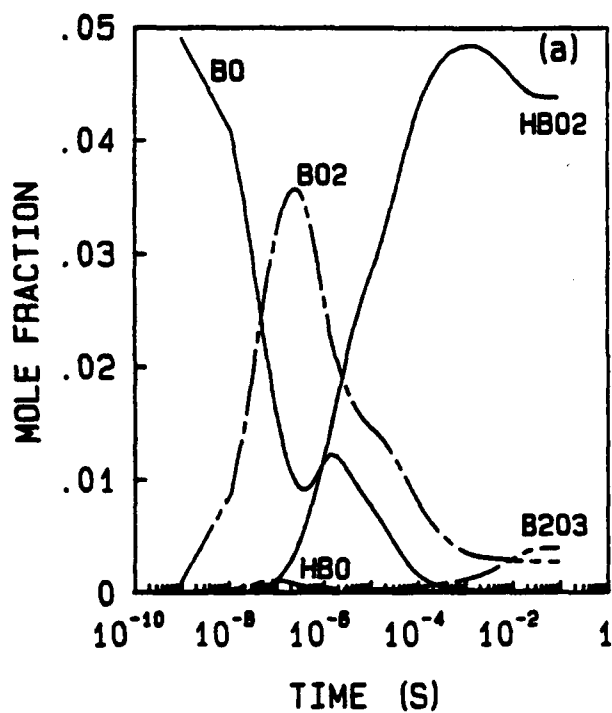
Figure 3.13. Boron Speciation Profiles for Four Related BO, $H_2$, CO, $O_2$ and $N_2$ Mixtures: (a) system is carbon-free; (b) system is free of $H_2$; (c) system is oxygen deficient; and (d) system is free of $H_2$ and carbon.

Examination of the concentration and temperature profiles suggest that for stoichiometric and oxygen excess systems (i.e., systems with reaction products dominated by $HBO_2$ and $B_2O_3$), the reaction proceeds in a sequential, partially overlapping process with the following order of events (events here referring to the formation of major intermediates and final products),

$$HBO \xrightarrow{\text{A}} BO \xrightarrow{\text{B}} BO_2 \xrightarrow{\text{C}} HOBO \xrightarrow{\text{E}} B_2O_3 \qquad ; \qquad HOBO \xrightarrow{\text{D}} B_2O_3$$
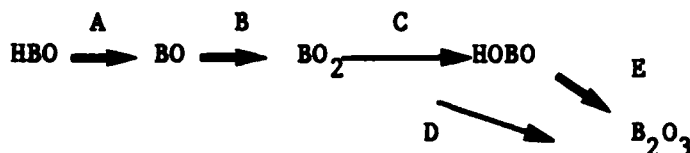
The amount of $HBO_2$ vs $B_2O_3$ in the products is determined by the final temperature and the amount of water vapor (or more generally, hydrogen containing species) in the system, which is governed to a large extent by the equilibrium relation

$$HOBO + HOBO = B_2O_3 + H_2O \quad .$$

The equilibrium constant for this reaction is shown in Figure 3.14, and as can be seen the reactants are generally favored with the equilibrium shifting toward the products with increasing temperature. Over the temperature range 1800 - 2400 K, steps A and B are observed to be fast and are generally completed within a few micro-seconds. The total energy release for these lean systems occurs over a lengthy period of time starting at a few micro-seconds and lasting a couple of milliseconds. Step B accounts for approximately 33-55% of the total energy release from the boron containing species, Step C (and/or D) accounts for the remaining 50-66% of the energy release.

For oxygen deficient systems, parallel and competing steps become important as represented by the following network of events
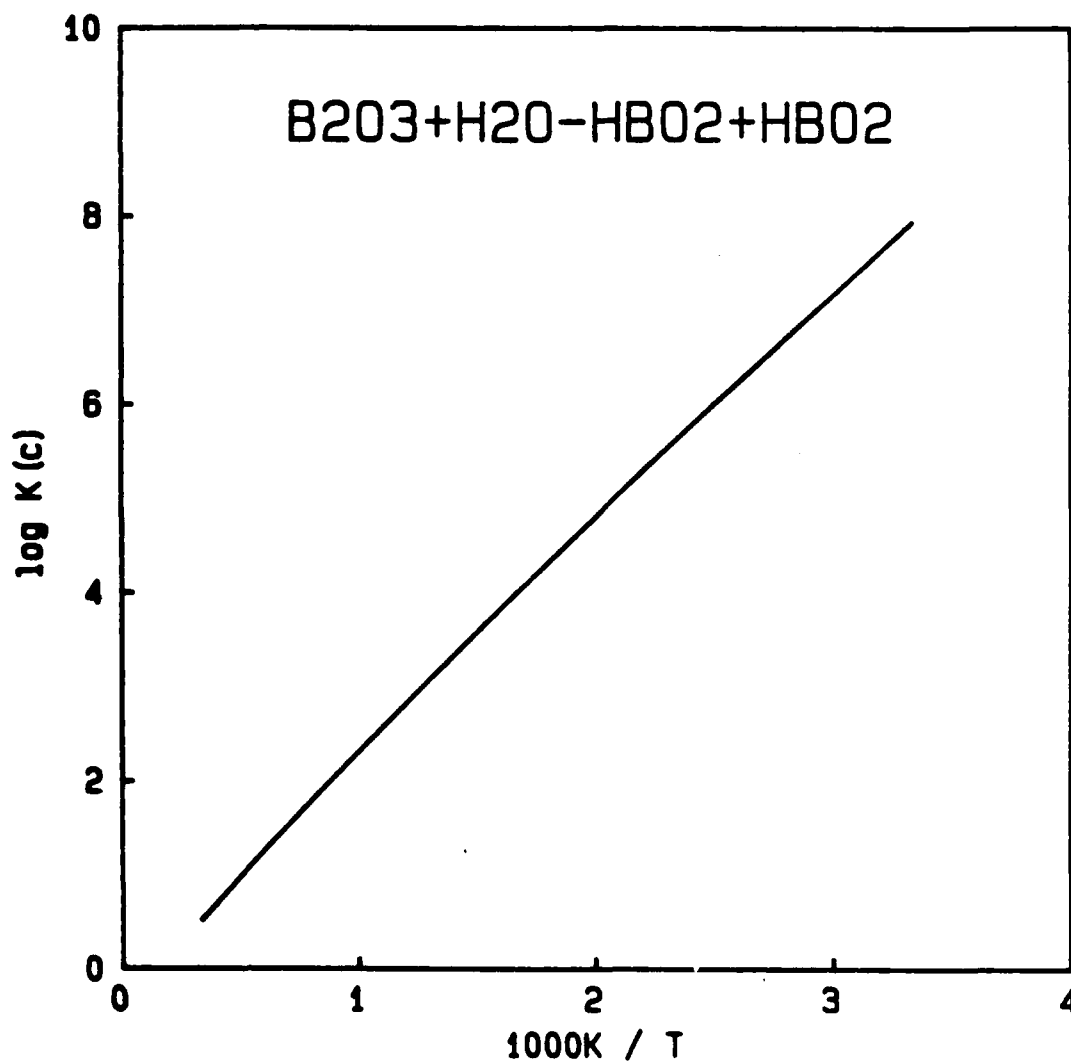
**Figure 3.14.** Equilibrium Constant, Log (K) Versus 1000/T, for $B_2O_3$ + $H_2O$ → $HBO_2$ + $HBO_2$ Reaction

3-43

$$HBO \longrightarrow BO \longrightarrow BO_2 \longrightarrow HOBO$$

with $B_2O_2$ branching up from $BO_2$ and down to $HOBO$, and $B_2O_3$ branching down from $HOBO$.

$$BO \longrightarrow BO_2 \longrightarrow HOBO$$

with $HBO \longrightarrow B_2O_2$ above, branching to $HOBO$, and $B_2O_3$ below.
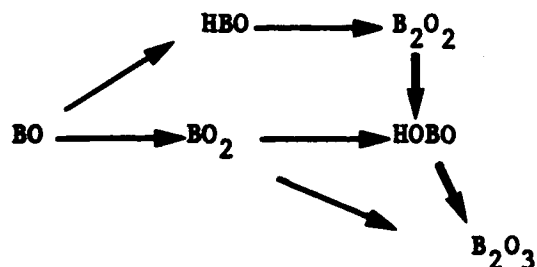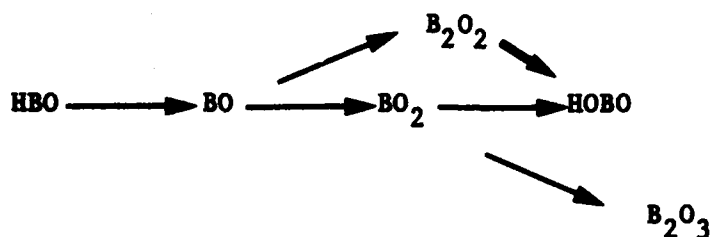
Furthermore, the reaction times are substantially longer and the reaction products are dominated by HBO, BO, $B_2O_2$ and HOBO in oxygen deficient systems.

The presence of CO or $CO_2$ can have a minor effect on reaction times and a more pronounced affect on the amount of $BO_2$ formed during the reaction process (as seen in Figures 3-11c and 3-11d and Figures 3-13c and 3-13d).

The influence of hydrogen on the reaction is shown by comparing Figure 3-13a with Figures 3-13d or 13b. In addition to shortening the time required for equilibrium, the presence of hydrogen plays a more important role in accelerating the oxidation of intermediates (i.e., BO and $BO_2$). This is particularly important with regard to the energy release of the system. Note that in comparing Figures 3-13a with 3-13b, the energy release duration (as denoted by the time to the peak in the $HBO_2$ concentration profile (Figure 13a) or the time to the peak in the $B_2O_3$ concentration profile (Figure 13b)) is about 100 times shorter with hydrogen present.

Comparison of all the system with HBO present initially with those with BO present as a reactant shows an important characteristic difference among these two types of systems. HBO systems have induction periods whereas BO

systems do not. Since induction periods play an important role in ignition phenomena and inhibition processes, the two systems for $O_2$ excess conditions (and of course $O_2$ deficient systems) could behave drastically different in certain environments. The differences in these two types of systems will be discussed further with the sensitivity analysis.

## 3.5 Sensitivity Analysis

### 3.5.1 System Equations

The role of sensitivity analysis in the present study has been to provide a means for assessing the importance or contribution of the various system parameters, $\alpha$, with respect to objectives of interest. The system parameters of interest here are the specific reaction rate constants, the equilibrium constants of the reactions, and the initial concentrations or initial temperature. The coefficients

$$S_{ij} = \frac{\partial c_i}{\partial \alpha_j} \qquad (3.5.1)$$

provide a direct measure of how the $j$-th parameter controls the behavior of the $i$-th dependent variable at time $t$.

The equations that the first order elementary sensitivity coefficients satisfy are obtained by differentiating the system equations (i.e., eqs. (1) and (2) or eq. (21)) with respect to each system parameter of interest. For simplicity, the sensitivity equations for the isothermal constant volume problem are given below as

$$\frac{\partial^2 c_i}{\partial t \partial \alpha_j} = \frac{\partial \dot{\omega}_i}{\partial \alpha_j} + \sum_{s=1}^{N} \left( \frac{\partial \dot{\omega}_i}{\partial c_s} \right) \left( \frac{\partial c_s}{\partial \alpha_j} \right) . \qquad (3.5.2)$$

This set of equations is solved in closed form to give the result

$$\frac{\partial \underline{c}}{\partial a_j} = G(t,0)\left(\frac{\partial \underline{c}}{\partial a_j}\right)_0 + \int_0^t G(t,t')\left(\frac{\partial \underline{\dot{q}}}{\partial a_j}\right) dt' , \qquad (3.5.3)$$

where Green's function satisfies

$$\left[\underline{1}\frac{\partial}{\partial t} - \underline{J}(t)\right] G(t,t') = 0 , \qquad t > t' \qquad (3.5.4)$$

and $G(t',t') = \underline{1}$. $J(t)$ is the $N \times N$ Jacobian matrix with elements $\partial \dot{q}_i/\partial c_j$. The initial condition $(\partial \underline{c}/\partial a_j)_0$ is the zero vector, unless $a_j$ is the initial concentration of the i-th species, in which case the initial condition is a vector whose components are all zero except the i-th component, which has the value 1. The sensitivity equations are solved with the AIM computer code.

### 3.5.2 Green's Function Gradients

The Green's function matrix has an important physical interpretation. The elements of the Green's function matrix may be identified as the gradients $G_{ij} = \partial c_i(t)/\partial c_j(t')$, $t \geq t'$. These terms may be directly interpreted as "memory functions" in that each term presents the sensitivity of species i at time t with respect to variations of species j at prior time t'. The result is a very detailed probe for the operational mechanistic pathways of a complex chemical system. When t' equals zero, these gradients are equivalent to the linear sensitivity gradients where the perturbed parameter is the initial species concentrations or initial temperature of the system. Furthermore, these gradients are measurable in the laboratory.

Examples of these initial condition sensitivity gradients are shown in Figures 3.15 through 3.18. The examples are taken from the two kinetic systems illustrated in Figures 3.10 and 3.12. Figures 3.15 and 3.17 show
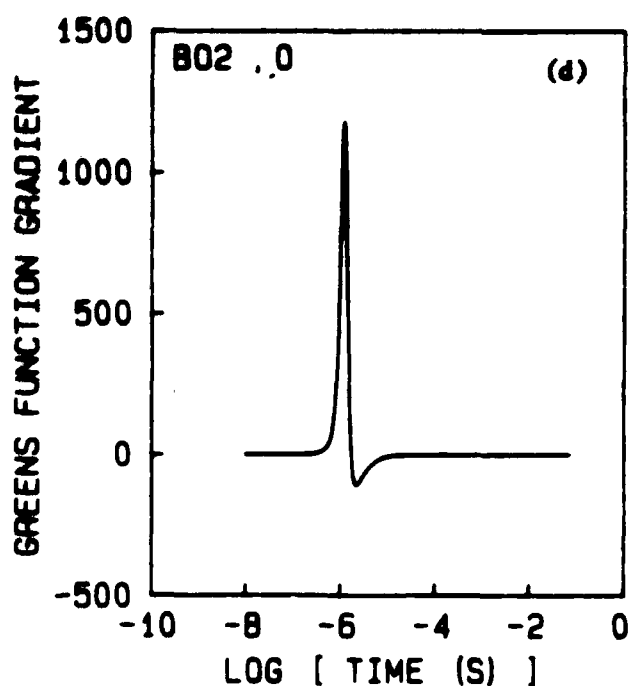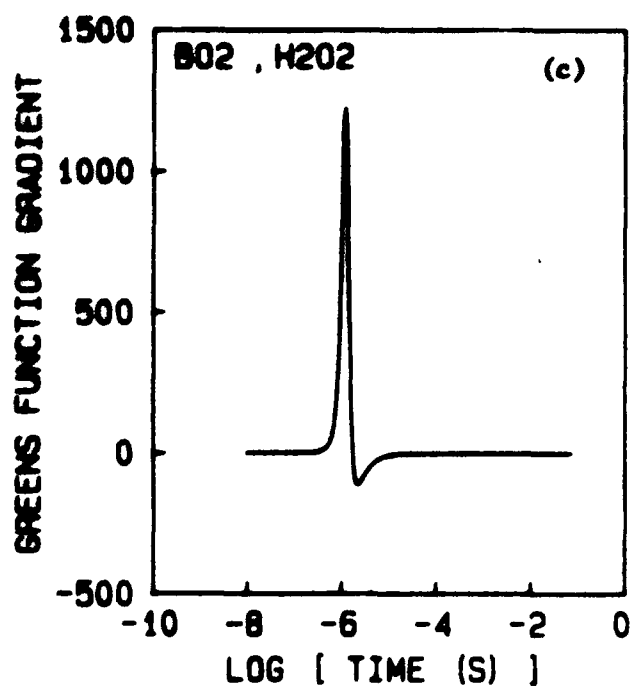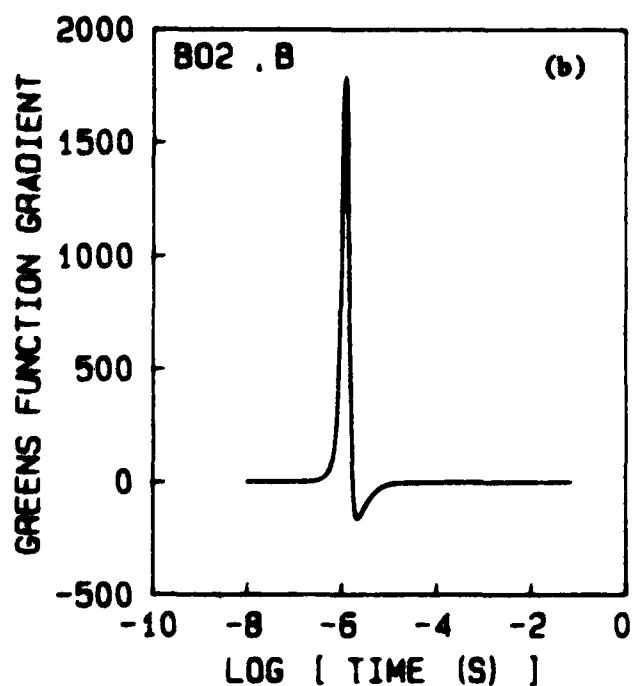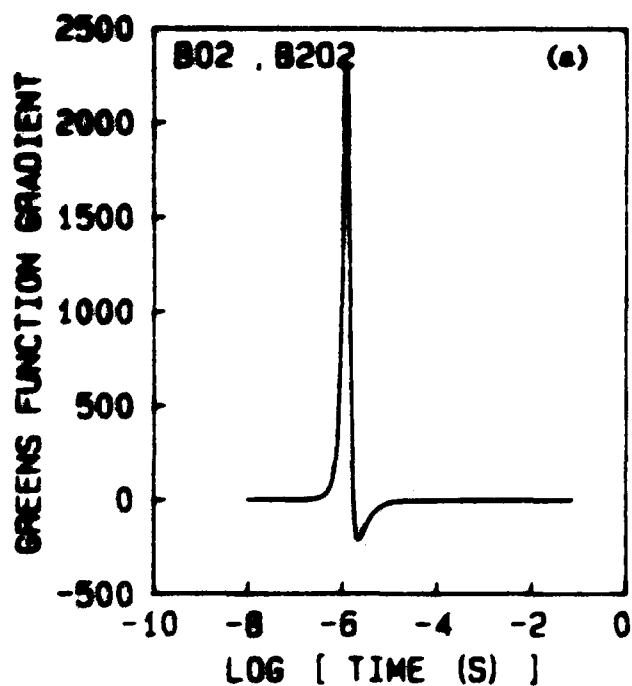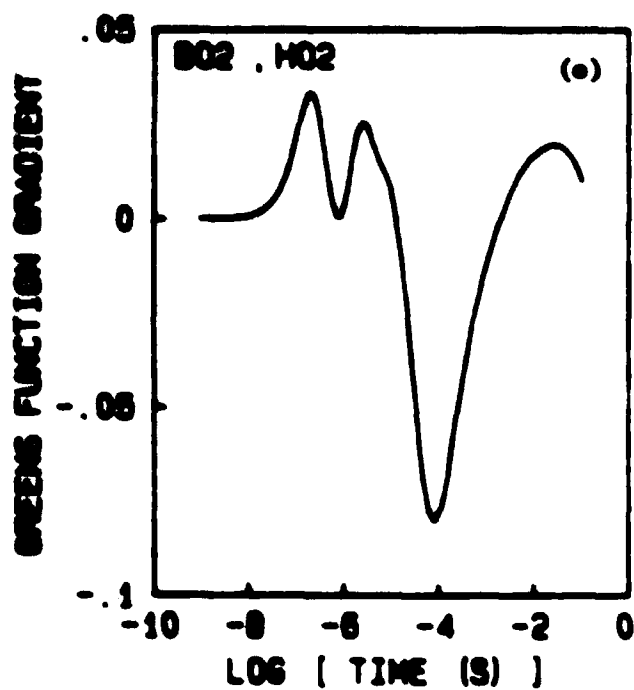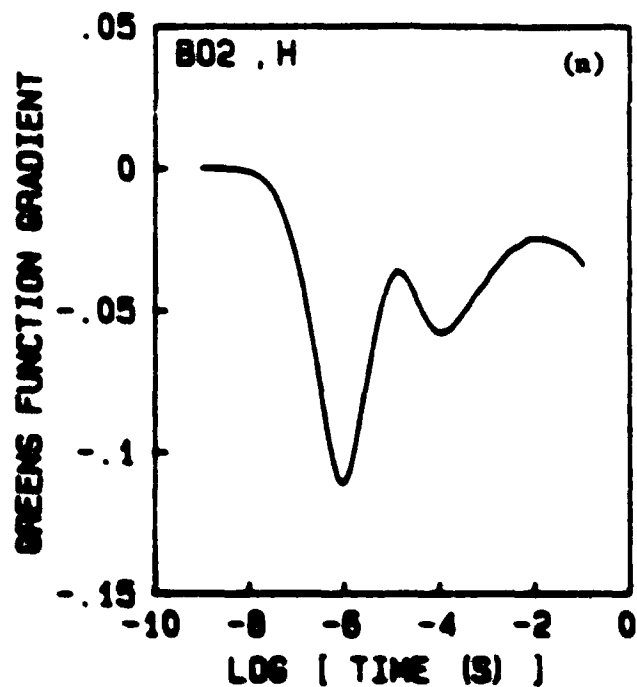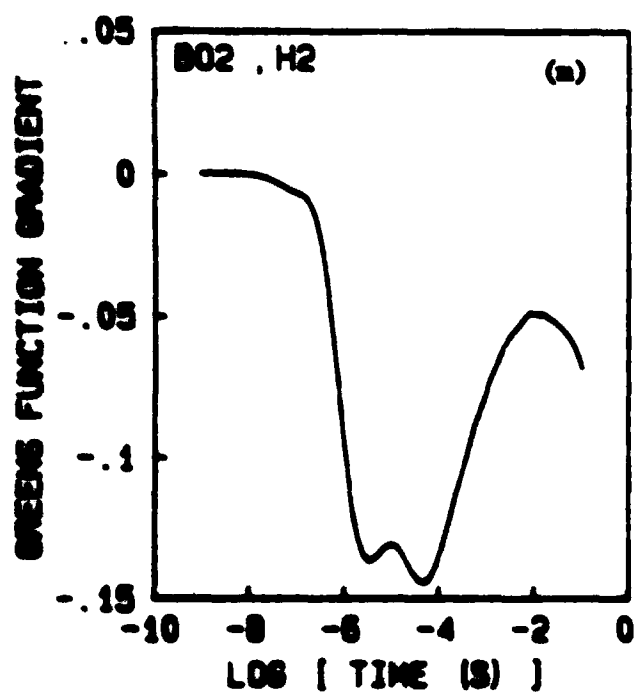
Figure 3.15. Sensitivity of $HO_2$ Concentration Versus Time to Variations in the Concentration of Several Reactants in an Isothermal, Constant Volume Mixture of HBO, $H_2$, $CO_2$, $O_2$ and $N_2$

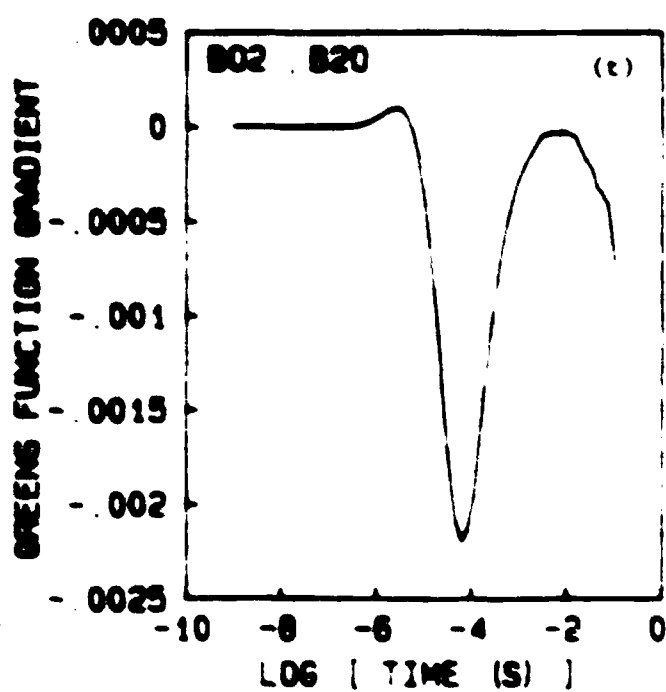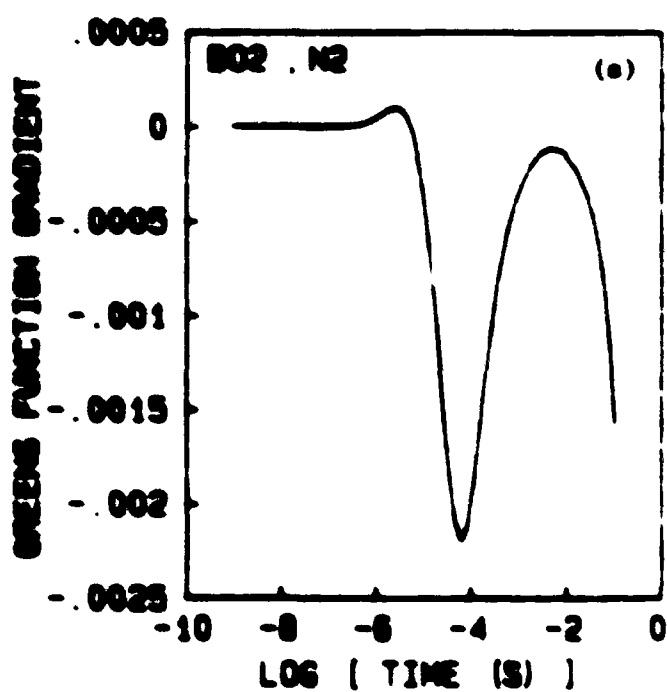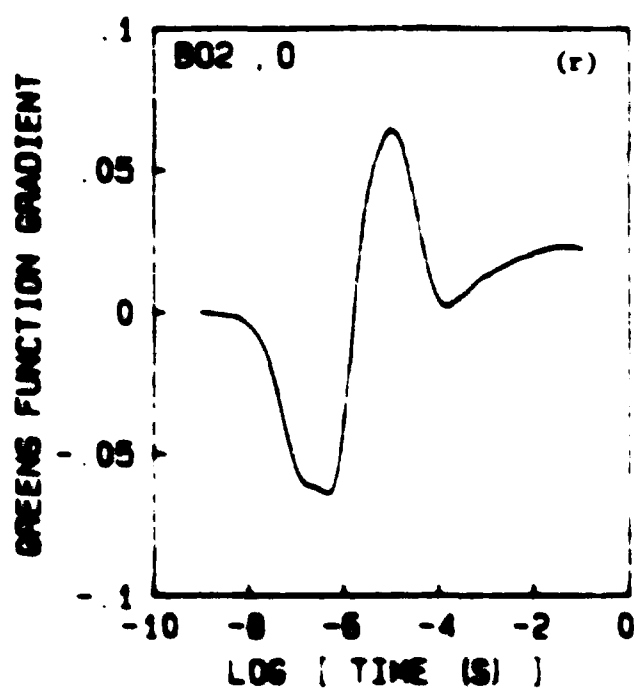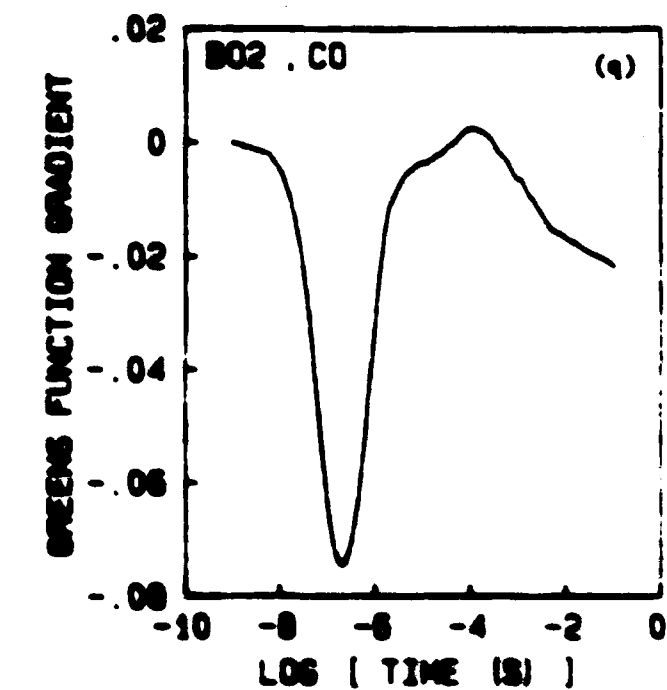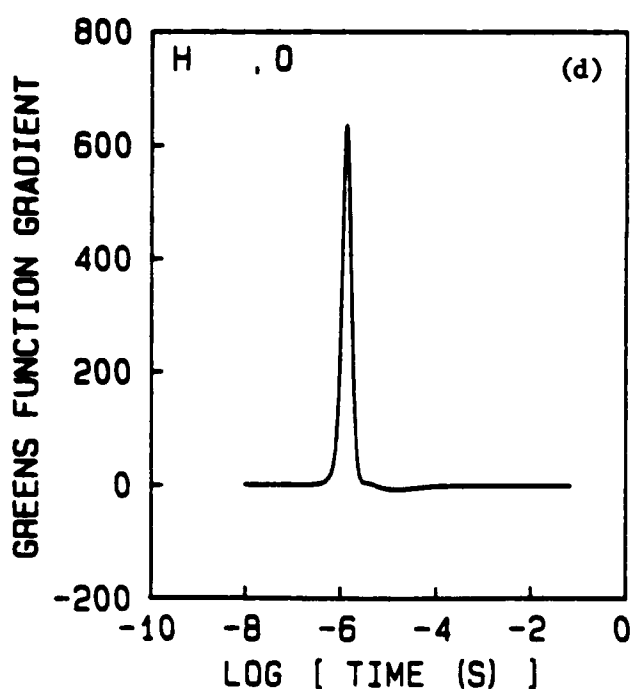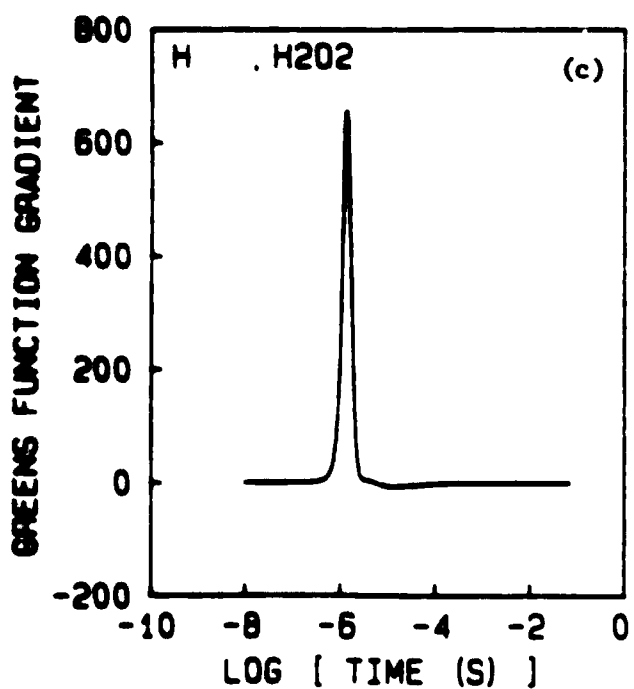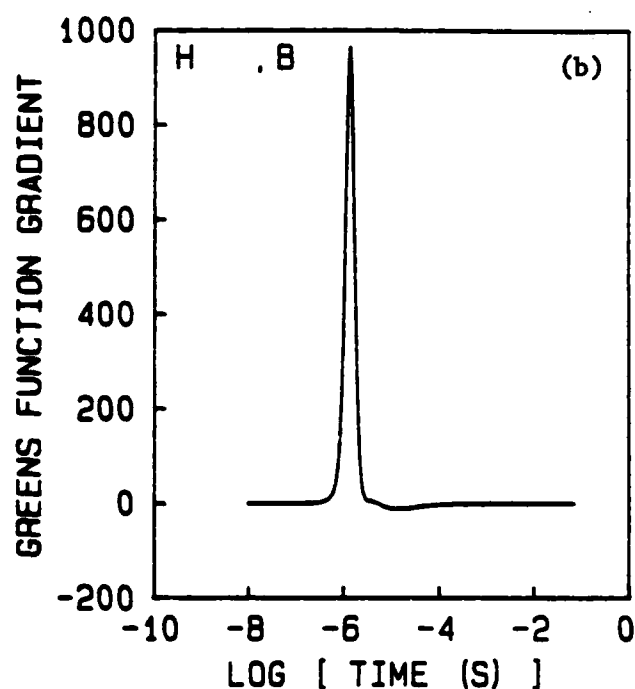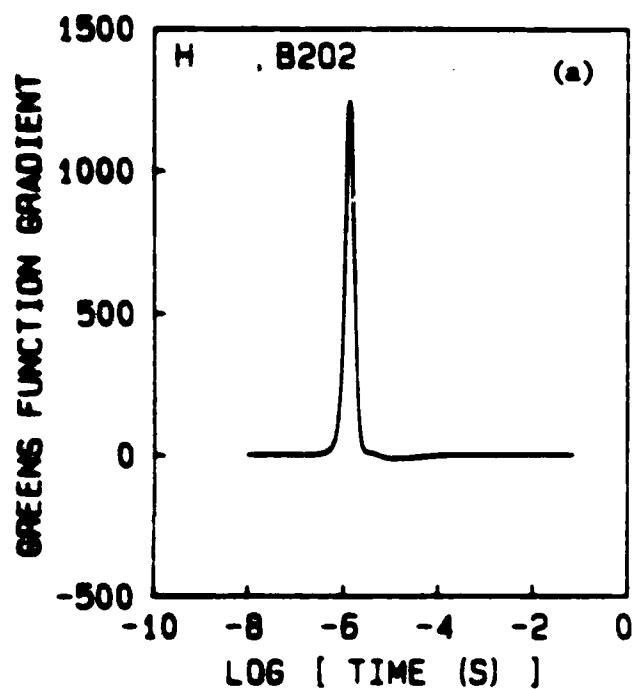Figure 3.15. (Continued) Sensitivity of $BO_2$ Concentration Versus Time to Variations in the Concentration of Several Reactants in an Isothermal, Constant Volume Mixture of HBO, $H_2$, $CO_2$, $O_2$ and $N_2$

Figure 3.15. (Continued) Sensitivity of $BO_2$ Concentration Versus Time to Variations in the Concentration of Several Reactants in an Isothermal, Constant Volume Mixture of HBO, $N_2$, $CO_2$, $O_2$ and $N_2$

Figure 3.15. (Continued) Sensitivity of $HO_2$ Concentration Versus Time to Variations in the Concentration of Several Reactants in an Isothermal, Constant Volume Mixture of $H2O$, $H_2$, $CO_2$, $O_2$ and $N_2$
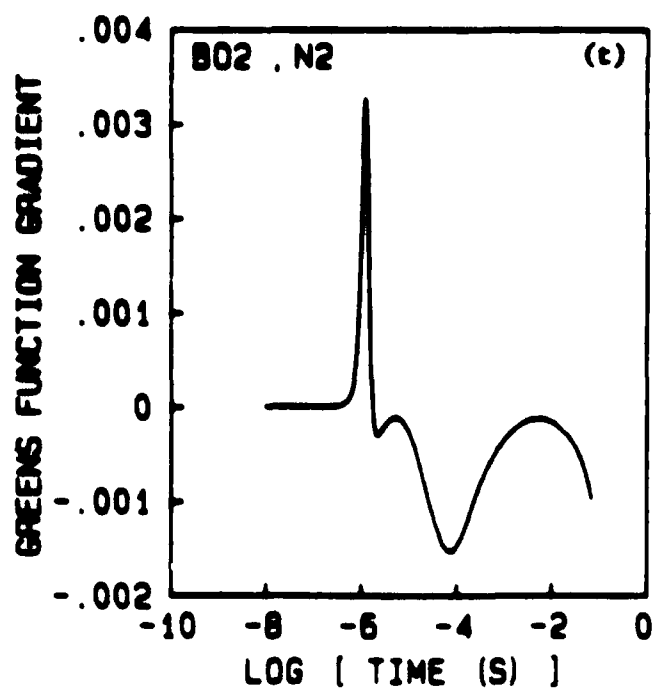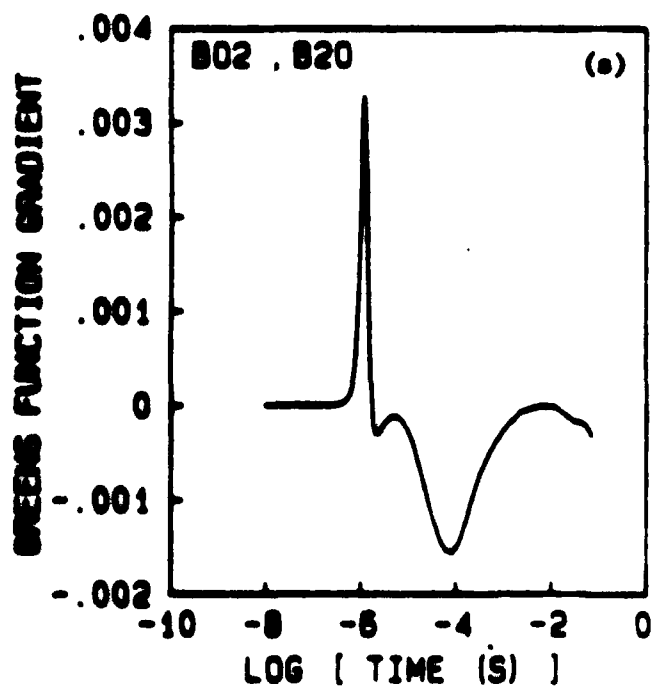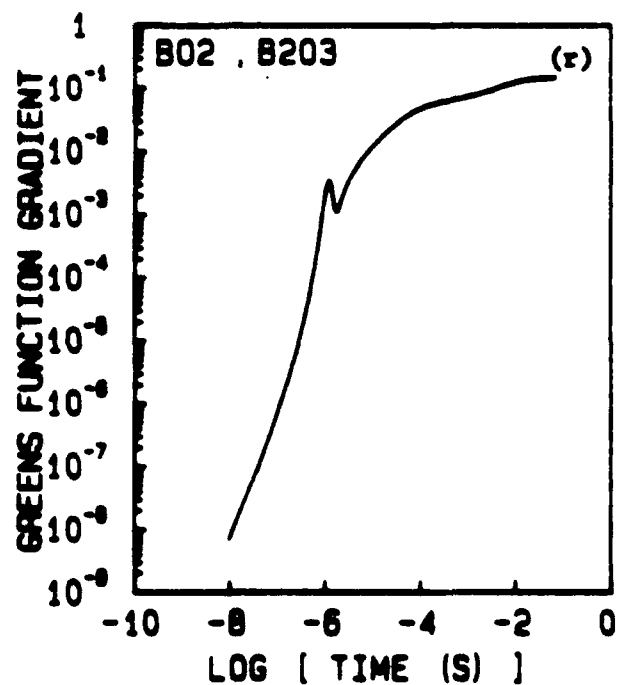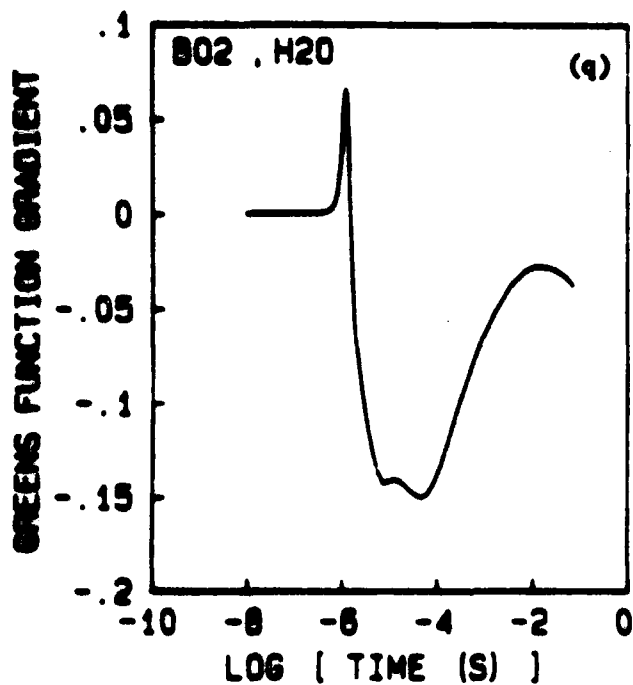
Figure 3.15. (Continued) Sensitivity of $HO_2$ Concentration Versus Time to Variations in the Concentration of Several Reactants in an Isothermal, Constant Volume Mixture of HBO, $H_2$, $CO_2$, $O_2$ and $N_2$
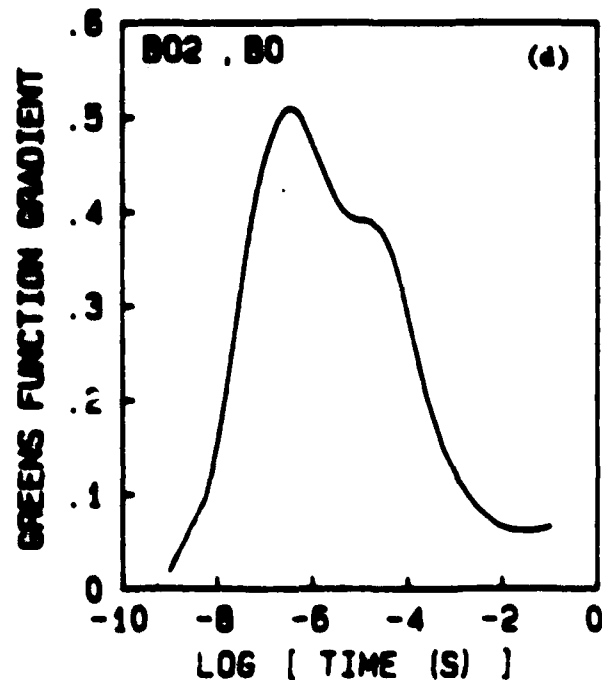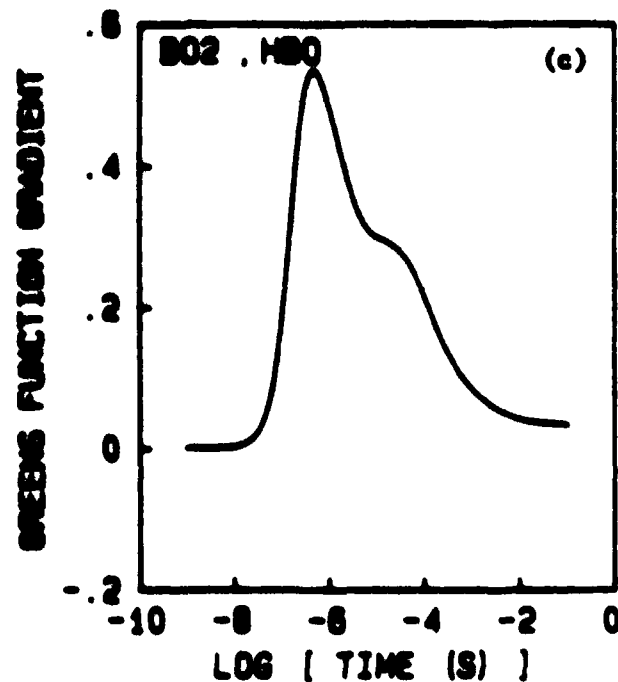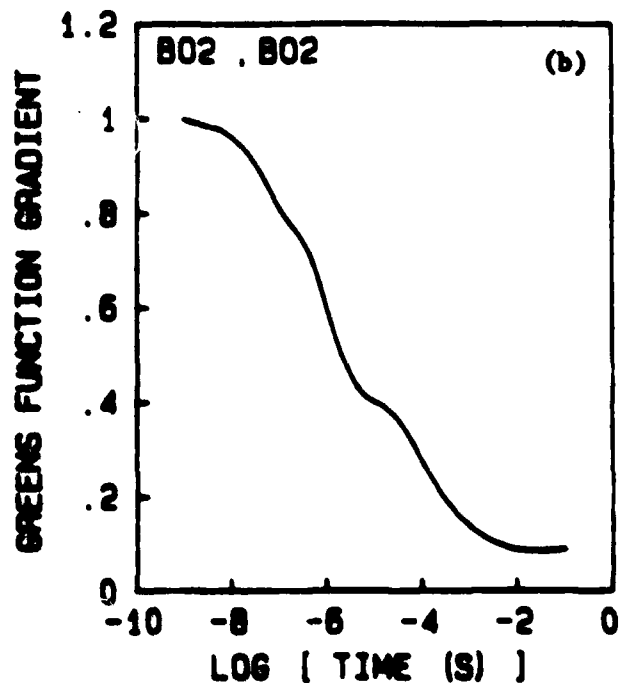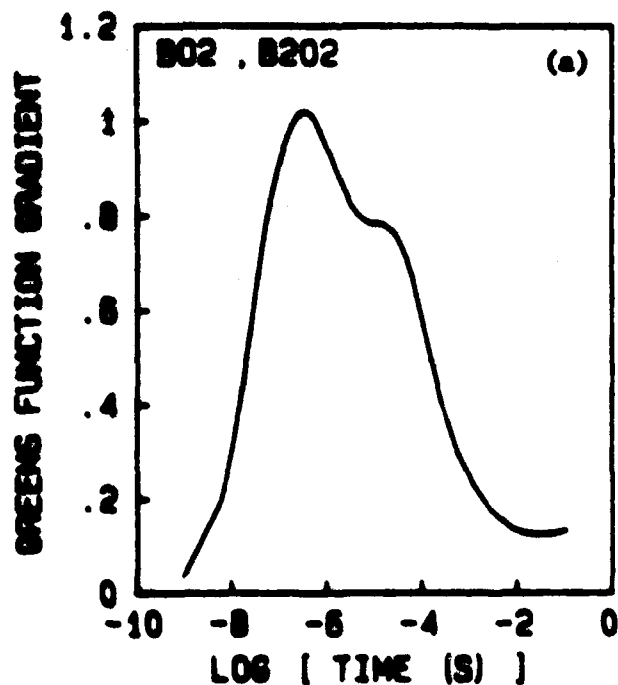
Figure 3.16. Sensitivity of H Concentration Versus Time to Variations in the Concentration of Several Reactants in an Isothermal, Constant Volume Mixture of HO, H₂, CO₂, O₂ and N₂

3-52

Figure 3.16. (Continued) Sensitivity of N Concentration Versus Time to Variations in the Concentration of Several Reactants in an Isothermal, Constant Volume Mixture of NO, $H_2$, $CO_2$, $O_2$ and $N_2$

Figure 3.16. (Continued) Sensitivity of H Concentration Versus Time to
Variations in the Concentration of Several Reactants in an
Isothermal, Constant Volume Mixture of HO, $H_2$, $CO_2$, $O_2$ and $N_2$

Figure 3.16. (Continued) Sensitivity of H Concentration Versus Time to Variations in the Concentration of Several Reactants in an Isothermal, Constant Volume Mixture of HO, $H_2$, $CO_2$, $O_2$ and $N_2$

Figure 3.16. (Continued) Sensitivity of N Concentration Versus Time to Variations in the Concentration of Several Reactants in an Isothermal, Constant Volume Mixture of NO, $H_2$, $CO_2$, $O_2$ and $N_2$

Figure 3.17. Sensitivity of H Concentration Versus Time to Variations in the Concentration of Several Reactants in an Isothermal, Constant Volume Mixture of HBO, $H_2$, $CO_2$ $O_2$ and $N_2$

Figure. Sensitivity of H concentration Versus Time to Variations in the concentration of several Reactants in an isothermal, constant Volume Mixture of H, O, and ...

the gradients of $\partial[BO_2(t)]/\partial c_j(0)$ and $\partial[H(t)]/\partial c_j(0)$, respectively, for the HBO system of Figure 3-10. Figures 3.16 and 3.18 report the same gradients except for the BO system of Figure 3.12. The chemical names in the upper left hand corner of each figure denote the gradient plotted. For example, the notation "$BO_2$, $B_2O_2$" of Figure 3.15(a) represents the gradient $\partial[BO_2(t)]/\partial[B_2O_2(0)]$. The physical interpretation of this gradient is simply that the nominal value of the $BO_2$ concentration is increased at a time of 1 $\mu s$ and then decreased slightly thereafter (relative to its original conc. profile shown in Figure 3.10) when the $B_2O_2$ concentration is perturbed at t=0. It also may be interpreted as a shift in the $BO_2$ concentration profile to shorter times, and thus, an acceleration in the overall reaction.

Without looking into the details of these sets of figures, they reveal an important characteristic feature about the two systems under consideration. Note in particular the similarities in many of the gradient profiles of the HBO system. This similarity indicates a high degree of dynamic coupling among the various species. Furthermore, the magnitudes of the coefficients are much larger for the HBO system, and hence, this system is much more responsive to perturbations. The high degree of coupling is only in the vicinity of HBO consumption and BO and $BO_2$ production. At times thereafter, the two chemical systems respond similarly to initial condition perturbations. This latter fact may be observed in Figures 3.15(p) and 3.16(m) or Figures 3.15(q) and 3.16(i) by comparing profiles at times greater than $10^{-5}$ s. The practical importance of these results are the following: first, for reaction times greater than approximately 1$\mu s$ (i.e., the period of energy release), both HBO and BO systems respond similarly, and hence, accurate information in the initial conditions (i.e., which species are coming off the metallic boron surface) is not critical to the present study of the gas phase chemistry. It is important, however, to realize that this statement pertains only to stoichiometric and oxygen excess systems. Secondly, the significant differences in the responses of these two systems (as indicated by the Green's function coefficients) may be used to differentiate if HBO or BO is the dominate species being produced at the surface. For example, note that $CO_2$

additions tends to inhibit the HBO system (or to decrease the $BO_2$ concentration), whereas $CO_2$ addition to the BO system accelerates it (and increases the $BO_2$ concentration).

### 3.5.3 Linear Parametric Sensitivities

Parametric sensitivities of the form $\partial \ln C_i / \partial \ln P_j$ have been investigated for several kinetic systems. Some results from three of the systems are discussed here. These include the $O_2$ excess HBO system of Figure 3.10, the $O_2$ excess BO system of Figure 3.12, and the $O_2$ deficient HBO system of Figure 3.11c.

Although one may apply and interpret the above parametric derivatives in several ways, the most elementary interpretation is used here. In particular, its gradient $\partial \ln C_i / \partial \ln P_j$ will be interpreted as the relative response of species $C_i$ at time $\tau$ to a variation in the kinetic rate constant parameter $P_j$.

Figures 3.19 and 3.20 show the gradients, $\partial \ln (BO_2)/\partial \ln P_j$, for the oxygen excess, HBO and BO systems, respectively. The sequence of Figures (a) through (p) includes the first 16 reaction rate parameters of greatest importance on the $BO_2$ concentration profile. The figures are arranged in a decreasing order of importance as determined by the maximum gradient (absolute) value over the time interval studied. Furthermore, the gradients plotted are normalized to their maximum values, i.e.,

$$\left\{ \frac{\dfrac{\partial \ln C_i}{\partial \ln P_j}}{\left| \dfrac{\partial \ln C_i}{\partial \ln P_j} \right|_{max}} \right\}$$
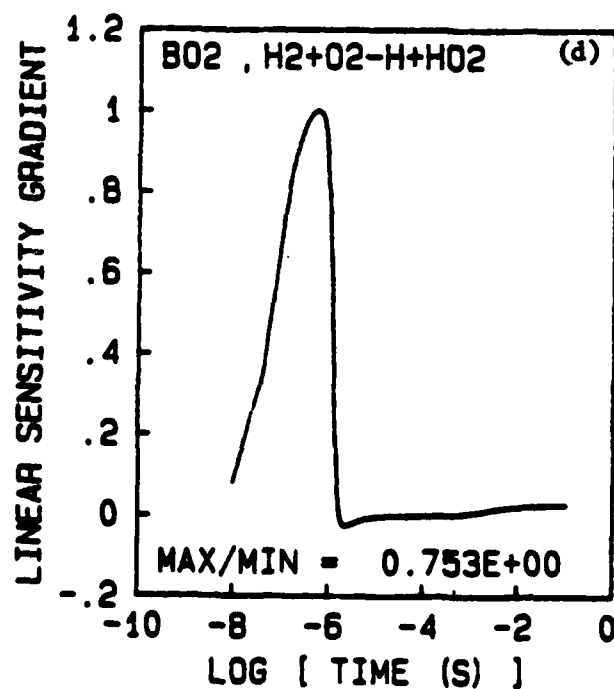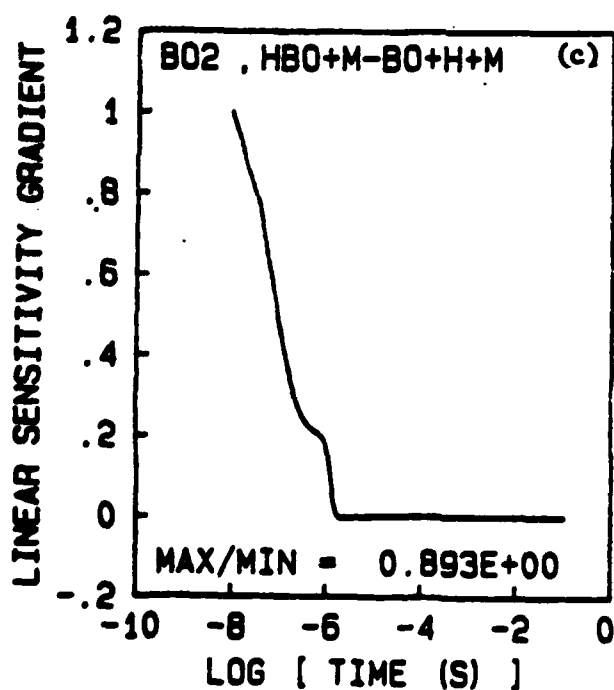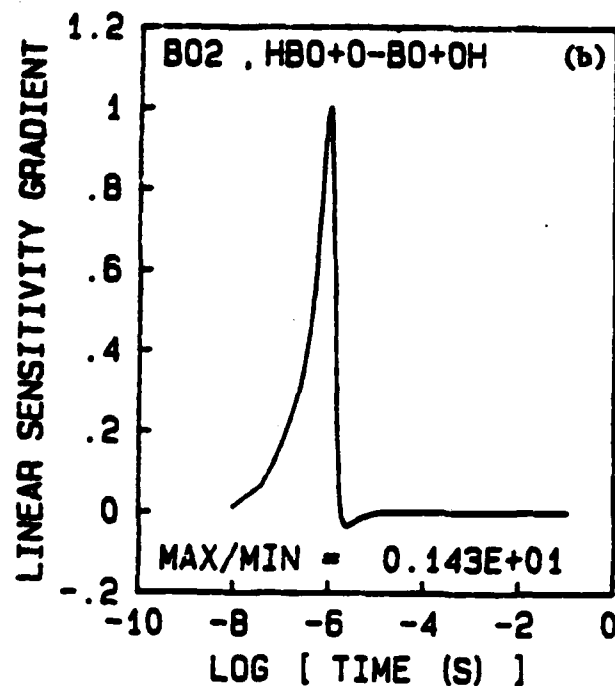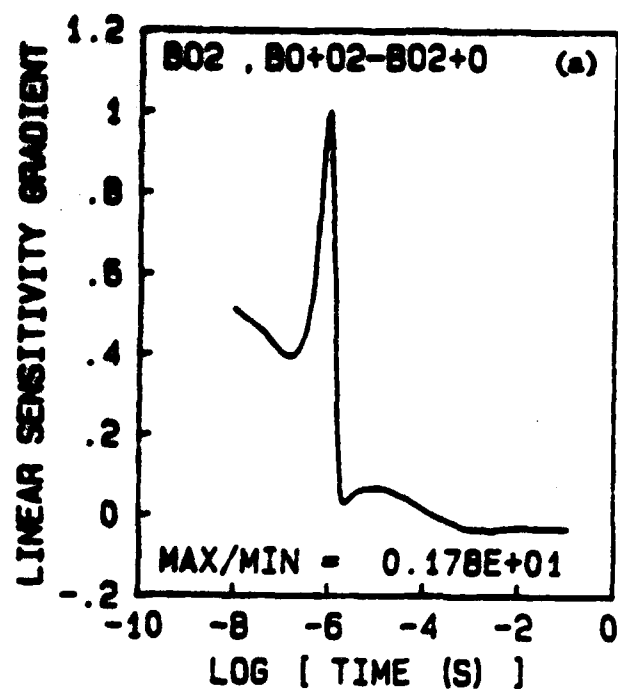
Figure 3.19. Sensitivity of $BO_2$ Concentration Versus time to Variations in Kinetic Rate Constants for an Isothermal, Constant Volume Mixture of HBO, $H_2$, $CO_2$, $O_2$ and $O_2$
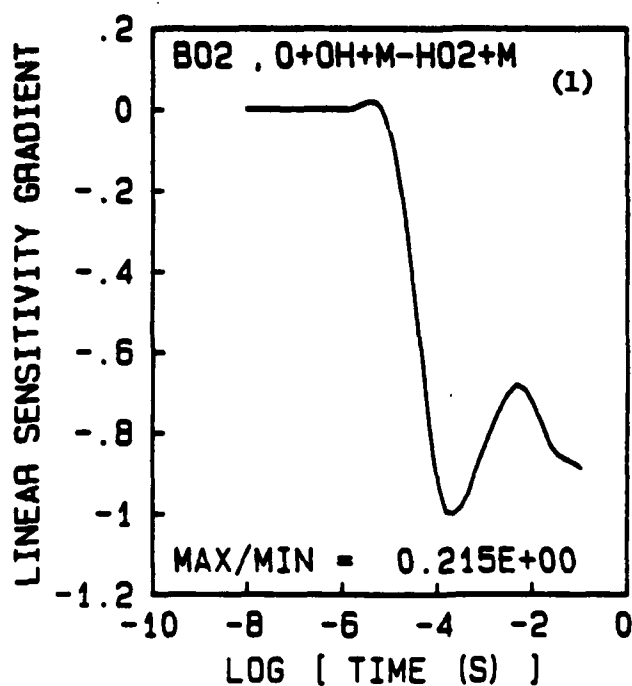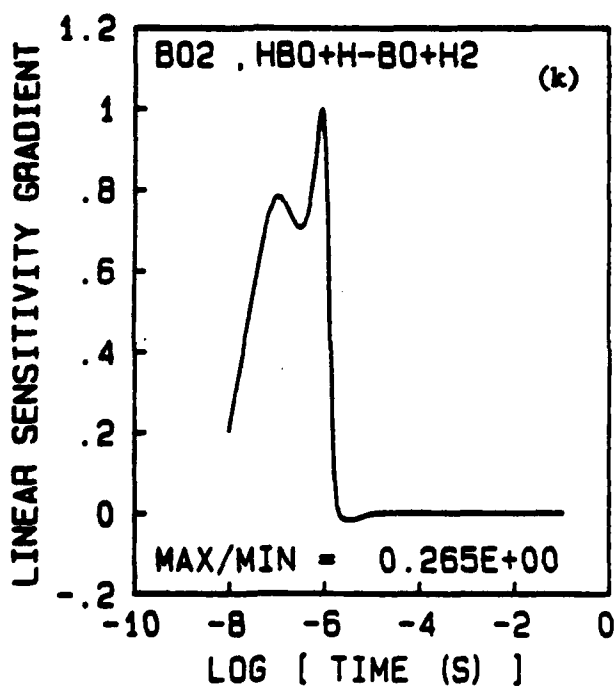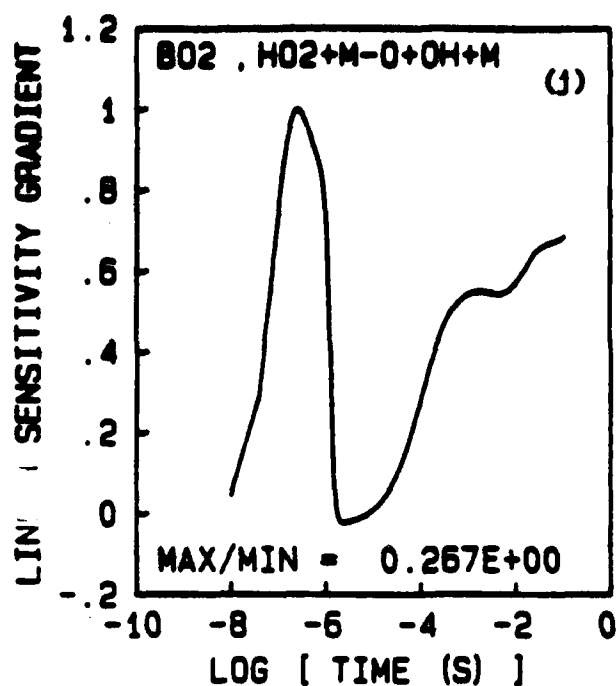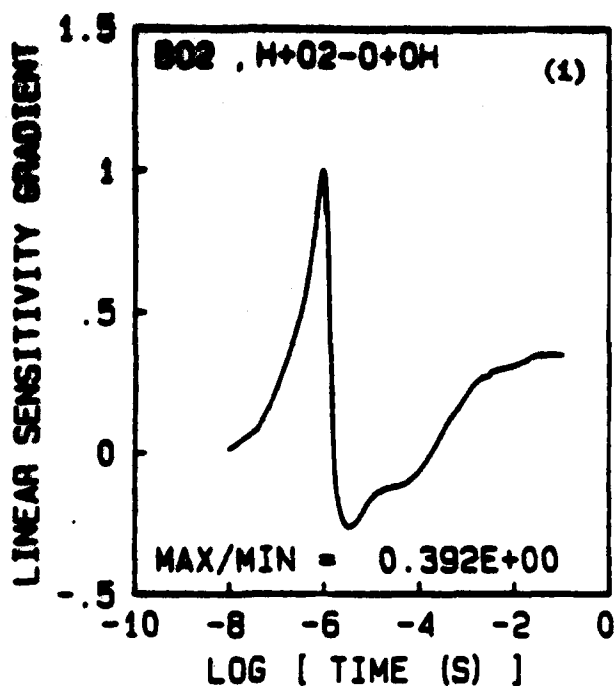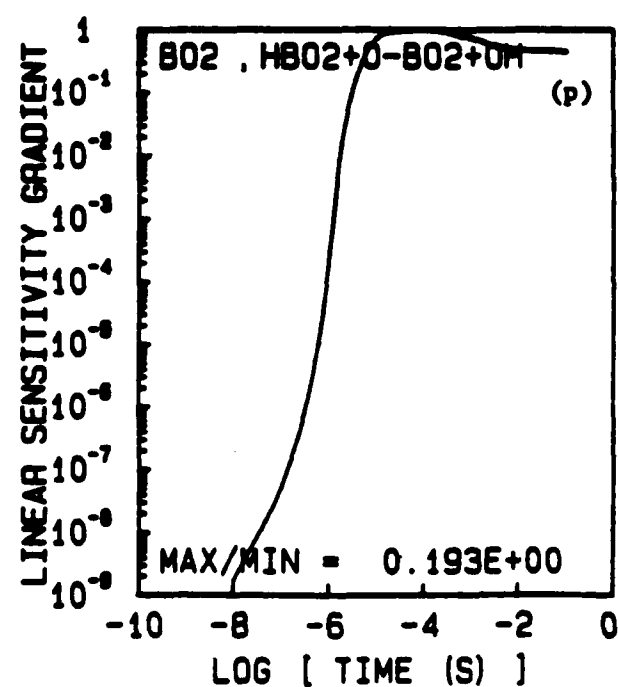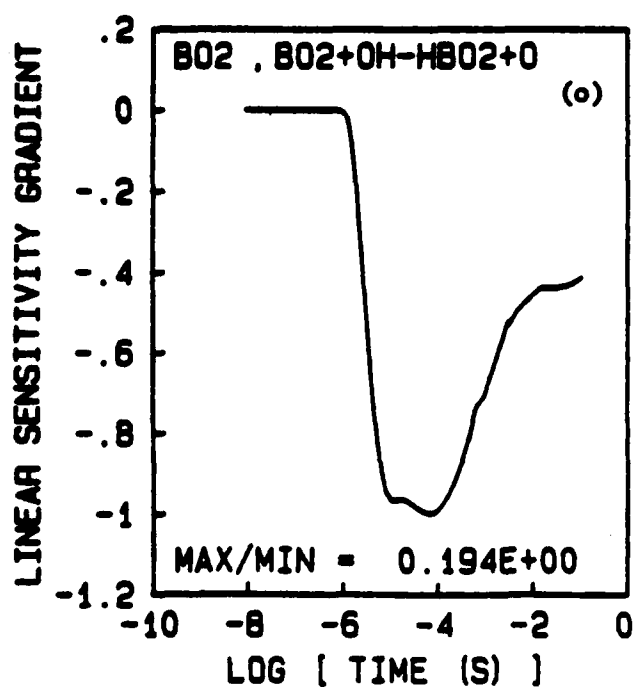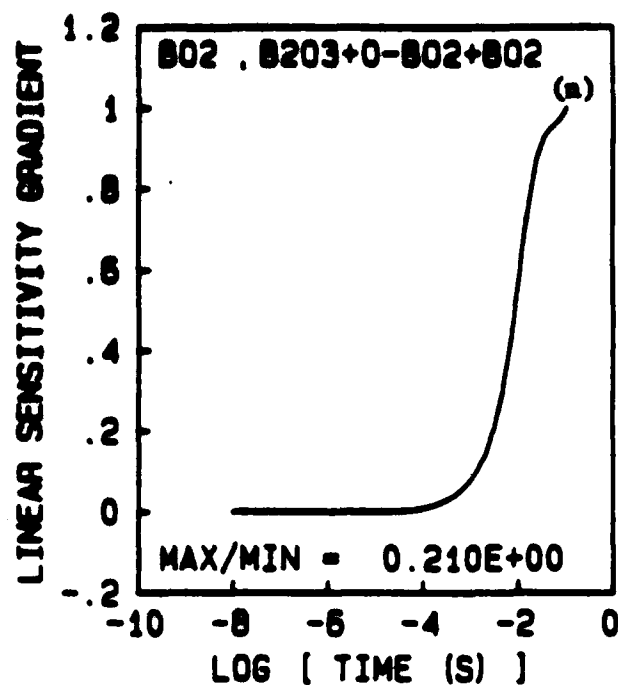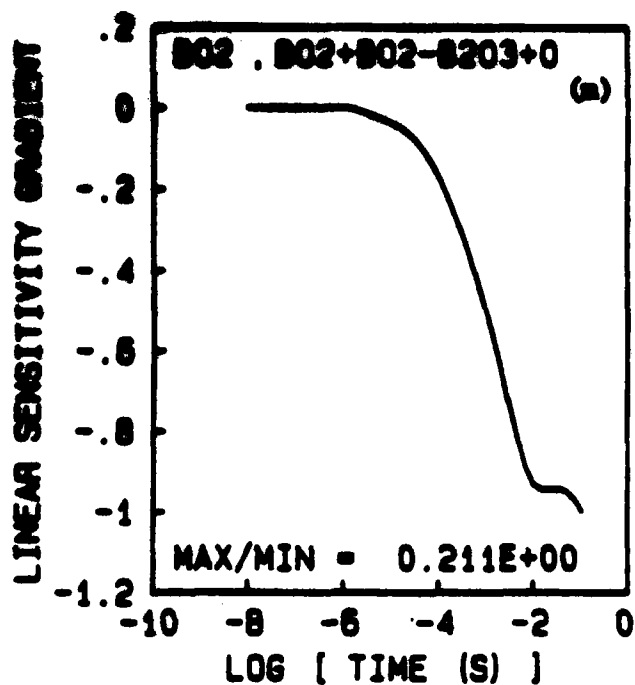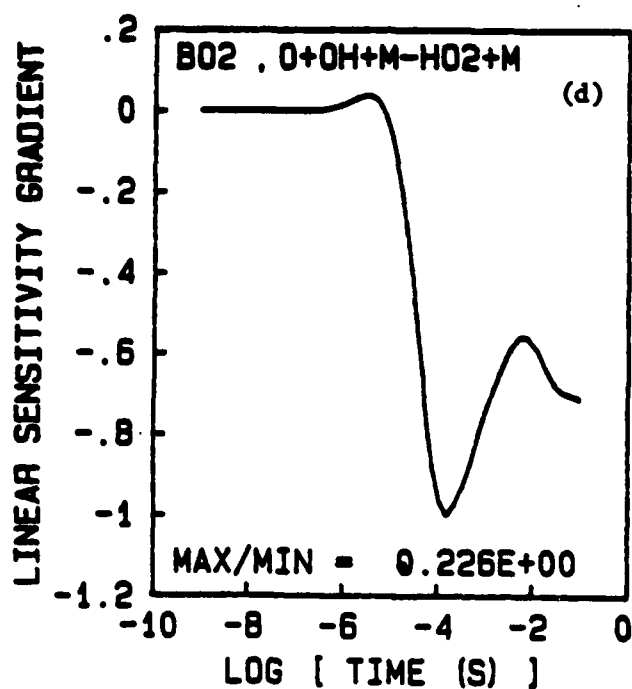
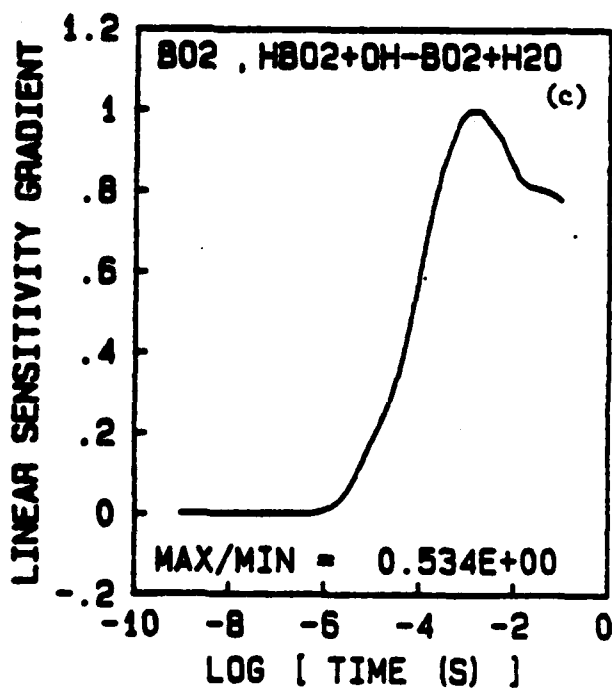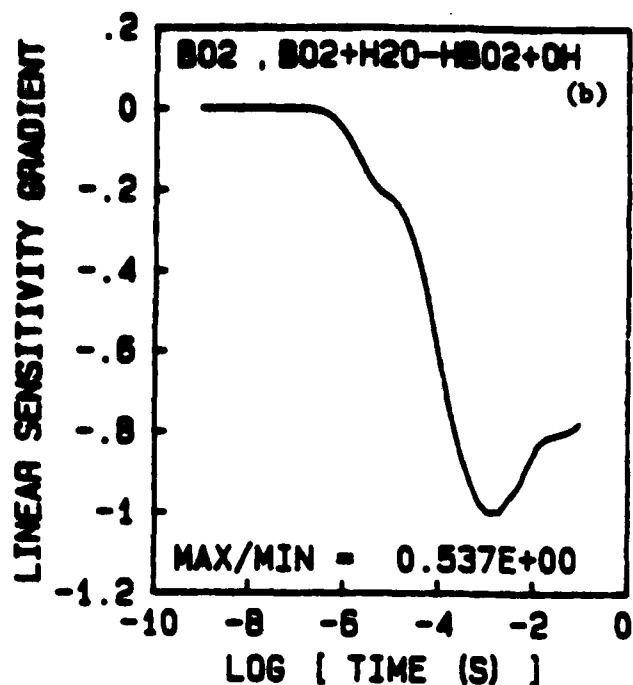Figure 3.19. (Continued) Sensitivity of $BO_2$ Concentration Versus time to Variations in Kinetic Rate Constants for an Isothermal, Constant Volume Mixture of HBO, $H_2$, $CO_2$, $O_2$ and $O_2$

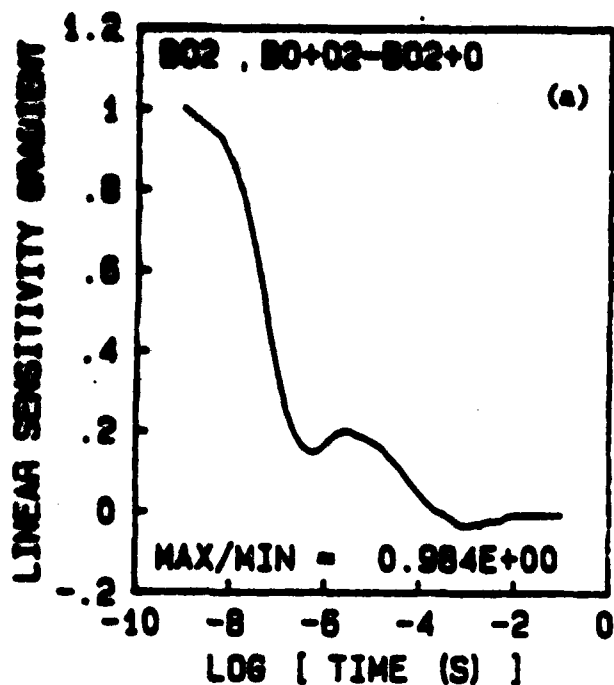Figure 3.19. (Continued) Sensitivity of $BO_2$ Concentration Versus time to Variations in Kinetic Rate Constants for an Isothermal, Constant Volume Mixture of HBO, $H_2$, $CO_2$, $O_2$ and $O_2$
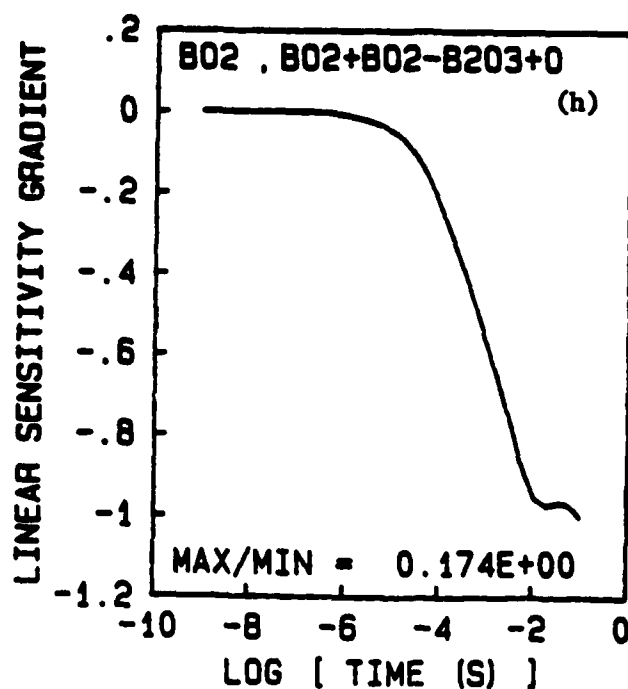
3-63

Figure 3.19. (Continued) Sensitivity of $BO_2$ Concentration Versus time to Variations in Kinetic Rate Constants for an Isothermal, Constant Volume Mixture of HBO, $H_2$, $CO_2$, $O_2$ and $O_2$

Figure 3.20. Sensitivity of $BO_2$ Concentration Versus Time to Variations in Kinetic Rate Constants for an Isothermal, Constant Volume Mixture of BO, $H_2$, $CO_2$, $O_2$ and $N_2$
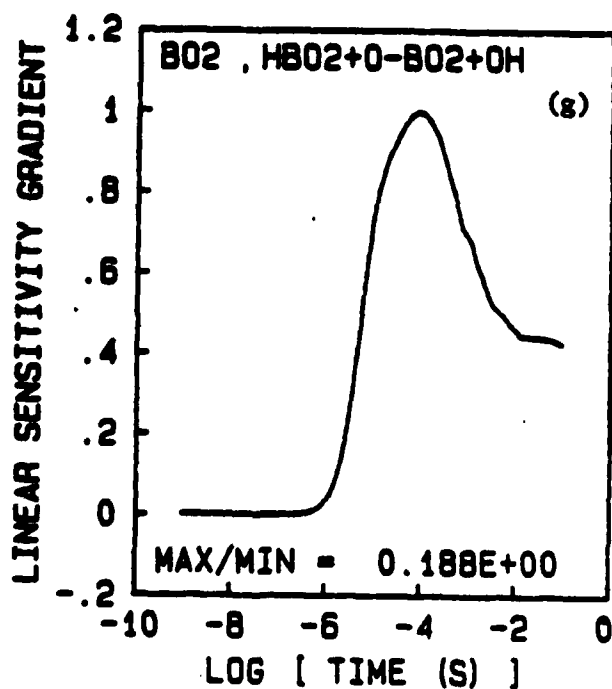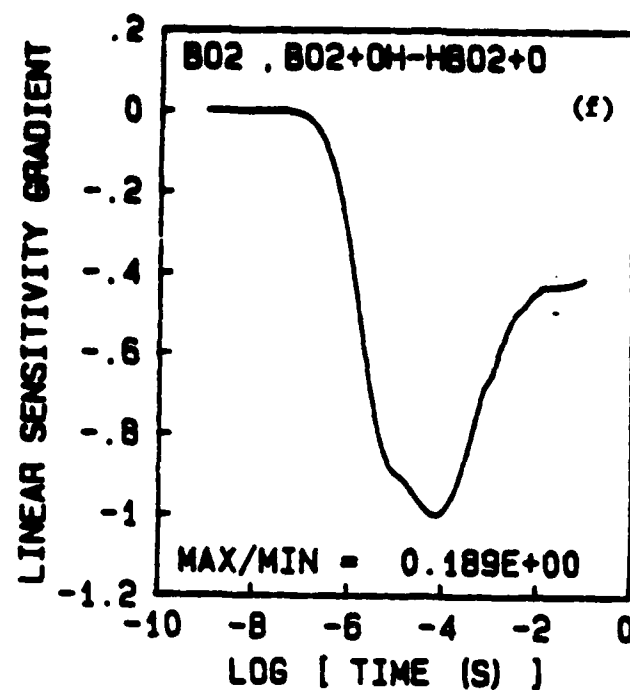
Figure 3.20. (Continued) Sensitivity of $BO_2$ Concentration Versus Time to Variations in Kinetic Rate Constants for an Isothermal, Constant Volume Mixture of BO, $H_2$, $CO_2$, $O_2$ and $N_2$
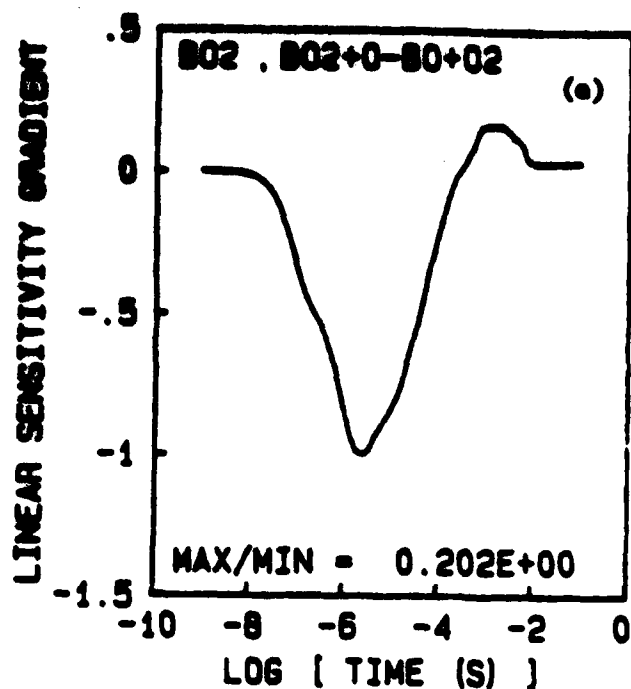
3-66

Figure 3.20. (Continued) Sensitivity of $BO_2$ Concentration Versus Time to
Variations in Kinetic Rate Constants for an Isothermal,
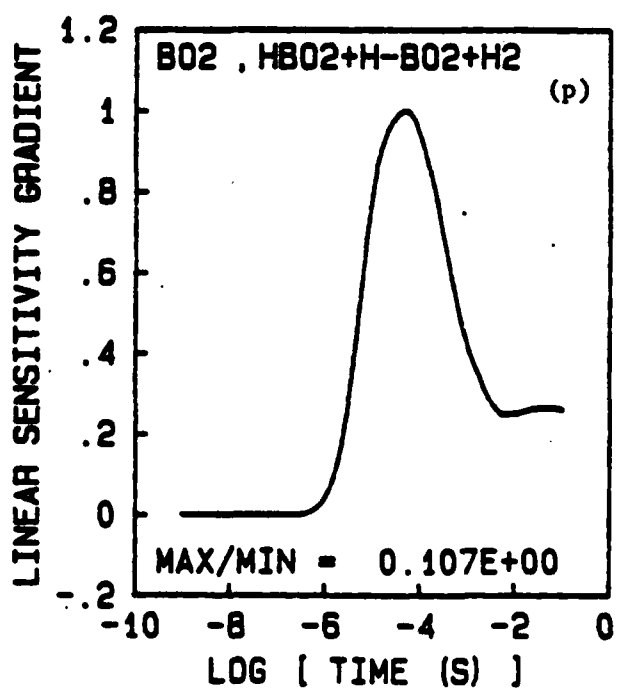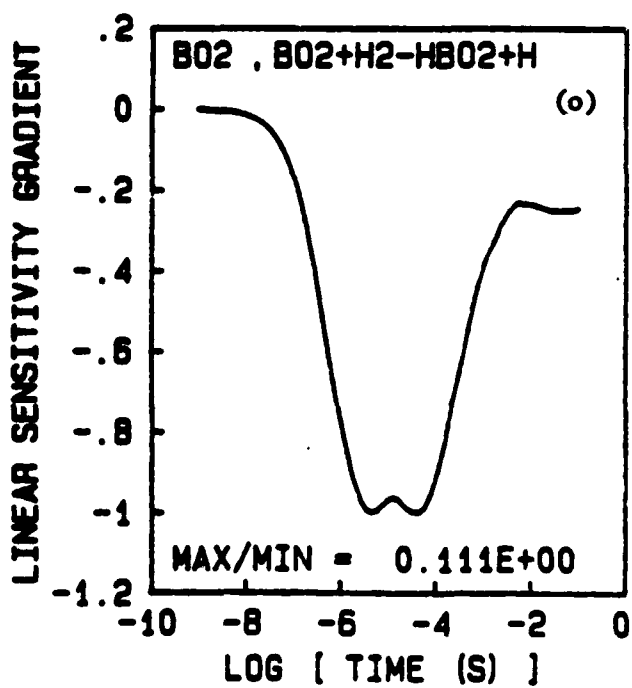Constant Volume Mixture of BO, $H_2$, $CO_2$, $O_2$ and $N_2$
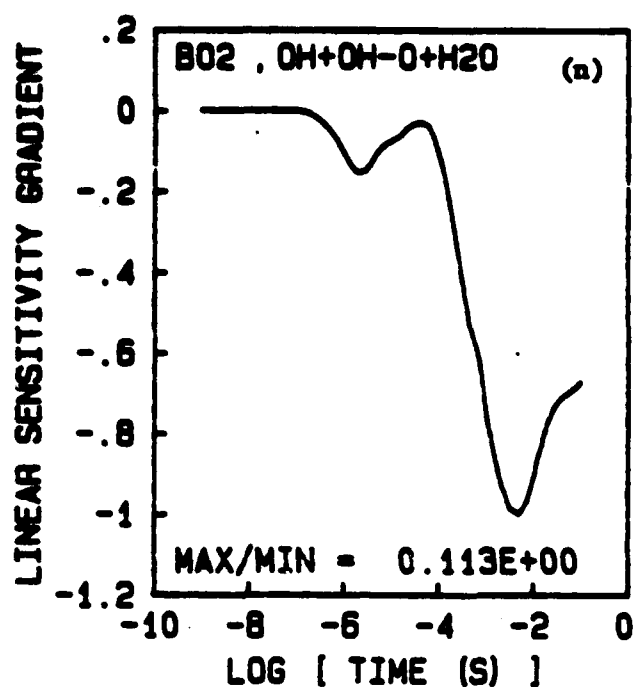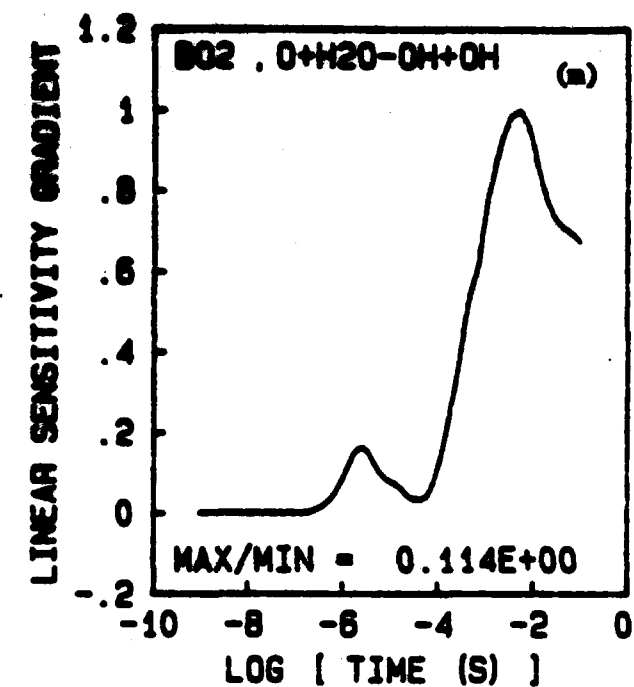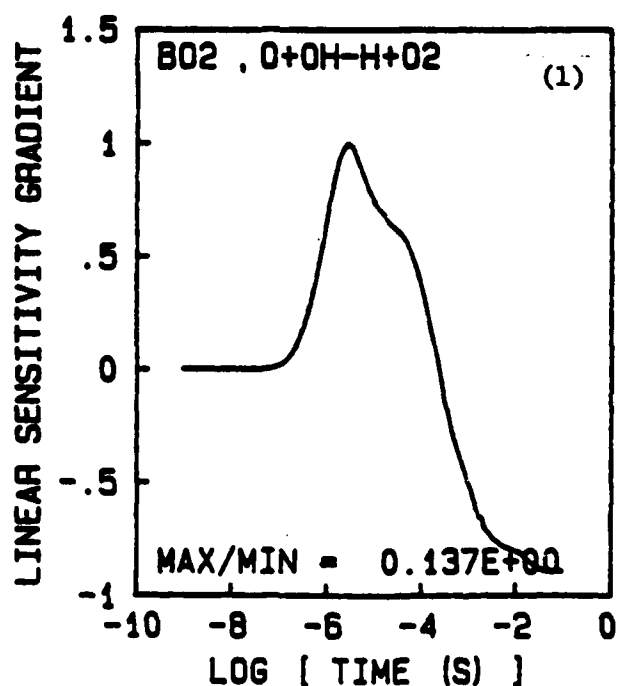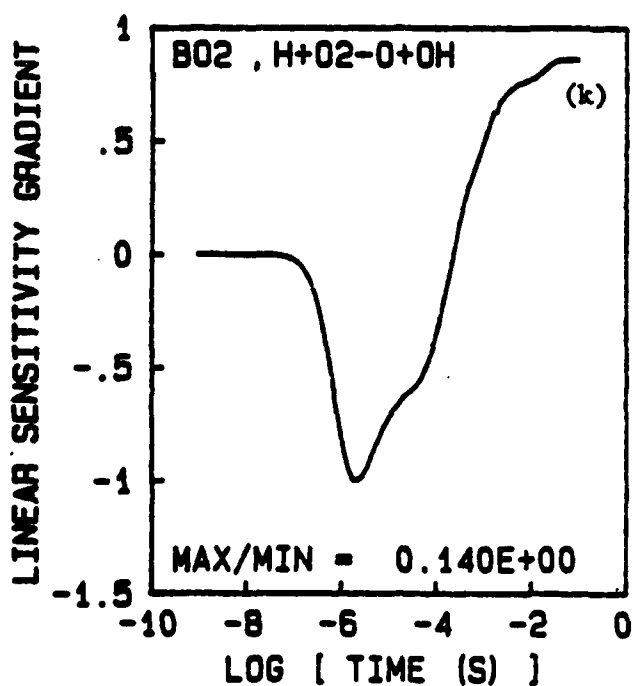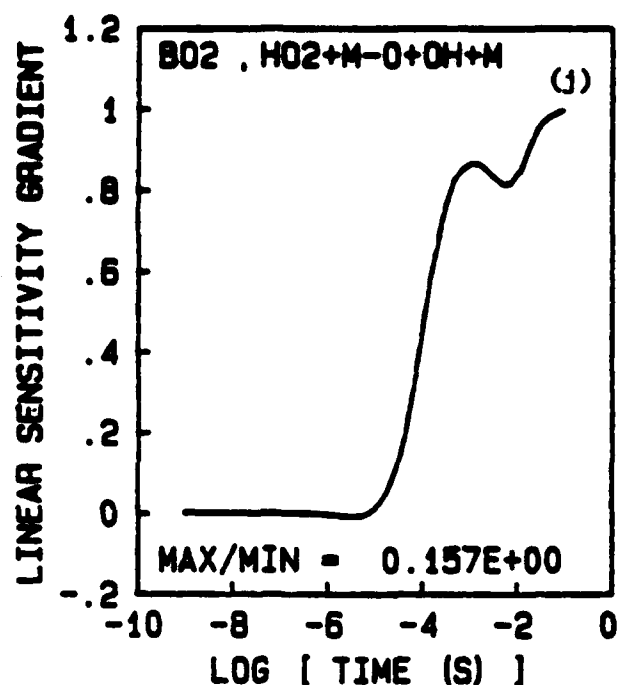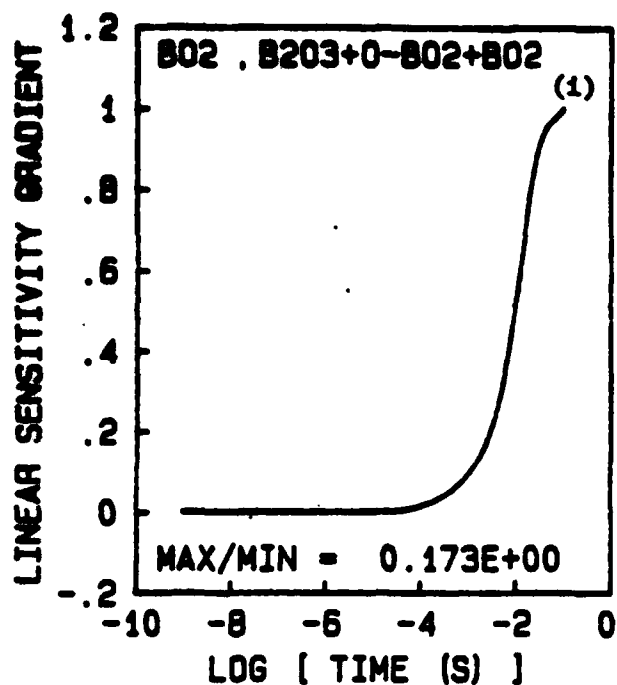
Figure 3.20. (Continued) Sensitivity of $BO_2$ Concentration Versus Time to Variations in Kinetic Rate Constants for an Isothermal, Constant Volume Mixture of BO, $H_2$, $CO_2$, $O_2$ and $N_2$

Considering the HBO system, the reactions most important to the production of $BO_2$ are the branching reaction

$$BO + O_2 \rightarrow BO_2 + O, \tag{R1}$$

the dissociation reaction

$$HBO + M \rightarrow H + BO + M, \tag{R2}$$

and the three abstraction reactions

$$HBO + O \rightarrow BO + OH \text{ (branching)} \tag{R3}$$

$$HBO + OH \rightarrow BO + H_2O \tag{R4}$$

$$HBO + H \rightarrow BO + H_2. \tag{R5}$$

The reactions important to $BO_2$ destruction are,

$$BO + H_2O \rightarrow HBO_2 + OH \tag{R6}$$

$$BO_2 + BO_2 \rightarrow B_2O_3 + O \tag{R7}$$

$$BO_2 + OH \rightarrow HBO_2 + O \tag{R8}$$

and $\quad BO_2 + H_2 \rightarrow HBO_2 + H$ (not shown). $\tag{R9}$

The CO oxidation reaction

$$BO_2 + CO \rightarrow BO + CO_2 \tag{R10}$$
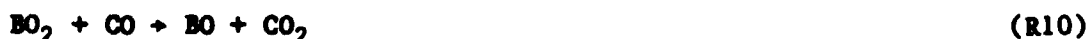
also has significant influence on the $BO_2$ concentration profile.

From the $CO/H_2/O_2$ reaction submechanism, the reactions important to the $BO_2$ concentration profile are the initiation reaction

$$H_2 + O_2 \rightarrow HO_2 + H \tag{R11}$$

and the branching reactions

$$H + O_2 \rightarrow OH + O \tag{R12}$$

$$O + H_2O \rightarrow OH + OH \text{ (not shown)} \tag{R13}$$

and $\quad HO_2 + M \rightarrow O + OH + M.$ $\tag{R14}$

In contrast, the results of Figure 3.20, i.e., the BO system, indicate that the most sensitive reaction to $BO_2$ production is R1. However, the same reactions (R6-R9) are important to $BO_2$ consumption. Since BO reacts directly with molecular oxygen, the initiation reaction, R11, is not important, but the $H_2/O_2$ branching reactions, R12 and R13, remain important.

The significance of backward reactions having gradients of the same magnitude, but of opposite sign as their corresponding forward reactions, as shown in several parts of Figures 3.19 and 3.20, are an indication of the importance of these reactions equilibrium constants on the concentration profile of interest. For example, Figures 3.20(b) and 3.20(c) show that for times greater than approximately 100 µs, the equilibrium constant of $BO_2 + H_2O - HBO_2 + OH$ is more important on the $BO_2$ concentration profile than either the forward or backward reaction rate constants.

Examples of gradients for the H-atom concentration profiles for the three kinetic systems of Figure 3.10, 3.12 and 3.11(c) are shown in Figure 3.21, 3.22, and 3.23, respectively. Comparison of these gradients with those of Figures 3.19 and 3.20 illustrates that the ranking of reactions can change with each species of interest. However, examination of the gradients for all species reveal a general grouping of important reactions. The results of this grouping are reported in the next section.

A detailed examination of the linear sensitivity gradients, as depicted in Figure 3.19 through 3.23, reveals an unlimited amount of information about the underlying kinetic processes. For example, note from Figure 3.22((a) that the formation of HBO in the excess oxygen BO system results from the initiation step

$$BO + H_2 \rightarrow HBO + H \tag{R15}$$

The HBO is rapidly converted back to BO mainly through the propagation reaction
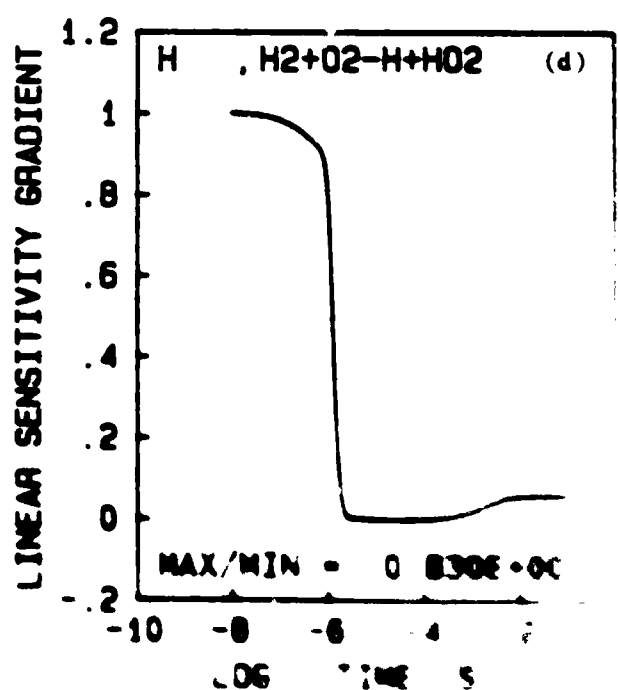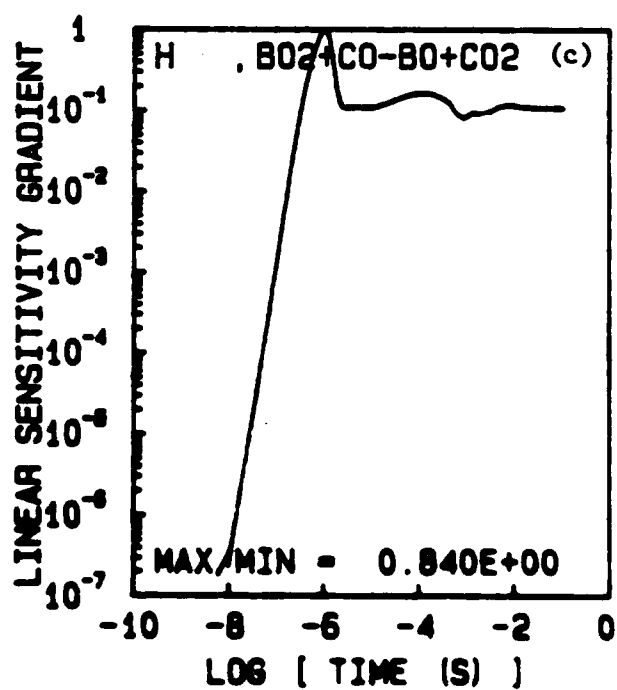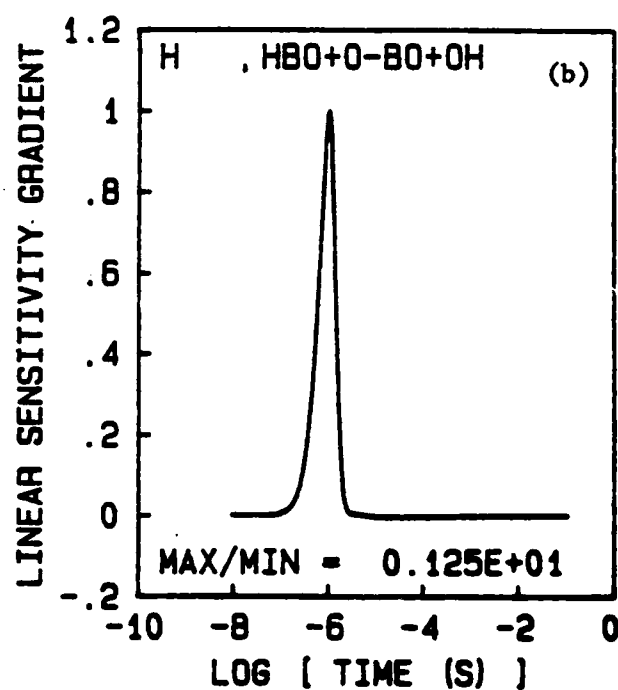
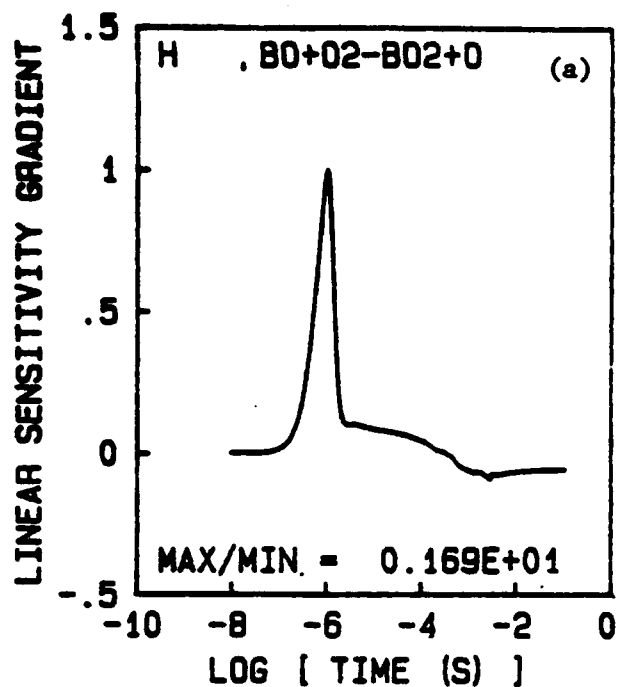$$HBO + OH \rightarrow BO + H_2O \tag{R?}$$

Figure 3.21. Sensitivity of H Concentration versus Time
Kinetic Rate Constants for an isothermal
Mixture of NBO, Hydrocarbon and ... 
Oxygen
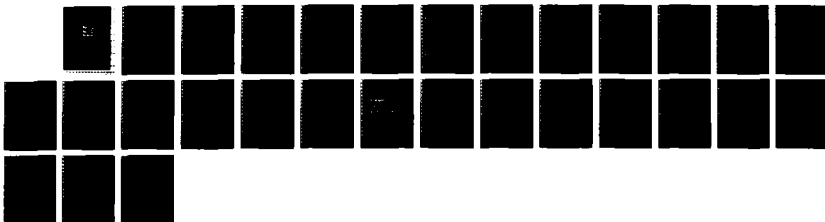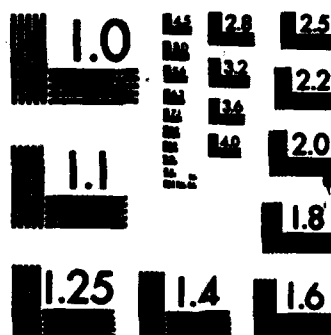
MICROCOPY RESOLUTION TEST CHART
NATIONAL BUREAU OF STANDARDS-1963-A

Figure 3.21. (Continued) Sensitivity of H Concentration Versus Time to Variations in Kinetic Rate Constants for an Isothermal, Constant Volume Mixture of HBO, Hydrocarbon Combustion Products and Excess Oxygen

Figure 3.21. (Continued) Sensitivity of H Concentration Versus Time to
Variations in Kinetic Rate Constants for an Isothermal,
Constant Volume Mixture of HBO, Hydrocarbon Combustion
Products and Excess Oxygen

Figure 3.21. (Continued) Sensitivity of H Concentration Versus Time to Variations in Kinetic Rate Constants for an Isothermal, Constant Volume Mixture of HBO, Hydrocarbon Combustion Products and Excess Oxygen
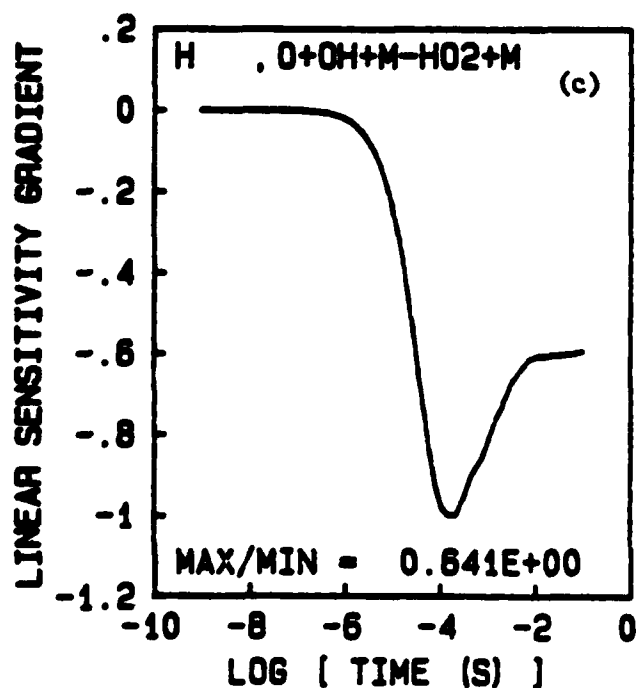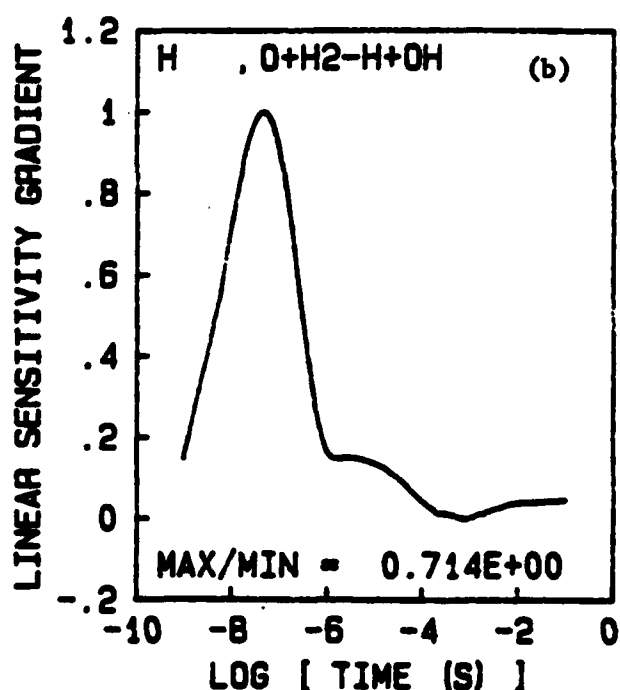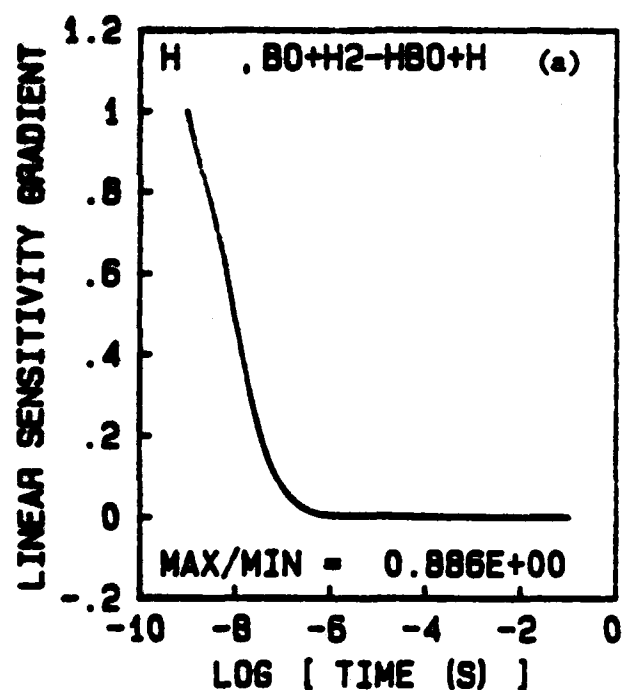
Figure 3.22. Sensitivity of H Concentration Versus Time to Variations in Kinetic Rate Constants for an Isothermal, Constant Volume Mixture of BO, Hydrocarbon Combustion Products and Excess Oxygen

Figure 3.22. (Continued) Sensitivity of H Concentration Versus Time to Variations in Kinetic Rate Constants for an Isothermal, Constant Volume Mixture of BO, Hydrocarbon Combustion Products and Excess Oxygen
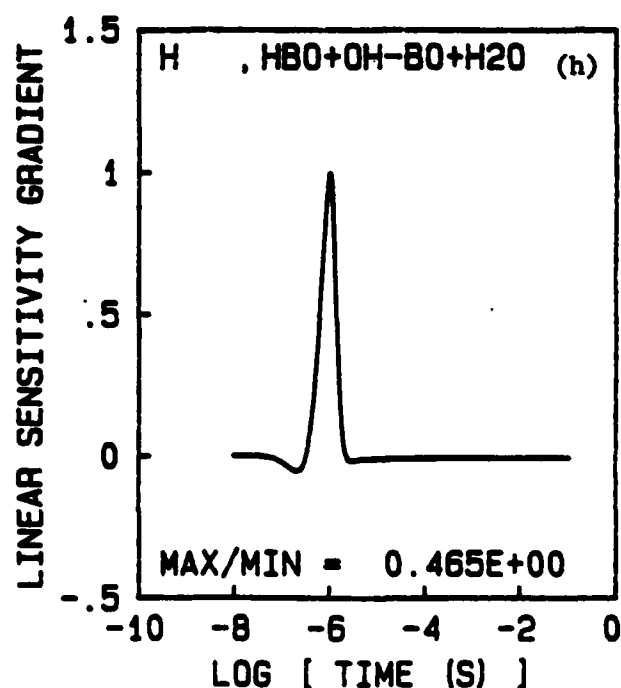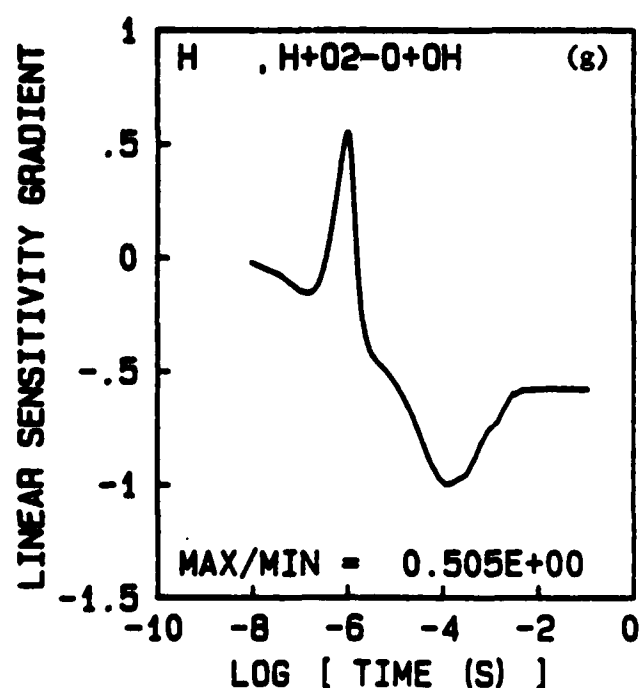
Figure 3.22. (Continued) Sensitivity of H Concentration Versus Time to Variations in Kinetic Rate Constants for an Isothermal, Constant Volume Mixture of BO, Hydrocarbon Combustion Products and Excess Oxygen
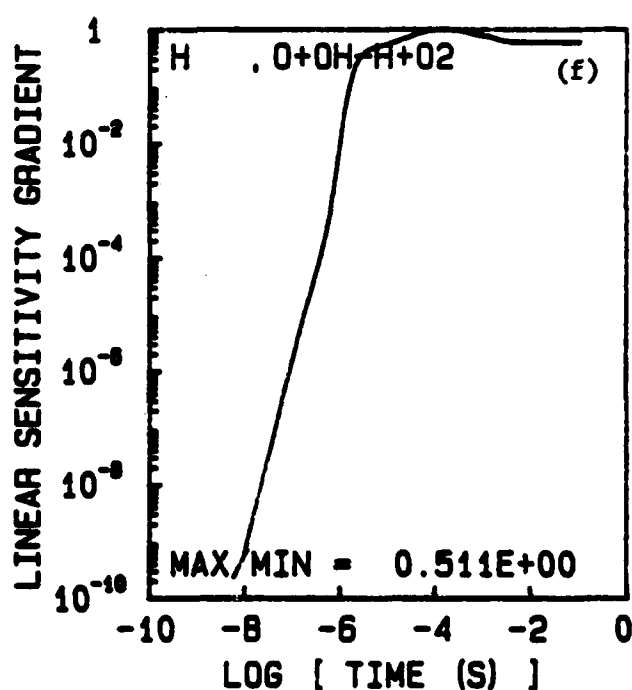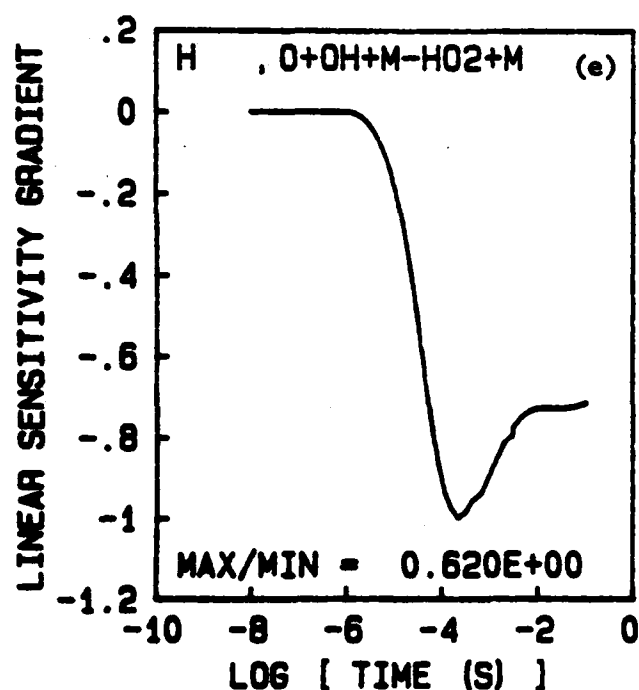
3-77

Figure 3.22. (Continued) Sensitivity of H Concentration Versus Time to Variations in Kinetic Rate Constants for an Isothermal, Constant Volume Mixture of BO, Hydrocarbon Combustion Products and Excess Oxygen

Figure 3.22. (Continued) Sensitivity of H Concentration Versus Time to Variations in Kinetic Rate Constants for an Isothermal, Constant Volume Mixture of BO, Hydrocarbon Combustion Products and Excess Oxygen
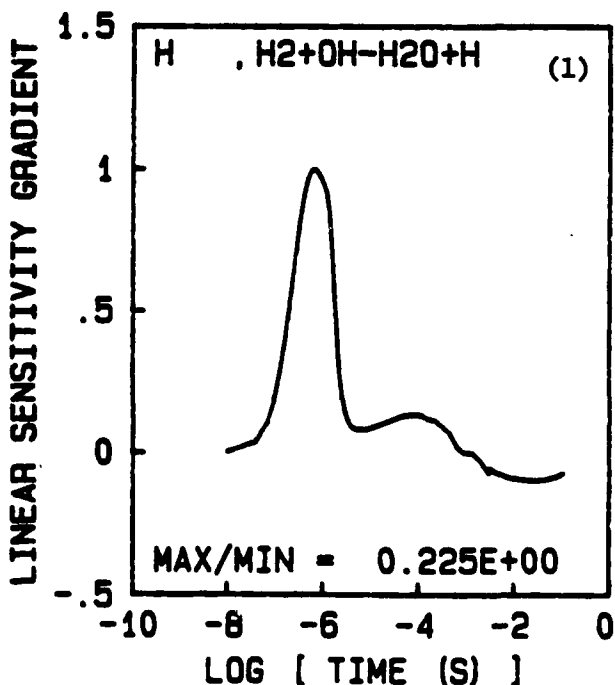
Figure 3.22. (Continued) Sensitivity of H Concentration Versus Time to Variations in Kinetic Rate Constants for an Isothermal, Constant Volume Mixture of BO, Hydrocarbon Combustion Products and Excess Oxygen
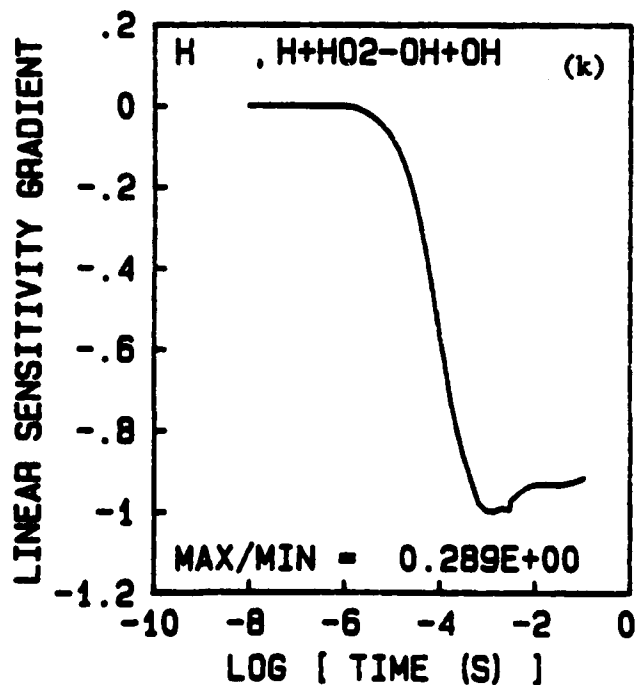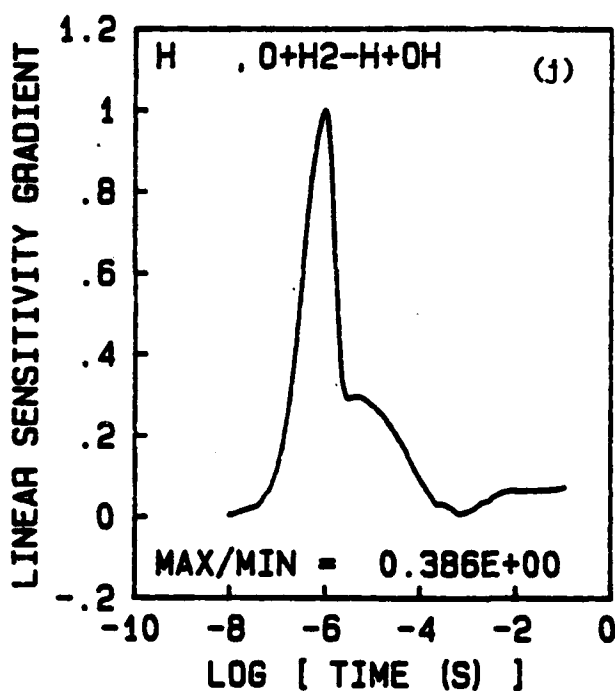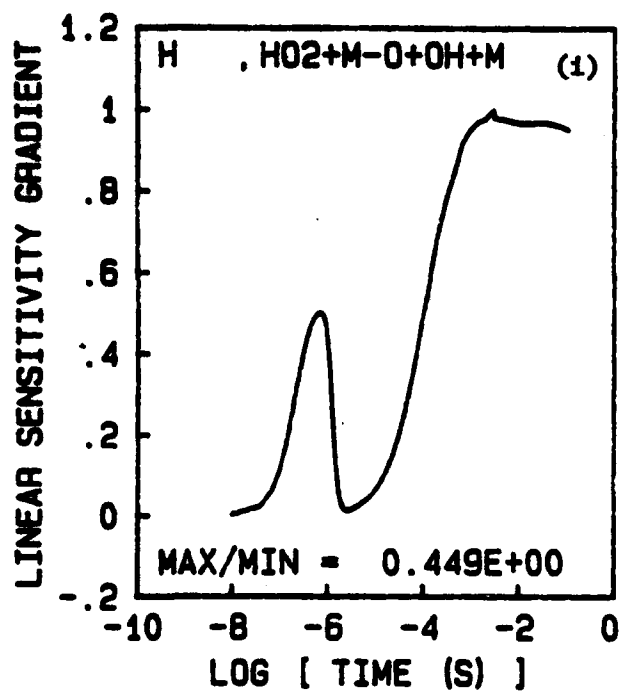
3-80

Figure 3.23. Sensitivity of H Concentration Versus Time to Variations in Kinetic Rate Constants for an Oxygen Deficient Mixture of HBO and Hydrocarbon Combustion Products

Figure 3.23. (Continued) Sensitivity of H Concentration Versus Time to Variations in Kinetic Rate Constants for an Oxygen Deficient Mixture of HBO and Hydrocarbon Combustion Products
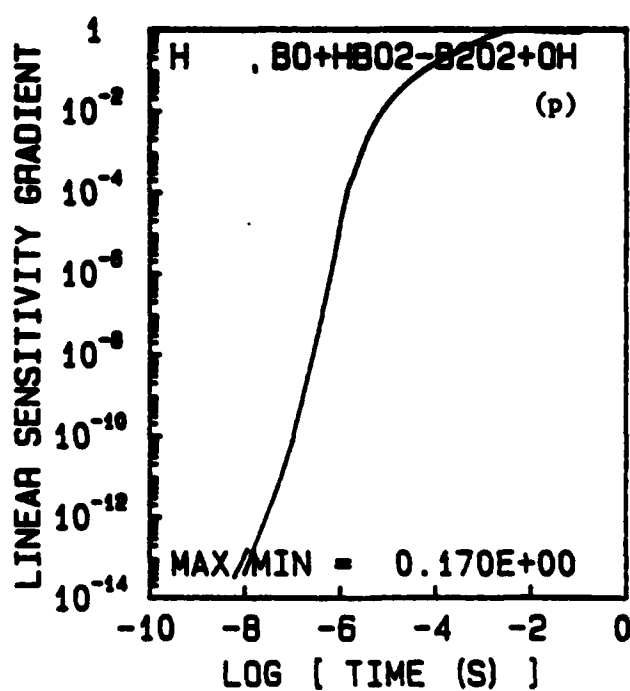
Figure 3.23. (Continued) Sensitivity of H Concentration Versus Time to
Variations in Kinetic Rate Constants for an Oxygen Deficient
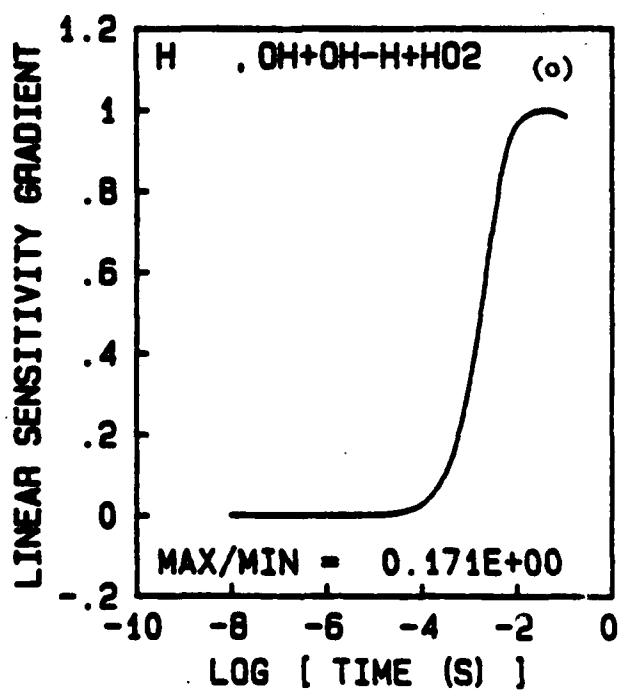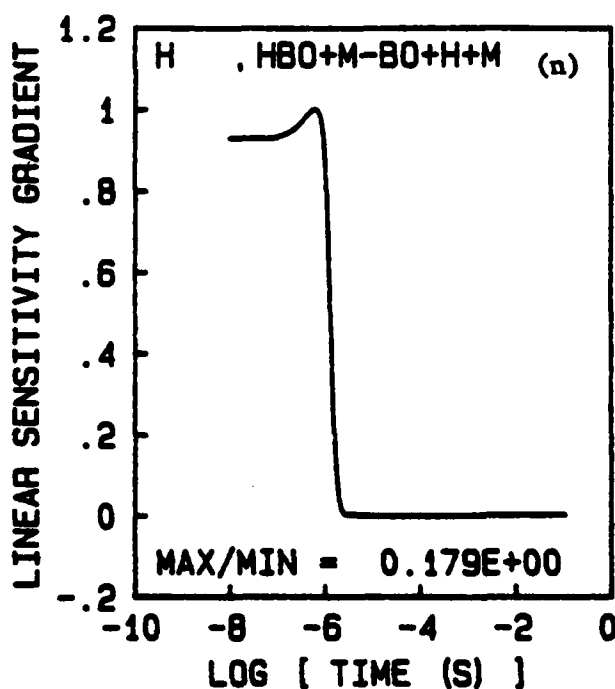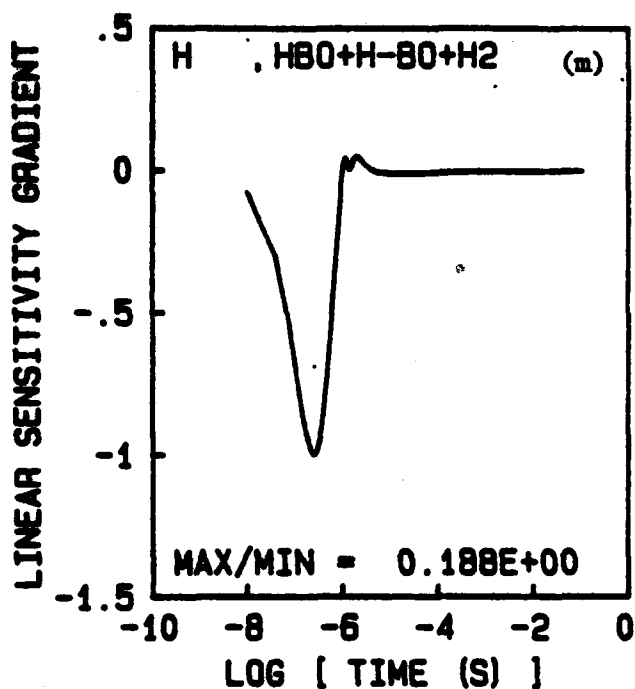Mixture of HBO and Hydrocarbon Combustion Products

3-83

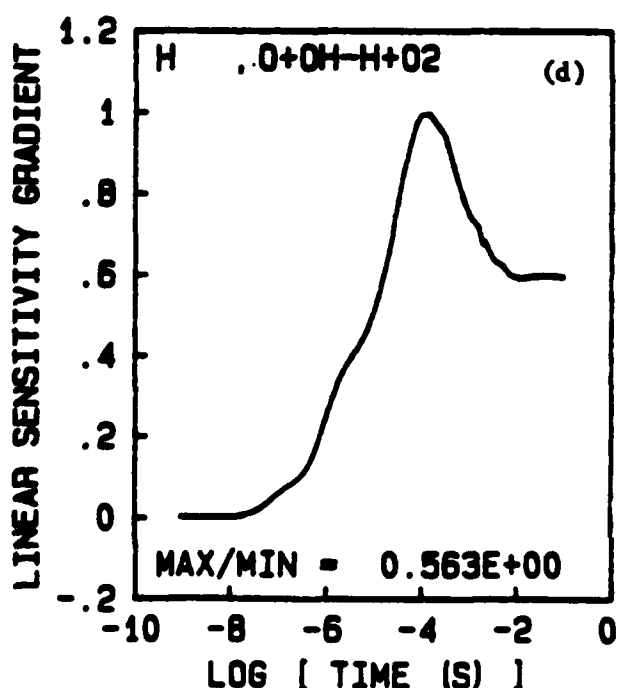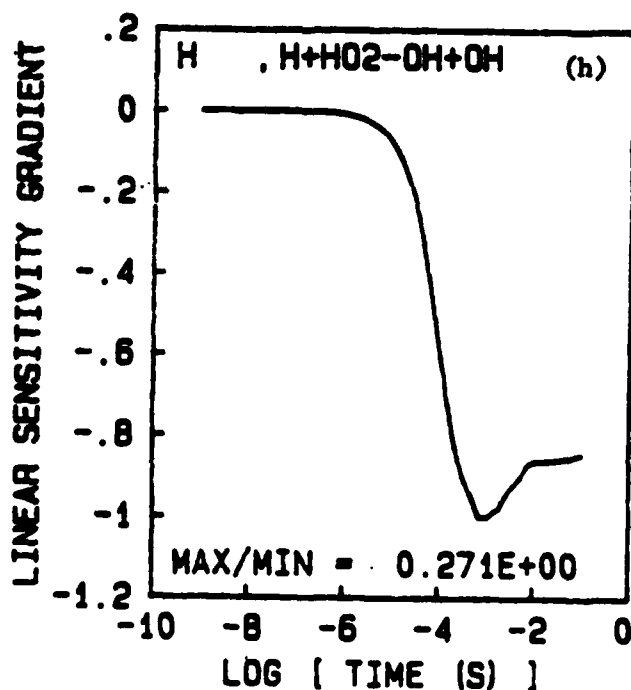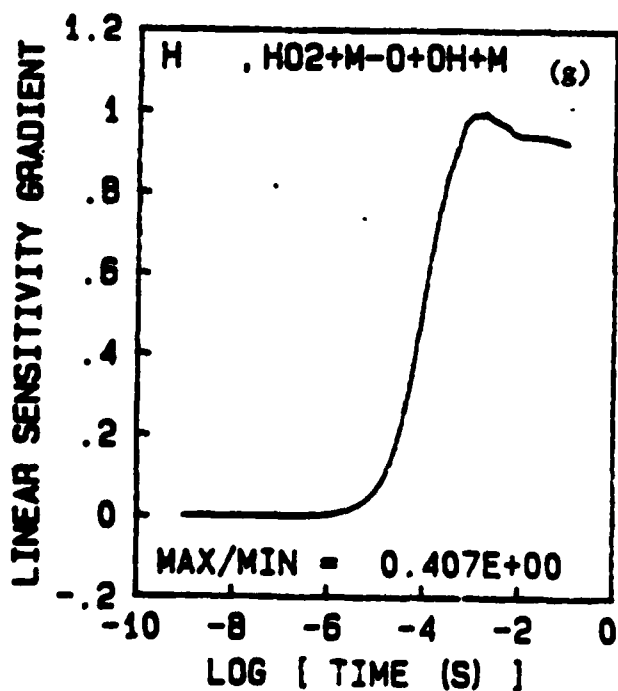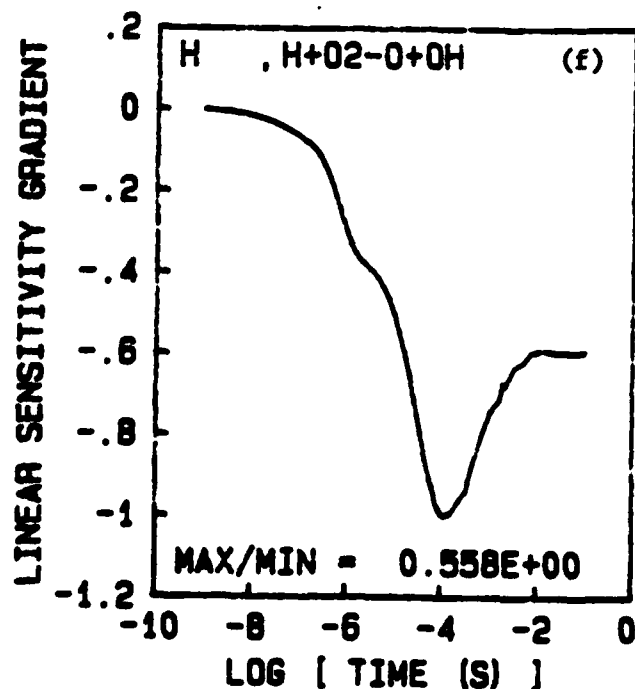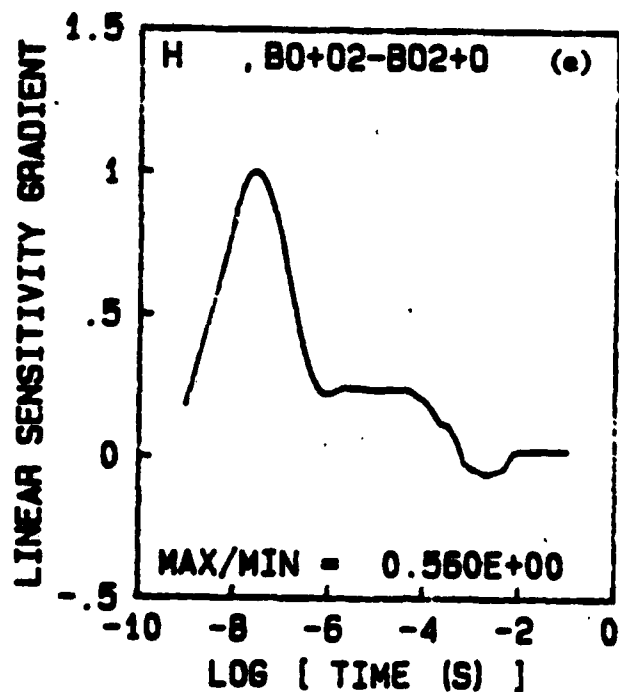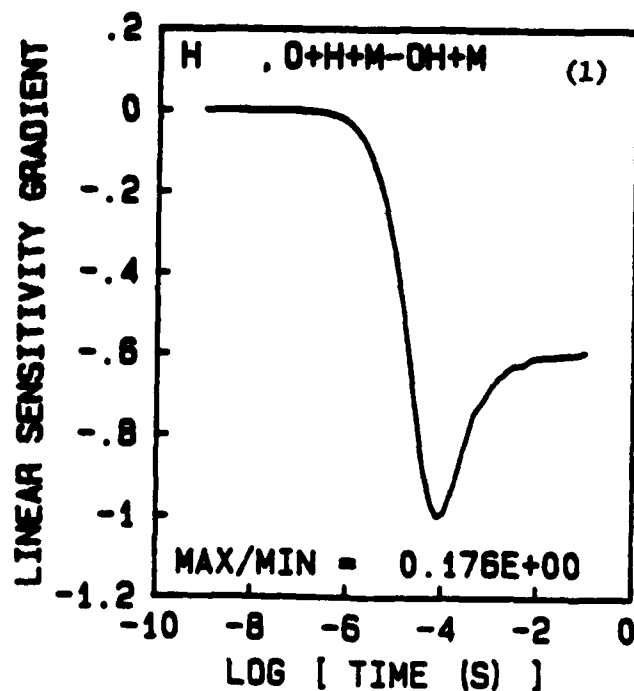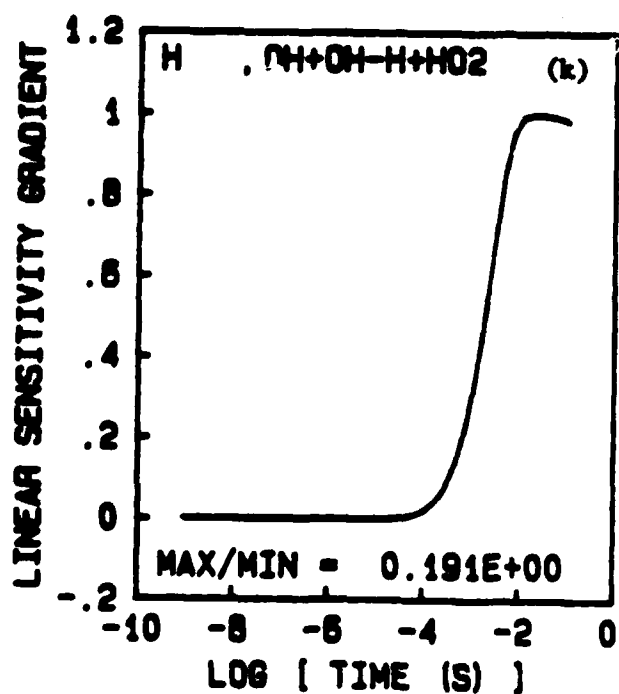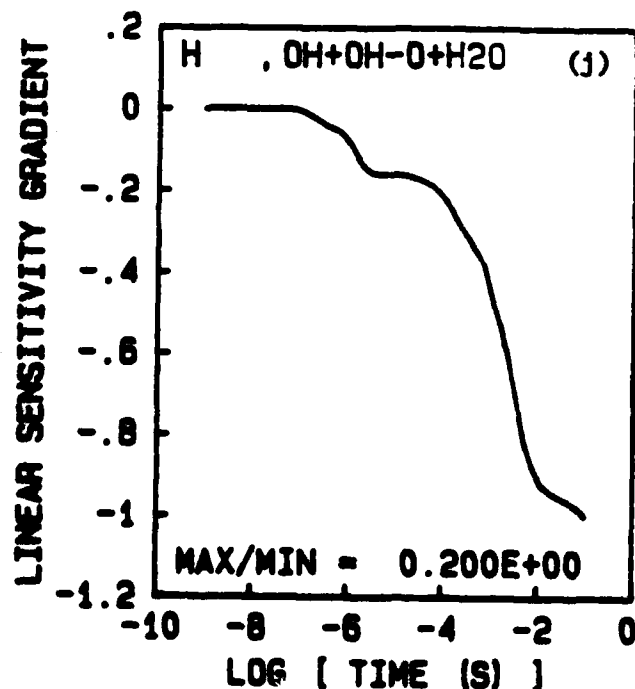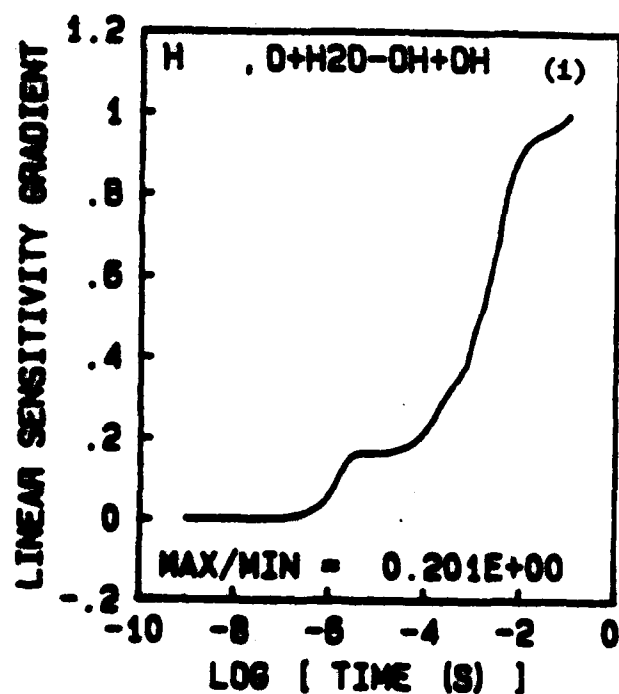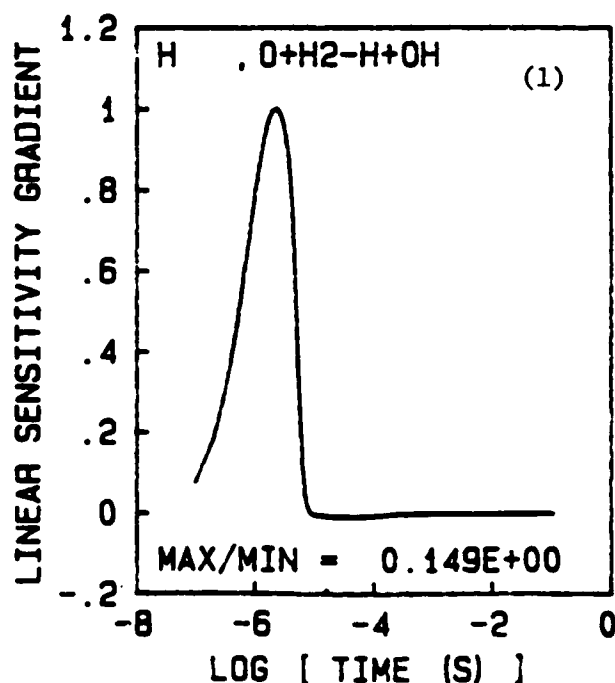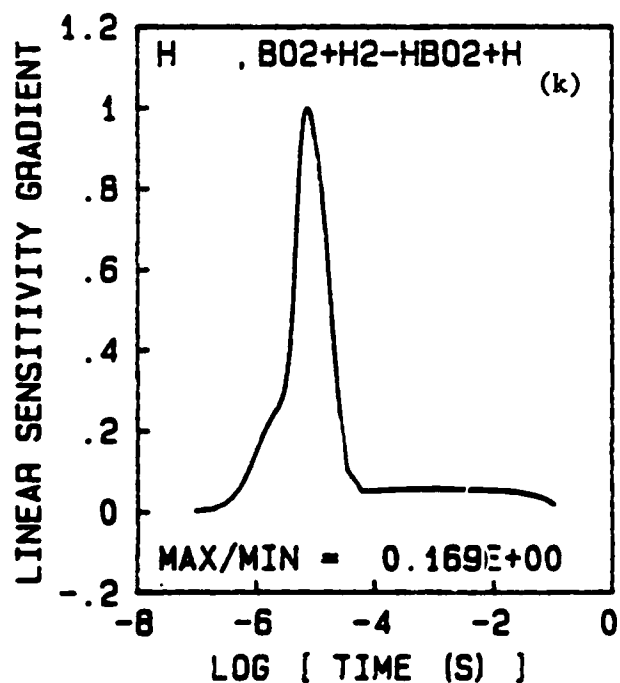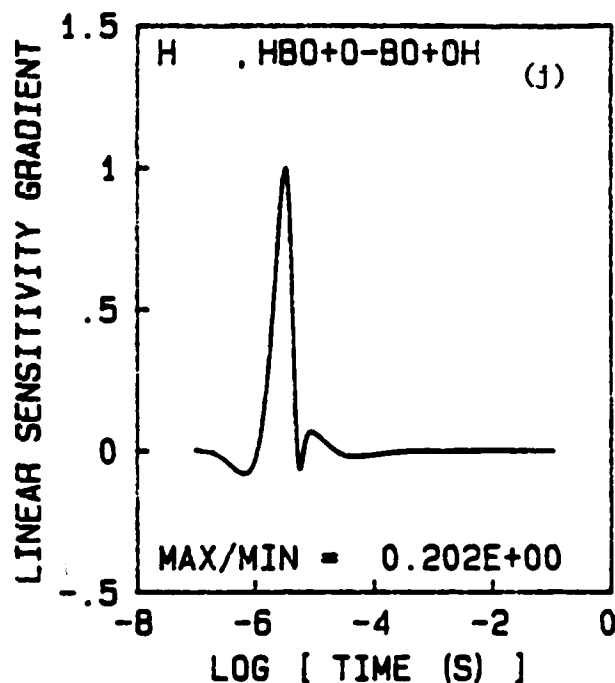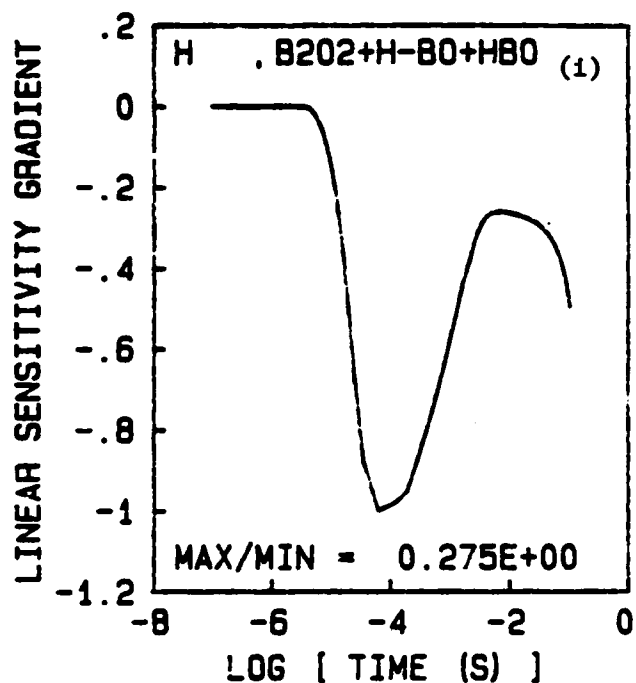Figure 3.23. (Continued) Sensitivity of H Concentration Versus Time to Variations in Kinetic Rate Constants for an Oxygen Deficient Mixture of HBO and Hydrocarbon Combustion Products

Or note that in the $O_2$ deficient system, the reaction $BO + O_2 \rightarrow BO_2 + O$ is again an important branching reaction.

## 3.6 Critical Reaction Pathways

The critical reaction pathways were determined by examining all the linear sensitivity gradients $\partial \ln C_i / \partial \ln P_j$. The most sensitive boron reactions were selected as those which had gradient values within 2 orders of magnitude of the maximum gradient value for a particular species. The results of this ranking for excess oxygen systems is tabulated in Table 3-8. For oxygen deficient systems, the $B_2O_2$ reactions listed in Table 3-9 were found important in addition to those reactions listed in Table 3-8.

## 3.7 Extension of Sensitivity Analysis Techniques

Currently available sensitivity analysis techniques have already been put to significant use in the first-phase of our boron combustion study (see Section 3.5 and 3.6 for details). The present studies have focused on gas-phase chemistry alone and we have therefore been able to directly utilize existing computer coding and experience gained from sensitivity and modelling studies of an allied nature. A complete model for particulate boron assisted hydrocarbon combustion, however, must incorporate heterogeneous and transport processes. In addition, the complexities of the physical and chemical events makes it highly desirable to search for any simplifying clues hidden in the kinetic behavior. This latter issue is directly connected with the possibility of scaling and self similarity behavior existing amongst the strongly coupled kinetic species in the boron particle combustion system. Therefore, in the first phase of this project we have examined two topics: a) the need for modifications of existing sensitivity analysis techniques for particle-gas phase transport and surface kinetics; b) the development, analysis and physical understanding of scaling and self-similarity behavior in kinetic systems. The current status of these two items is summarized below.

Table 3-8 - Critical Elementary Reactions for Oxygen Rich Combustion
Homogeneous

<u>HBO/BO REACTIONS</u>

$$HBO + OH \rightarrow BO + H_2O$$ (important when HBO
$$HBO + O \rightarrow BO + OH$$ is initial reactant)
$$HBO + O \rightarrow BO_2 + H$$
$$HBO + H \rightarrow BO + H2$$
$$HBO + M \rightarrow BO + H + M$$

$$BO + OH \rightarrow BO_2 + H$$ (important when BO
is initial rectant)

<u>BO_2 REACTIONS</u>

$$BO + O_2 \rightarrow BO_2 + O$$
$$BO_2 + CO \rightarrow BO + CO_2$$

<u>HBO_2 REACTIONS</u>

$$BO_2 + H + M \rightarrow HOBO + M$$
$$BO_2 + H_2O \rightarrow HOBO + M$$
$$BO_2 + OH \rightarrow HOBO + O$$
$$BO_2 + H_2 \rightarrow HOBO + H$$

$$HBO + OH \rightarrow HOBO + H$$ (important when HBO
is initial reactant)

<u>B_2O_3 REACTIONS</u>

$$BO_2 + BO_2 \rightarrow B_2O_3 + O$$
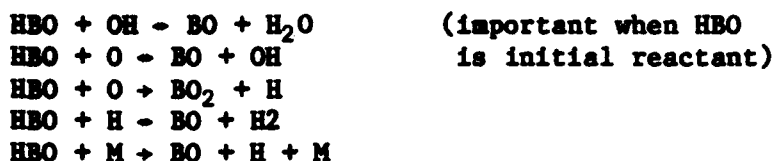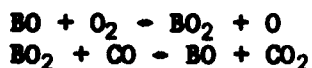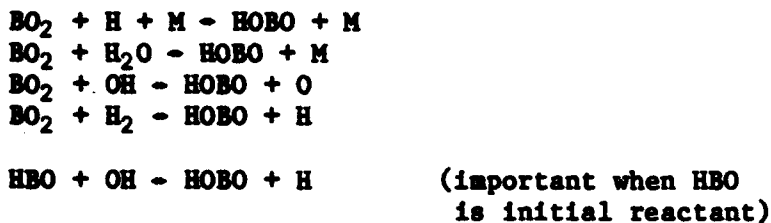
Table 3-9 - Critical Reactions for Fuel Rich Homogeneous Combustion

<u>B_2O_2 REACTIONS</u>

$$BO + HBO \rightarrow B_2O_2 + H$$
$$BO + BO + M \rightarrow B_2O_2 + M$$
$$BO + HOBO \rightarrow B_2O_2 + OH$$

3-86
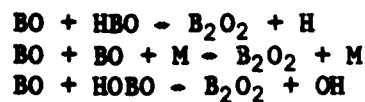
### 3.7.1 Sensitivity Analysis Techniques as Applied to Boron Particle-Gas Phase Transport and Heterogeneous Surface Reactions

Many of the general sensitivity analysis techniques needed to treat the various aspects of boron particle combustion are already available from prior applications to other kinetics problems. The one exception to this situation may be encountered when condensation phenomena are ultimately included. Since modeling of the product condensation phase of boron combustion will only occur at an advanced stage of the research it will not be discussed here. Instead we will focus on the initial heterogeneous burning phase. Currently, the basic two problems are 1) transport of chemical species and energy to/from the particle surface, and 2) reaction and transport on the particle surface. Regarding both types of problems it is important to note that other steady and unsteady reaction diffusion problems including sensitivity analysis have already been treated. The primary distinction is that these latter studies have thus far been restricted to one spatial dimension, although there is no inherent reason (except for the level of computational effort) constraining them in this way. One immediate application even in one dimension arises by treating the boron particle burn-up problem as purely radial. Relaxation of this idealization would require the introduction of an angular variable. The basic mathematical formulation is already in hand, but careful consideration to computer coding and efficiency would have to be made. In the case of adsorption, desorption, diffusion and reaction occurring on the boron particle surface, the physical and mathematical formulation is quite similar to the latter gas-phase processes. The surface problem is further compounded by the fact that the surface may be heterogeneous with defects. An important caveat is that the proper parametric values for virtually all of the surface processes are far more speculative than in the gas-phase. This situation calls for special care when interpreting the results, but also provides an even more serious role for sensitivity analysis as a means to guide further modeling and experimental efforts.

The gas-phase and surface processes are intrinsically coupled although a first cut at these problems would treat them separately involving source fluxes to/from each phase. For example, the current gas-phase modeling/sensitivity effort could easily be extended to include flux inputs and outputs of species and energy to/from the boron particle. Similarly, the processes on the particle surface could also be treated with gas-phase fluxes as source/sink terms. The full combination of both coupled system might still be fruitfully treated by splitting techniques whereby each aspect of the problem is alternatively solved in a bootstrap type process. All of the particulars of these issues will be explored and implemented in the insuing research.

### 3.7.2 Scaling and Self Similarity Relations in Kinetics

A kinetic system with N chemical species and M parameters may exhibit a variety of complex behavior regardless of whether it is steady or unsteady. In addition, the number of basic questions or interrelationships between the various variables will give rise to N(N+M) sensitivity coefficients as a measure of the system coupling. Each of these coefficients in turn will be a function of the coordinates and/or time. As we have already seen in the present first phase of the project the analysis of these coefficients can provide a critical guide to physical understanding and intelligent planning of subsequent experiments. From a number of previous kinetic studies an intriguing prospect of significantly simplifying this problem has arisen. In particular, evidence exists for the presence of scaling and self similarity relations amongst all the system sensitivity coefficients under appropriate conditions.

The scaling relations take on the following form for a purely temporal problem

$$\left[\frac{\partial C_n(t)}{\partial \alpha_j}\right] = \left[\frac{\partial C_m(t)}{\partial \alpha_j}\right]\left[\frac{\partial C_n}{\partial t} \quad \frac{\partial C_m}{\partial t}\right]^{-1}$$

where $\alpha_j$ is a system parameter such as rate constant and $C_n$ is a chemical species concentration. This scaling relation shows that knowledge of the sensitivities to one chemical species may be used to deduce others by simply scaling it with a ratio of the species fluxes. Even more remarkable are the self similarity conditions which have the form

$$\frac{\delta C_n(t)}{\delta \alpha_j} \propto \lambda_n(t)\sigma_j$$

where

$$\lambda_n(t) \propto \lambda_m(t) \left[\frac{\delta C_n}{\delta t}\right]\left[\frac{\delta C_m}{\delta t}\right]^{-1}$$

The functions $\lambda_n(t)$ are characteristic of the chemical mechanism and can most easily be identified from the temporal behavior of the sensitivity coefficients. In contrast, the coefficients $\alpha_j$ are constant in time but otherwise complicated functions of all the systems parameters. The self similarity relation is consistent with the scaling relation but goes further to imply that knowledge of one vector of constants $\bar{\sigma}$ and a single function $\lambda_m(t)$ will yield all of the system sensitivity coefficients.

The relations above are only approximate and a critical issue is to establish their realms of validity. The evidence available thus far implies that these relations are most valid when the system is characterized by a strong nonlinear coupling, such as through the temperature. Some of the current gas-phase boron combustion sensitivity analysis calculations show evidence of these relations and the matter will be explored further in the second phase of the research. The primary motivation for this effort is to fully utilize any systematic behavior found in the kinetic system. An important spin-off of these results concerns their potential generality since they should be applicable to a variety of other similar problems.

As in the present first phase study, it is anticipated that sensitivity techniques will continue to provide a powerful means to analyze the physical models. In addition as the experimental aspects of this project ultimately develop sensitivity analysis will be used in a recursive way to assess the theoretical and physical implications the new experimental information.

## 3.8 References for Section 3

3-1 JANAF Thermochemical Tables, 2nd Edition, Stull, D.R., Prophet, H., et. al., eds., NSRDS-NBS 37, US Govt. Printing Office, Washington, DC, 1971, and supplements.

3-2 Zynbina, F.S., Charkin, O.P. and Gurvich, L.V., "Ab Initio Calculations of the Potential Surfaces and Minimum Energy Paths of Intramolecular Rearrangements, 1. Heterovalent Isomerism in the System BOH → HBO," Translated from Zhurnal Structurnio Khimii, Vol. 20, No. 1, pp. 3-11, (1979).

3-3 Oldenborg, R.C. and Baughcum, S.L., "Gas Phase Oxidation of Boron Compounds," Abstracts of the 1986 AFOSR/ONR Contractors Meeting on Combustion, Standford University (June 1985).

3-4 DiGiuseppe, T.G. and Davidovits, P., "Boron Atom Reactions II Rate Constants with $O_2$, $SO_2$, $CO_2$ and $H_2O$," J. Chem. Phys. 74, 3287 (1981).

3-5 Llewellyn, I.P., Fontijn, A., and Clyne, M.A.A., "Kinetics of the Reaction of BO + $O_2$ → $BO_2$ + O," Chem. Phys. Letts. 84, 504 (1981).

3-6 DiGiuseppe, T.G., Estes, R., and Davidovits, P., "Boron Atom Reactions and Rate Constants with $H_2O$, $H_2O_2$, Alchols and Ethers," J. Phys. Chem. 86, 260 (1986).

# 4. CONCLUSIONS AND RESEARCH RECOMMENDATIONS

## 4.1 Summary of Results and Conclusions

The model results and sensitivity analysis presented in Section 3 fulfill the major goal of our first phase effort; the basic dependencies of homogeneous boron suboxide and boron oxyhydride oxidation are clearly elucidated and critical reaction paths (and their associated rate constants) and key interconversion equilibria are highlighted for further refinement. Our secondary goal of identifying issues to be addressed in extending the model to the heterogeneous ignition and product condensation phases was also addressed.

Among the major research conclusions are:

1) The presence of hydrogen containing species ($H_2O$, OH, H, $H_2$) has a significant impact on both the identity of species evolved from reacting boron particles and on their subsequent oxidation rate, as well as the rate of heat release.

2) The initial identity of the boron oxide and oxyhydride species evolved from the particulate boron influences the oxidation chemistry for a very short time period (typically on the order of a microsecond); subsequent oxidation chemistry at reasonable O/F ratios is only mildly dependent on the identity of initially vaporized species including B, BO, HBO and $B_2O_2$. This fact validates our decision to model the homogeneous combustion phase chemistry without being able to fully specify the kinetic distribution of initially volatilized boron species from ignited particles.

3) As revealed by our sensitivity analysis, a relatively small set of kinetic and equilibrium processes appear to dominate the boron oxidation pathways. As discussed in Subsection 4.2, this allows the identification of key kinetic and thermochemical parameters which need further experimental and/or theoretical refinement if a more accurate model is desired.

4) The most important issues associated with extending our boron combustion model and concomitant kinetic sensitivity analysis techniques to the initial particle ignition and heterogeneous burn phase of boron combustion have been identified. These include transport of chemical species and energy to/from the particle surface and kinetic processes on the surface. This initial analysis suggests that both processes may be treated with existing sensitivity analysis techniques by invoking two simplifications. First, the gas phase and surface processes would be treated separately (as in the present work), but source and sink terms corresponding to species and energy fluxes would be incorporated into the kinetic equations. Second, reaction and transport to and from the particle surface would be modeled for one spatial dimension (e.g., the radial dimension). This would provide an initial model for the heterogeneous burn, a more realistic model for the gas phase oxidation kinetics, and build in a coupling between the two phases using chemical species fluxes. On the basis of this work, it would be possible to evaluate the validity of scaling and self-similarly relations.

5) A better defined (but possibly incomplete) model of homogeneous boron assisted hydrocarbon combustion now exists and can be used to study a number of energetic combustion and propulsion systems of interest to the Department of Defense community. Several of these are discussed in Subsection 4.3.

## 4.2  Recommendations for Further Research

The work described in this report has significantly increased our current understanding of the homogeneous gas phase kinetics for boron-assisted hydrocarbon combustion. However, achieving a reliable model for a boron fueled combustor will require further research on several fronts. This includes the development of models for the initial heterogeneous burn and final condensation stages of boron-assisted combustion, in conjunction with experimental work which can provide accurate values for key thermochemical and kinetic parameters, as well as validation of the various combustion models.

In subsections 4.2.1 and 4.2.2 below, we briefly discuss our recommendations for further experimental and modeling work. It is imperative, however, to note that real progress in this field requires that the modeling and experimental work be closely interrelated. In particular, modeling of either the initial ignition and heterogenous oxidation or the final condensation processes will rely heavily on the homogeneous combustion model presented in this report.  Consequently, any further development in the combustion modeling must be carefully coordinated with experimental studies which can be used to validate the present homogeneous combustion model. Similarly, as key reaction mechanisms in the other stages of boron combustion are identified, additional experimental work will be required to provide accurate values for the input parameters and for comparisons with model predictions.

### 4.2.1  Further Basic Experimental and Theoretical Research

In the present program, sensitivity analysis was used to identify the critical chemical and physical parameters which control the homogeneous combustion process. The capability to identify the most important gas phase reactions allows researchers to preferentially select those rate parameters whose magnitudes, temperature dependence, and product branching ratios need to be carefully evaluated with further experimental work. Such experimental studies are particularly important for modeling of boron-assisted fuels

4-3

because of the large uncertainties in both the overall boron combustion process and specific input parameters. Thus, while the estimated rate parameters from the present and earlier work were adequate for initial modeling efforts, they cannot be expected to be accurate enough for the modeling which will be required to optimize boron combustion systems.

Based on the results from the present modeling of the homogeneous combustion phase, it is clear that experimental measurements of the kinetic rate parameters and product branching ratios for HOBO, HBO, BO, $BO_2$, and $B_2O_2$ reactions (Table 3-6) are needed. The kinetic sensitivity analysis described in Sections 3.5 and 3.6 suggests that experimental studies should particularly concentrate on the reactions listed in Tables 3-8 and 3-9 since the gas phase kinetics has been shown to be particularly sensitive to these elementary reactions.

To date, relevant laboratory studies have been limited to reactions of atomic B(g) and BO(g) with simple stable oxidants such as $O_2$, $CO_2$, and $H_2O$. A similar situation exists in for boron/halogen systems where only a few reactions of BF and BCl with oxidants such as $O_2$, O, and $NO_2$ have been studied. While these past and on-going studies are important, only the work on BO, initially studied by Fontijn[4-1] and more recently by Oldenborg and Baughcum,[4-2] is relevant to boron-assisted hydrocarbon oxidation, since only BO, of the gaseous species studied to date, is expected to be vaporized from boron particles burning in a hydrocarbon/oxygen combustion system. Consequently, further progress in formulating a reliable boron combustion model requires extensive experimental research on key reactions involving the other boron oxides and oxyhydrides which play important roles in the combustion process.

The sensitivity analysis summarized in Subsection 3.5 has also indicated a need for more accurate thermochemical data. Equilibrium constants for key reactions involving $HBO_2$ (g) formation and conversion to $B_2O_3$ (g) are particularly important. Specifically, equilibrium data for two reactions

$$BO_2 + H_2O \rightarrow HOBO + OH$$

$$HBO_2 + HBO_2 \rightarrow B_2O_3 + H_2O$$

appear to be particularly critical. Better values for the equilibrium constants for these key processes would come from the experimental kinetics community (by independent determination of forward and reverse rate constants), the experimental thermodynamics community through second and third law $\Delta H^f$ and $\Delta S$ determinations, or from the theoretical molecular structure community through better molecular parameters for HBO (g), $B_2O_3$ (g), and $BO_2$ (g). In general, reference to Table 3-1 illustrates the crucial need for more accurate (hopefully to the 0.1 kcal/mole range) molecular structure data over the temperature range of 300 to 3000°K.

### 4.2.2 Further Modeling Work

Coupled to the experimental studies described in 4.2.1, additional modeling of both the heterogeneous burning of a boron particle and condensation of the gas phase combustion products is needed to develop a complete model for the overall combustion process. The most logical extension of the present work is to model the gas phase chemistry in the presence of a clean solid or liquid boron/boron oxide surface. From a practical viewpoint, this extended model will represent the clean particle burning phase described in Section 2.2. From a more fundamental perspective, the same model could be applied to analyze simple heterogeneous kinetic experiments [see for example, Ref. 2.23].

This is a particularly important aspect of the practical combustion problem since earlier work, as well as the results of the present study indicate the boron oxidation is dominated by heterogeneous, surface oxidation processes. This preliminary work would emphasize the oxidation kinetics of B(s) by the various gas phase species expected in the boron/hydrocarbon combustion system. Subsequent work should focus on the boron particle

ignition and the elementary chemical and physical processes of boron oxide film growth and vaporization. Particular attention should be given to the competing diffusion processes of the various species in $B_2O_3$ which control oxide growth and the chemical transformations affecting the oxide removal at temperatures lower than the vaporization temperature of $B_2O_3$ [e.g., $B_2O_3(l)$ + $H_2O$ (g)]. The modes of heat transfer should be an important phase of this modeling since it has been shown experimentally that particle self-heating is negligible during the ignition process.

Finally, the condensation process which occurs downstream from the burning stage should be treated. This phase may be initially studied separately from the heterogeneous particulate boron oxidation and subsequently coordinated with the other submodels to provide a complete description of the full process.

## 4.3 Related Areas of Application

The work presented in this report was specifically motivated by the current interest in boron-assisted hydrocarbon combustion for air-breathing propulsion systems. However, metallic boron and borane based propellants are also being actively considered for a variety of related applications. Although each potential application has unique physical and chemical characteristics, there will undoubtedly also be strong similarities in the basic combustion chemistry. It is worthwhile, therefore, to briefly review the relation between our modeling program and ongoing research in other laboratories.

The use of boron enhanced fuels in decoy flares is one area of application of current interest. Infrared decoy flares deployed from both tactical and strategic aircraft must present a hot infrared spectral signature which will divert a missile seeker away from the aircraft nozzle and exhaust plume. In order to be successful, a decay flare must achieve very rapid and efficient combustion while simultaneously providing the appropriate spectral signature. Current magnesium/teflon flares have significant deficiencies on

both accounts. Ongoing work at Aerodyne Research, the Naval Weapons Support Center and other laboratories have identified several boron enhanced fuels which may have both combustion and exhaust spectral signatures that could result in improved, advanced infrared decoys. The knowledge gained in the present AFOSR boron combustion modeling program will be directly relevant to the evaluation of these new decoy concepts.

Another related area of interest is the addition of borane or borane/amine adduct compounds to liquid rocket propellants in conjunction with a variety of oxidizers including nitrogen oxides, oxygen, oxygen halides, or interhalogens. Attack warning issues have stimulated a great deal of Department of Defense sponsored research effort focused on determining the exhaust plume afterburning chemical kinetics and spectral properties of boron containing exhaust species from such "advanced" liquid rocket propellants.

Borane-based propellants may also have significant applications as burn rate modifiers for NC and NC/HMX propellants and ignitors in large and medium caliber guns and telescoped ammunition, and as propellants for advanced gun propulsion concepts such as consumable sabot, FILMBAL and the traveling charge concept.[4-3] Conventional chemical gun propulsion is intrinsically inefficient for obtaining muzzle velocities greater than 2 km/sec. In a traveling charge configuration, a projectile is accelerated by a combination of gas pressure and impulse produced by a very fast burning propellant attached to and moving with the projectile. Initial calculations indicate that burn rates between 100 m/s and 1000 m/s are required to obtain the desired muzzle velocities.

Much of the recent work on very high burn rate (VHBR) propellant formulations has focused on a series of borane salts (B10B10-2, B12H12-2) known generically by the trade name of Hivelite. Although these salts have been shown to be very effective burn rate promoters, there is very little understanding of the basic mechanisms through which they act. It is generally accepted that VHBR materials burn by a convective mechanism in which the

combustion zone propagates by the infiltration of hot combustion products through pores in in the propellant sample. This is followed by a transition to a very rapid combustion which takes place throughout the whole sample.

In borane-assisted combustion, the initial ignition and volatilization combustion phase associated with metallic boron propellants is replaced by a simpler and much faster pyrolysis of the borane. However, the chemical kinetics of the subsequent combustion phases should closely parallel the reaction kinetics discussed in Section 3.5. Specifically, as the borane ion breaks up and undergoes some initial oxidation, the resulting combustion gases will probably contain many of the same oxides and oxyhydrides which characterize the homogeneous phase of metallic boron combustion. Consequently, the homogeneous boron combustion model described in Section 3.5 should be a very useful in research on the mechanisms by which the gaseous combustion products influence the burn rate. The first step in generalizing the reaction list in Table 3-6 to borane-assisted propellants would be to include oxidation reactions for BH fragments and substitution reactions for the highly reactive 5-coordinated boron atoms in the deca-borane salt. Some evidence for the similarity between borane and metallic boron assisted combustion can be seen in Table 4-1. The table gives combustion product concentrations for a representative sample of a VHBR-borane.

Table 4-1 - Combustion Products of VHBR-Borane Propellant and a
Conventional High Impetus Propellant

| Species | Concentration |
|---------|---------------|
| $HBO_2(g)$ | 0.186 |
| $B_2O_3(g)$ | 0.0072 |
| $HBO(g)$ | 0.092 |
| $B_2O_3(l)$ | 1.88 |

It anticipated that as the present modeling efforts are extended to the heterogeneous phases of metallic boron combustion, the resulting combustion models and mathematical framework developed to extend sensitivity analysis to include heterogeneous processes will be extremely useful in understanding the basic mechanisms responsible for the action of VHBR propellants based on boranes.

## 4.4 References for Section 4

4-1 Llewellyn, I.P., Fontijn, A., and Clyne, M.A.A., "Kinetics of the Reaction of $BO + O_2 \rightarrow BO_2 + O$," Chem. Phys. Lett. 84, 504 (1981).

4-2 Oldenborg, R.C. and Baughcum, S.L., "Gas Phase Oxidation of Boron Compounds," Abstracts of the 1986 AFOSR/ONR Contractors Meeting on Combustion, Stanford University, (June 1985).

4-3 Juhasy, May I.W., and Aungst, W.P., "Combustion Studies of Very High Burning Rate (VHBR) Propelant," Army Armament Research and Development Command Aberdeen Proving Ground, MD Ballistic Laboratory, Report No. IL162618AH80.

END

7-87

DTIC